Methodology for the Enantioselective Synthesis of Isochromanes and their Dimers

Sameshnee Govender

Methodology for the Enantioselective Synthesis of Isochromanes and their Dimers

Sameshnee Govender

Supervised by Prof. C. B. de Koning and Dr W. A. L. van Otterlo

A dissertation submitted to the Faculty of Science,
University of the Witwatersrand, Johannesburg,
in fulfillment of the requirements for the
Degree of Master of Science

November 2005

DECLARATION

I declare that the work presented in this dissertation was carried out exclusively by myself under the supervision of Prof. C. B. de Koning and Dr W. A. L. van Otterlo. It is being submitted for the degree of Master of Science at the University of the Witwatersrand, Johannesburg. It has not been submitted before for any degree or examination at any other university.

Sameshnee Govender
November 2005

ABSTRACT

Pyranonaphthoquinones are biologically important molecules found in a wide variety of bacteria, microbial fungi and plant species. Their biological activity is proposed to be a consequence of their ability to function as bioreductive alkylating agents. This class of compounds, which include monomeric and dimeric examples, contain the basic naphtho[2,3-*c*]pyran-5,10-dione skeleton, usually with substituents at the C-1 and C-3 positions of the pyran ring. The aim of the first part of the project was to develop a novel method for the synthesis of enantiomerically pure 5,8-dimethoxy-isochroman-4-ol, which will provide a handle for stereoselectively adding substituents to the C-1 and C-3 positions of the pyran nucleus. In the second part of the project we wished to attempt to synthesize the naturally occurring compound, cardinalin 3, the dimer of ventiloquinone L previously synthesized in the Wits laboratories. The synthesis of the enantiomerically pure isochromanol began with 2,5-dihydroxybenzoic acid, which was subjected to a diallylation followed by a Claisen rearrangement. The phenols were protected by a methylation reaction and the ester moiety was reduced to give (2-allyl-3,6-dimethoxyphenyl)methanol. It was then allylated to produce a suitable precursor for a one pot/two step ruthenium mediated isomerisation/ring closing metathesis reaction to produce 5,8-dimethoxy-1*H*-isochromene in an overall yield of 47%. It was converted to racemic 5,8-dimethoxy-isochroman-4-ol through a hydroboration-oxidation reaction in a yield of 84%. The separation of the enantiomers was achieved by acetylating the alcohol to form 5,8-dimethoxy-3,4-dihydro-1*H*-isochromen-4-yl acetate and then a lipase enzyme was used to stereospecifically deacetylate one enantiomer, while leaving the other enantiomer untouched. The second part of the dissertation discusses the progress towards the synthesis of cardinalin 3. This project began with the formation of the C-C biaryl axis starting from 1,3-dimethoxybenzene. The synthesis then continued with the diformylation of the biphenyl to give 2,2’,6,6’-tetramethoxy[1,1′-biphenyl]-3,3′-dicarbaldehyde. This was subjected to a Stobbe condensation and a Friedel-Crafts acylative cyclisation to produce diethyl [4,4′-diacetoxy-6,6′,8,8′-tetramethoxy-7,7′-binaphthalene]-2,2′-dicarboxylate. The synthesis will be continued in the PhD, using methodology previously developed for the formation of the monomer, as well as methodology developed here.

ACKNOWLEDGEMENTS

I am truly indebted to my supervisor and mentor Professor Charles de Koning. This project would not have been possible without his support, guidance and most of all his understanding. I truly value all our conversations about chemistry and life!

To my co-supervisor Dr Willem van Otterlo, for all his encouragement and Professor Jo Michael for invaluable advice, thank you.

I would like to thank Professor Laurence Carlton, Mr. Richard Mampa and Mr. Stephen Pelly for running numerous NMR spectra; Mr. Tommie van der Merwe for the many mass specs and Mr. Manuel Fernandes for the XRD analysis of crystal structures as well as data analysis.

I would like to express my sincere appreciation to Dr Dean Brady and Mr. Daniel Visser of the CSIR Biochemtek at Modderfontein for adding a wonderful dimension to my project and teaching me about enzymes. Thank you for your patience and the kind use of your facilities.

I am very grateful for financial support from the University of the Witwatersrand and the National Research Foundation.

To all my fellow members of the Organic Research Group, thank you for a enjoyable working environment, and for all the useful advice as I found my feet in the lab.

To my family, thank you for all your support and encouragement, throughout everything.

And finally to my own personal ‘knight in shining armour’ Stephen, I cannot express in words how grateful I am for having met you and having you in life. You are truly wonderful.

TABLE OF CONTENTS

LIST OF ABBREVIATIONS

Ac	acetyl
aq.	aqueous
Bn	benzyl
cat.	catalytic
cm^{-1}	wavenumber
DMAP	4-dimethylaminopyridine
DMF	*N*,*N*-dimethylformamide
DNA	deoxyribonucleic acid
Et	ethyl
H	hour(s)
Hz	hertz, s^{-1}
IR	infrared
Me	methyl
min	minute(s)
mp.	melting point
NMR	nuclear magnetic resonance
PCC	pyridinium chlorochromate
Ph	phenyl
ppm	parts per million
pr	propyl
rt	room temperature
Salcomine	*N*,*N*′-bis(salicylidene)ethylenediiminocobalt(II)

CHAPTER 1: INTRODUCTION AND AIMS

1.1 Biologically Important Benzoisochromane Quinones

Pyranonaphthoquinone antibiotics have been isolated from various strains of bacteria and fungi of microbial origin.[1] They are typified by the presence of a basic naphtho[2,3-*c*]pyran-5,10-dione skeleton **1** (**Figure 1**). Examples of this class of compounds include simple monomeric, dimeric and carbohydrate derived pyranonaphthoquinones. Also a common feature in many of these molecules is the presence of substituents in the C-1 and C-3 and sometimes in the C-4 position. In this dissertation, we will focus primarily on the monomeric and dimeric representatives of these biologically viable compounds and the next sections will describe some pertinent examples.

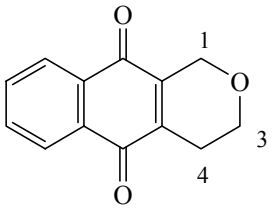

1

Figure 1

1.1.1 Naturally Occurring Monomeric Quinones

The pyranonaphthoquinone family of antibiotics display an extensive range of biological activity which include activity against a wide range of gram positive bacteria, pathogenic fungi and yeasts as well as antiviral activity.[1] Simple examples of this are eleutherin **2** and its C-3 epimer, isoeleutherin **3** (**Figure 2**). They were isolated from the tubers of *Eleutherine bulbosa* (Iradaceae).[2] Eleutherin exhibits activity against *Pycoccus aureus* and *Streptococcus haemolyticus A*.[3]

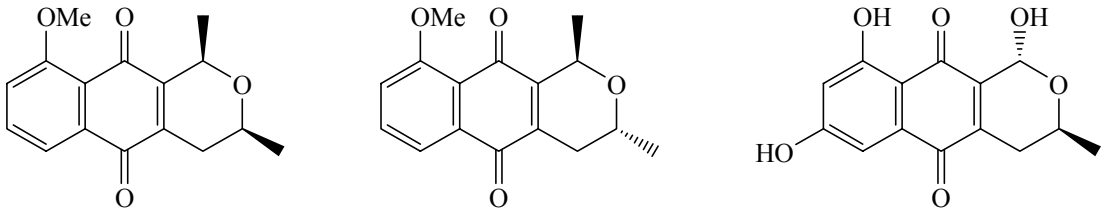

2 **3** **4**

Figure 2

Thysanone **4** (**Figure 2**), a pyranonaphthoquinone isolated from *Thysanophora penicilloides* exhibits activity against the human rhinovirus 3C protease.[4] It has thus provided a lead compound for the development of chemotherapeutic agents for the common cold.[1]

The ventiloquinones are another series of closely related examples of monomeric pyranonaphthoquinone compounds, also with substituents in the C-1 and C-3 positions (**Figure 3**). Ventiloquinones A-E **5-9**, were isolated[5] from the acetone extracts of the root of the barks of two Indian plant species *Ventilago maderaspatana* and *Ventilogo calcyculata* while ventiloquinone L **10**, was isolated from the root bark of *Ventilago goughi*.[6]

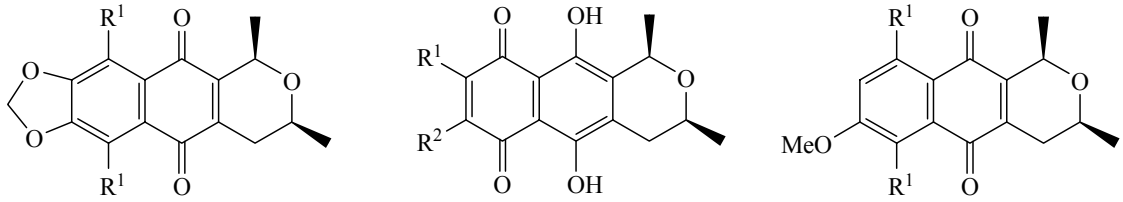

5 R^1=OH(OMe); R^2=OMe(OH) **7** R^1=OH(OMe); R^2=OMe(OH) **9** R^1=R^2=OMe
6 R^1=OMe; R^2=OMe **8** R1=OMe; R^2=OMe **10** R^1=OH; R^2=H

Figure 3

The anti-fungal pigment kalafungin **11** (**Figure 4**), which was extracted from the fermentation broth of *Streptomyces tanashiensis*,[7] was found to be inhibitory *in vitro*

against a variety of pathogenic fungi, protozoa, yeasts, gram-positive bacteria and some gram-negative bacteria.[8] More recently, it was also found to be cytotoxic, displaying inhibitory activity against L5178Y mouse leukemic cells[9] and to be an antithelmintic agent.[10] This pyranoquinone contains an additional γ-lactone ring fused to the dihydropyran moiety and hence substituents at the C-1, C-3 and C-4 positions. Nanaomycin D **12**, (**Figure 4**) isolated from *Streptomyces rosa*, was found to be the enantiomer to kalafungin, and to possess almost identical antibacterial properties.[11]

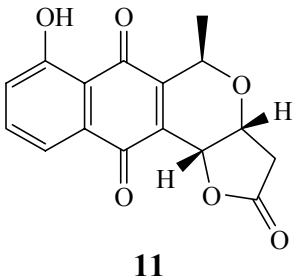

11

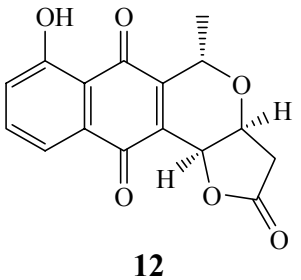

12

Figure 4

Also structurally similar to kalafungin, are the frenolicins, isolated[12] from *Streptomyces fradiae* (**Figure 5**). Frenolicin B **13,** contains a propyl side chain at C-1, instead of the usual methyl group. Frenolicin **14**, and it's reduced form, deoxyfrenolicin **15**, also have the propyl side chain as well as a carboxylic acid side chain at C-3, as a result of the ring opening of the γ-lactone.

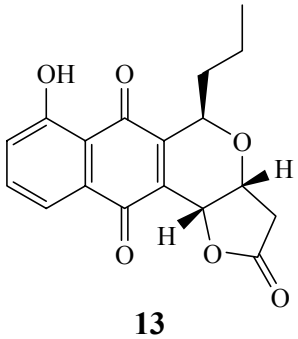

13

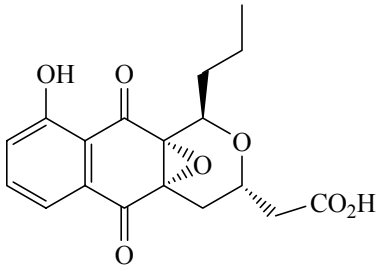

14

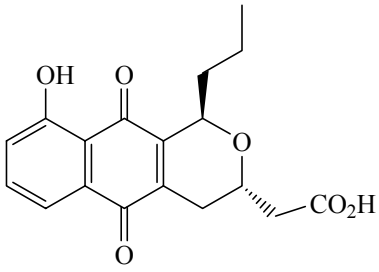

15

Figure 5

While frenolicin **14**, shows only weak antibacterial activity[13], deoxyfrenolicin **15**, possesses significant *in vitro* activity against a variety of fungi[14] and frenolicin B **13**, strongly inhibits platelet aggregation.[15] Other novel kalafungin-type antibiotics were isolated from the fermentation broth of *Actinoplanes arizonaenis*. Arizonin A1 **16**, and arizonin B1 **17**, (**Figure 6**) both exhibit moderate activity against pathogenic strains of gram-positive bacteria[16] as does griseusin **18**, isolated from the cultures of *Streptomyces griseus* K-63.[17] Griseusin **18** is one of the more complex members of the pyranonaphthoquinone family. It contains a 1,7 dioxaspiro[5,5]undecane ring system fused to a juglone moiety.

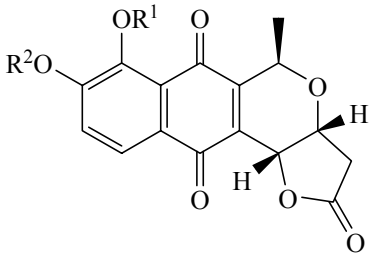

16 R^1=Me; R^2=H
17 R^1=H; R^2=Me

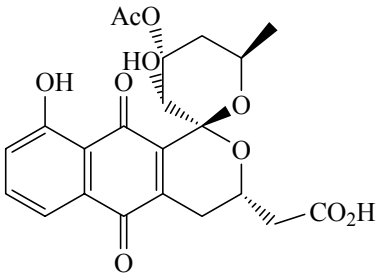

18

Figure 6

1.1.2 Naturally Occurring Dimeric Quinones

The first example in this section comes from a series of dimeric pigments from *Streptomyces coelicolor* known as the actinorhodins. Actinorhodin **19**, (**Figure 7**) contains a C8-C8′ biaryl linkage with the two halves exhibiting identical stereochemical features, whereas in δ-actinorhodin **20** there is a six-membered lactone supplementing the connection between the two halves as well as two γ-lactams. There has been reported activity of **19** against *Staphalococcus aureus*.[18]

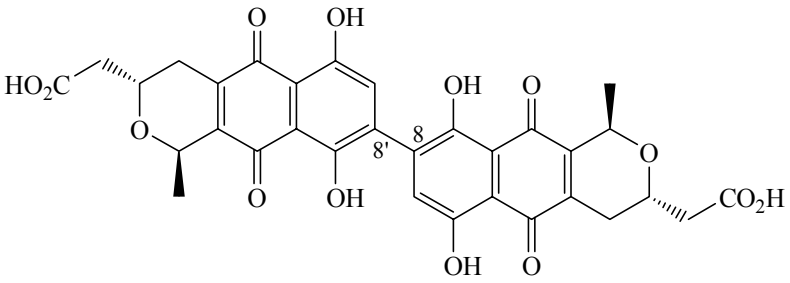

19

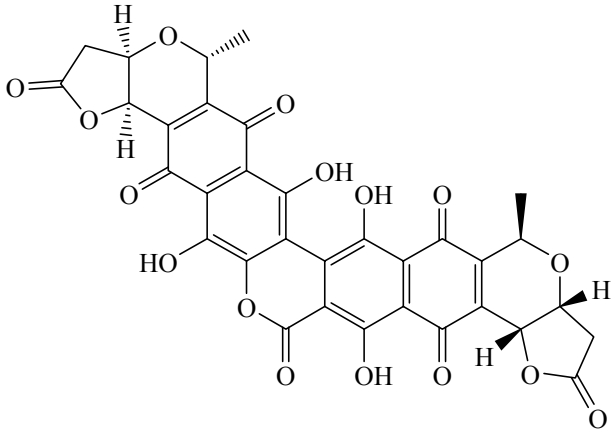

20

Figure 7

The major biologically active component of an antibiotic complex produced by a microorganism *Micromonospora purpureochromogenes* sub-species *halotolerans*, crisamycin A **21**, displays excellent activity against gram-positive bacteria, and has also exhibited *in vitro* activity against B16 murine melanoma cells, herpes simplex virus and vesicular stomatitis virus.[19] Also isolated from these extracts was crisamycin C **22**, the epoxide derivative of **21**. It exhibits the same range of activity as **21** but is much more potent.

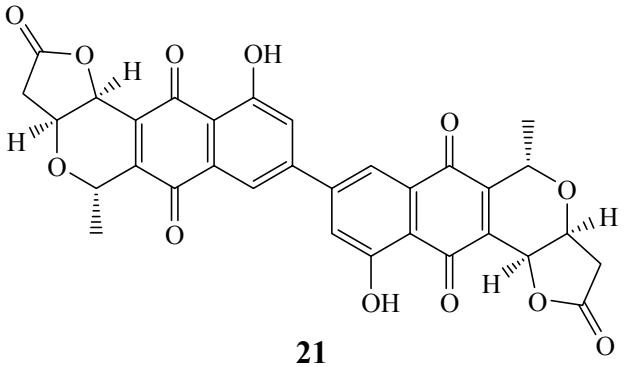

21

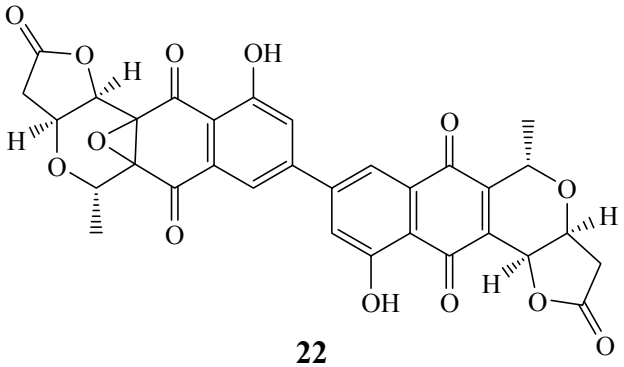

22

Figure 8

Another class of dimers, the cardinalins, were the first class of pyranonaphthoquinones to be isolated from higher order fungi.[20] They were isolated from the ethanol extracts of the toad stool *Dermocybe cardinalis*. The deep red ethanolic extracts showed significant cytotoxic activity (IC_{50} of 0.47 μg cm^{-3}) against a P388 murine leukemia cell line.[20] The individual components of the mixture were then separately examined. Some examples are given below in **Figure 9**. The symmetrical dimer cardinalin 3 **23** contains only the C8-C8′ biaryl linkage, with a bis-naphthoquinone skeleton, while cardinalin 4 **24** and its C-4a′ epimer cardinalin 5 **25**, have an ether linkage supplementing this linkage. Cardinalin 3 **23** shows no asymmetric doubling in either the ^{1}H or ^{13}C NMR spectra, and can therefore be assumed to occur as discrete atropisomers.[20] Comparison of the circular dichromism (CD) spectra of **23** with binaphthyls where the stereochemistry of the biaryl linkage is known, has shown that cardinalin 3 **23** possesses (*S*) chirality at the stereogenic axis.[20]

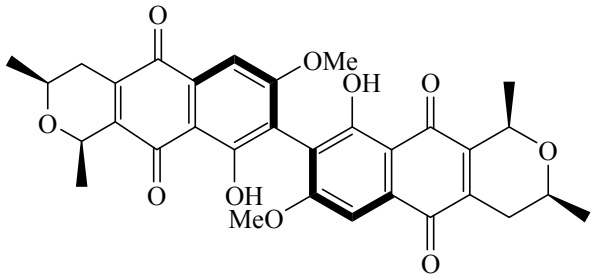

23

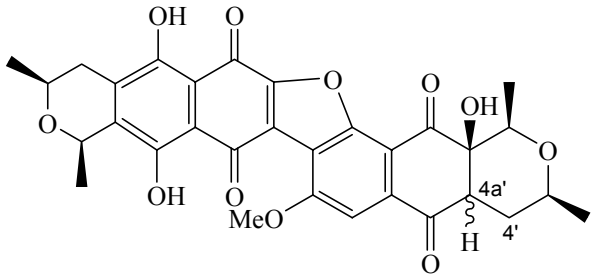

24 α-H
25 β-H

Figure 9

These monomeric and dimeric pyranonaphthoquinones are just a few representative examples of an extensive range of naturally occurring, biologically active molecules. Their biological activities are thought to be a consequence of their interesting chemical structures. While there are many proposed mechanisms of antineoplastic action, we will focus on the model of the bioactivation of quinones to produce quinone methides, which are proposed to behave as alkylating agents,[21,22] selectively forming covalent bonds with the DNA of cancer cells, resulting in the anticancer activity of the quinone.

1.2 Bioreductive Alkylating Agents

The term "bioreductive alkylation" was introduced by Lin.[23] This hypothesis was used to explain the biological activity of the pyranonaphthoquinones and to predict their important structural features. The idea behind bioactivation lies in the fact that a drug is introduced as a biologically inactive form, and only after *in vivo* activation is it able to

carry out its function. In the case of quinones e.g. **26**, *in vivo* bioreduction results in the hydroquinone **27**. The cleavage of a benzylic substituent from **27**, by the mesomerically assisted loss of HX results in the formation of a quinone methide **28**. The quinone methide can now form covalent adducts such as **29** with biological nucleophiles such as DNA, proteins or carbohydrates through a Michael addition to the reactive enone system of **28**. The formation of the covalent adduct with DNA for example, renders it incapable of carrying out its normal function, thus leading to cell death. Once this cytotoxic activity of the quinone has been carried out, the adduct can be oxidized, resulting in its biologically inactive form **30**.[24] This is depicted in **Scheme 1**.

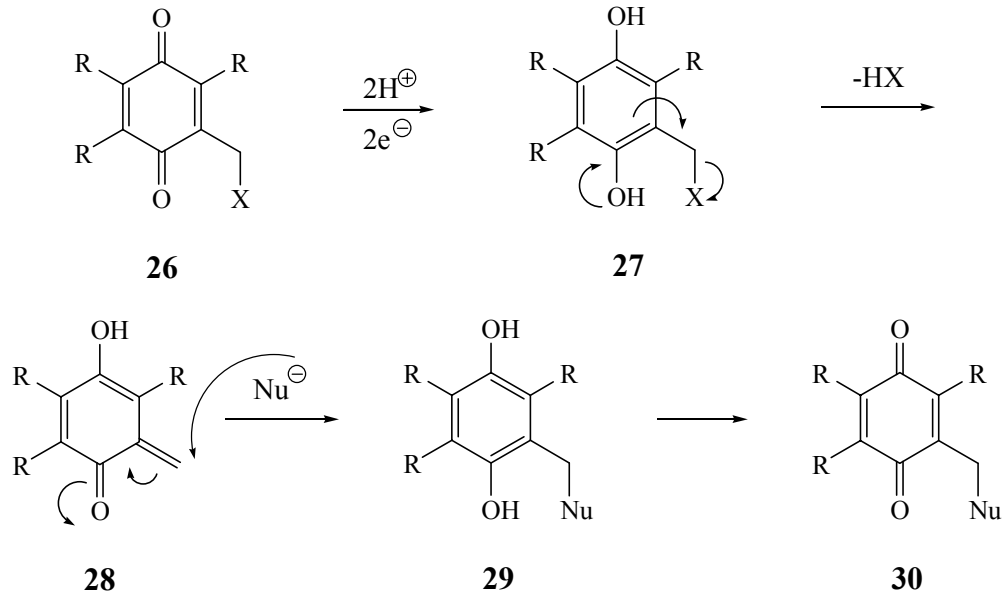

Scheme 1

The process depicted in **Scheme 1** will be discussed below, with specific examples; however they are general for many biologically active quinones.

1.2.1 *In vivo* Bioreduction

An example of a compound which requires bioactivation to achieve biological activity is the antibiotic mitomycin C **31** (**Figure 10**), a potent inhibitor of transplantable rodent

tumours. The compound is believed to function as an antitumour alkylating agent. It has been found that the anticancer agent **31**, which contains the quinone functionality, is inactive in aerobic conditions, and requires bioreduction to the hydroquinone for biological activity.[25,26]

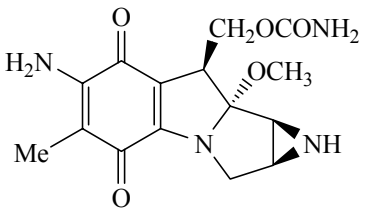

31

Figure 10

It was further shown by Iyer and Szybalsky that an NADPH-dependant reductase system was involved in this step.[26] NADPH is the reduced form of nicotinamide adenine dinucleotide phosphate, and is a non-specific electron donor. Several chemical, electrochemical and enzymatic methods have been used to bring about *in vitro* reductive activation. Koch and co-workers[27] described the reduction of daunomycin **32**, an anthracycline antitumour drug, containing a quinone moiety, using sodium dithionite in DMSO, to form the quinone methide **34**. (**Scheme 2**) They were also able to effect the reduction with 3,5,5-trimethyl-2-oxomorpholin-3-yl (TM-3) **33** and sodium borohydride. When using TM-3 **33**, a one electron donor, one equivalent of the reducing agent first produced a semiquinone and a second equivalent produces the 7-deoxydaunomycin **34**. In the case of the $NaBH_4$, the reaction proceeded through a hydroquinone borate followed by a quinone methide borate. In all cases reduction was found to take place preferentially under anaerobic conditions.

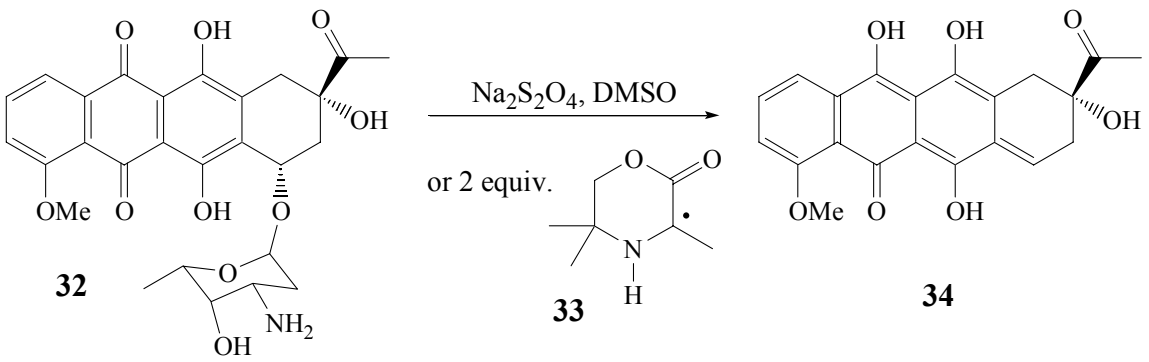

Scheme 2

For the successful treatment of cancerous tumours using chemotherapy it is essential for the drug to be able to differentiate between the host and target cells. This property of bioactivation under anaerobic conditions is an extremely beneficial property as it is possible to make the potential drug selective between host and target cells. The reason for this is that solid tumours have regions of poor vascularity due to their extremely rapid growth and hypoxic (oxygen deficient) cells may exist at the centre, remote from surrounding blood vessels.[28] This population of hypoxic cells allows the possibility of designing drugs that are capable of bioactivation in a hypoxic environment. As quinones are activated by a reductive mechanism, their potential for development as hypoxia selective cytotoxins is plausible[28] thus leaving analogous and healthy oxygen-rich cells unaffected.

1.2.2 Formation of Quinone Methides

Bioreductive alkylating agents can be classified according to the mechanism of formation of their quinone methides. Some simple models have been postulated and are described below.

1.2.2.1 Quinone Methide Formation by Bioreduction and Elimination

This model was proposed by Lin *et al.*[23] to explain the neoplastic activity of simple quinones containing one or more $–CH_2$-X substituents, where X is a leaving group (**Scheme 3**), e.g. **35** (with X = $OCOCH_3$). The elimination of HX to produce the quinone methide **37** can be enhanced when there are electron-releasing substituents on the ring, however the reduction to the hydroquinone **36** is then more sluggish. These quinones do however show enhanced biological activity when compared to those substituted with electron-withdrawing groups.[24]

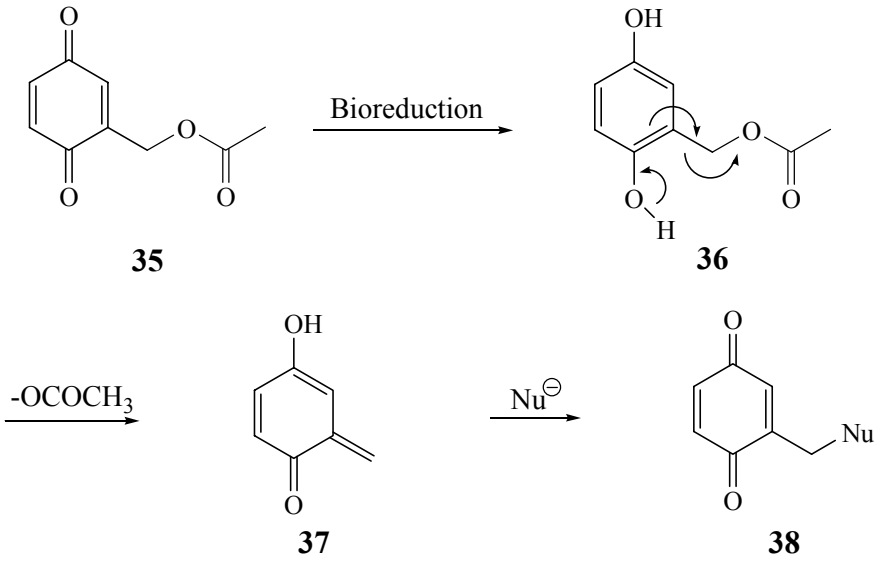

Scheme 3

The quinone methide can then undergo nucleophilic addition to form a covalently bonded adduct **38** to for example a cancer cell, inhibiting further activity and thus resulting in cell death.

1.2.2.2 Vinylogous Quinone Methides

This is a variation of the above mechanism, where the leaving group is substituted with an alkenyl group as in compound **39**. Reduction to the hydroquinone **40** and subsequent

loss of HX results in the vinylogous quinone methide **41**, which can then function as an alkylating agent by Michael addition of the biological nucleophile to form compound **42** (**Scheme 4**).

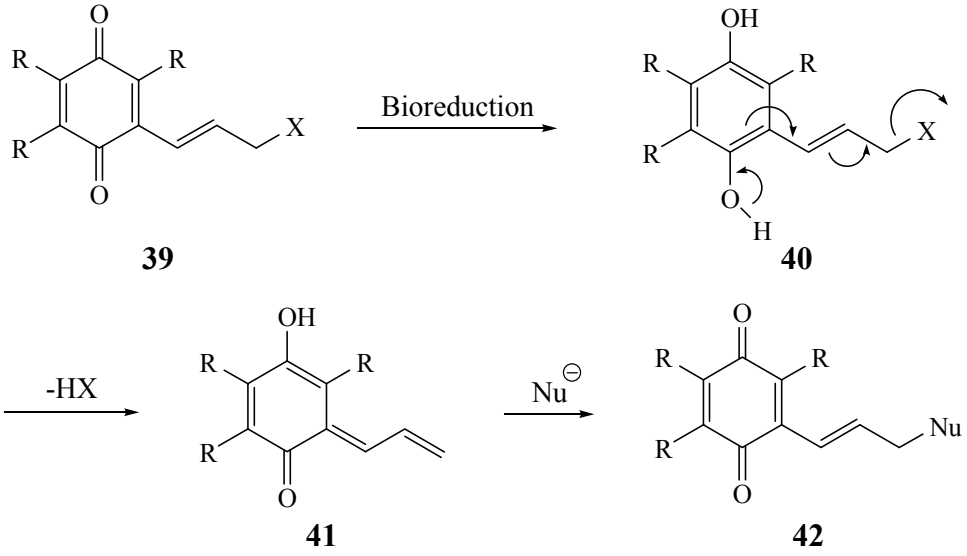

39 **40** **41** **42**

Scheme 4

1.2.2.3 Bis-alkylating Agents

Several quinones are capable of producing two alkylating sites, which tend to be arranged in a 1,4-cisoid dienyl arrangement as in structure **43** (**Figure 11**).

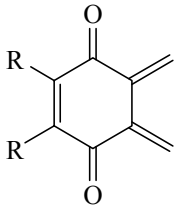

43

Figure 11

An example of this type of bis-alkylating agent can be produced from the fused pyrano-γ-lactone quinone, kalafungin **11**. Reduction of the naturally occurring compound **11** to the hydroquinone **44**, followed by molecular rearrangement and opening of the γ-lactone ring produces the quinone methide **45**, which may function as an alkylating agent. Further elimination of **45** could then result in the bis-quinone methide **46** (**Scheme 5**).[28]

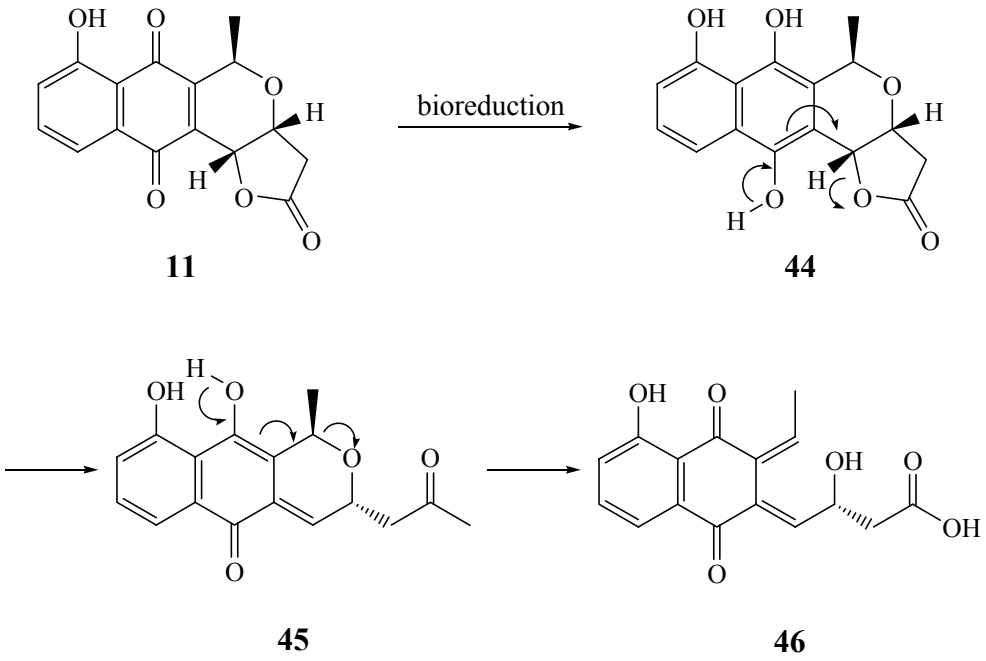

Scheme 5

1.2.3 Addition of Biological Nucleophiles to Quinone Methides

The mode of action of quinones at the DNA level still remains a topic of speculation and debate. Phillips and co-workers detected *in vitro* covalent adducts between adriamycin **47** (**Figure 12**) and DNA.[29] Their experimental evidence pointed to interstrand cross-links in the DNA which were found to contain the adriamycin chromaphore. The binding to this biologically important nucleophilic target would account for the inhibition of the template action of DNA, thus blocking the synthesis of DNA, RNA and proteins and leading to chromosomal abnormalities in cells exposed to these alkylating agents.

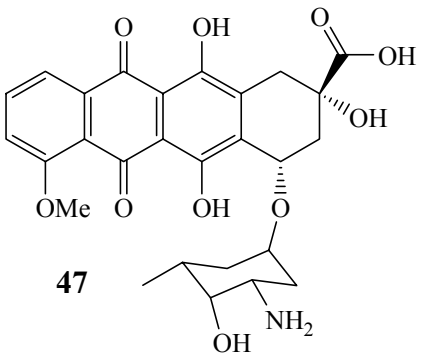

47

Figure 12

There has been much research carried out on the *in* vitro nucleophilic addition to quinone methides.[30-32] Koch and co-workers found that the treatment of the quinone methide **48** of andriamycin **47** with reduced glutathione **49** led to the glutathione conjugate **50**. (**Scheme 6**).[30] The same group also reported the addition of *N*-acetylcysteine **51** to the quinone methide **34** of daunomycin **32** to form the quinone adduct **52** (**Scheme 7**). Angle *et al.* showed that treatment of a quinone methide **53** with various nucleophiles led to the formation of conjugate addition adducts **53a-f**.[32] This is shown in **Scheme 8** with the list of nucleophiles.

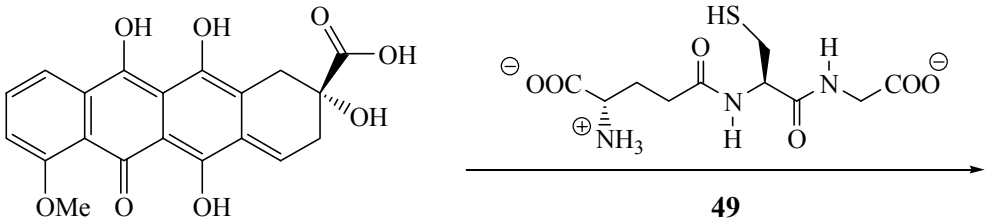

48 **49**

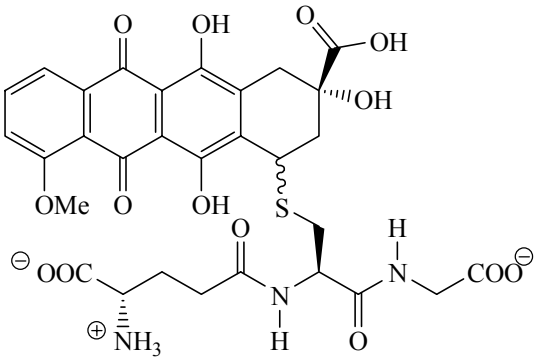

50

Scheme 6

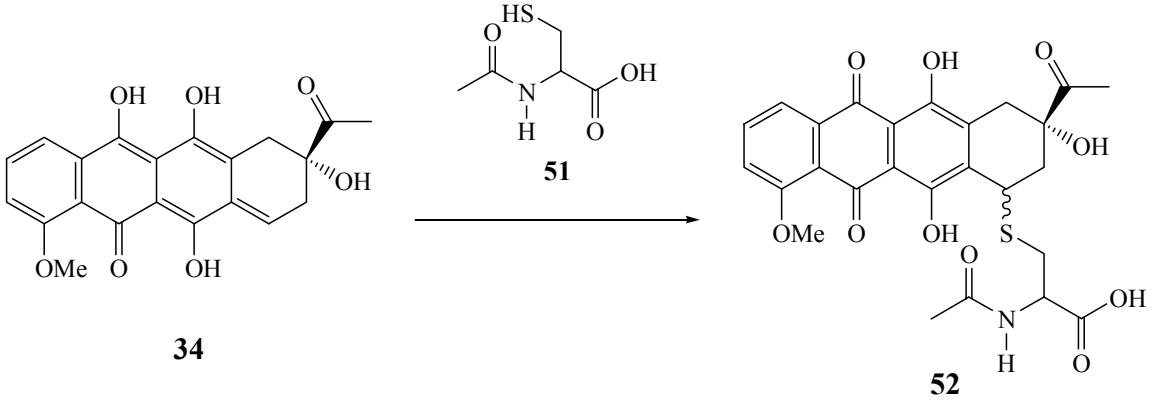

34 **51** **52**

Scheme 7

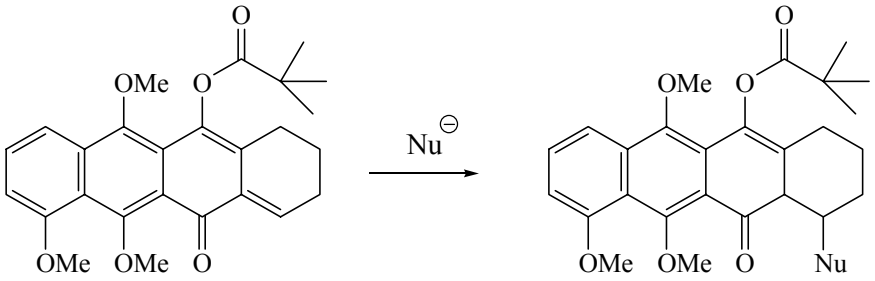

53

53a Nu = OEt

53b Nu = NHPh

53c Nu = SPh

53d Nu = SBu

53e Nu = CN

53f Nu = $CH(CO_2CH_3)_2$

Scheme 8

Once the formation of the covalent bond with the nucleophile has taken place the hydroquinone adduct can then be oxidized to the quinone. This adduct is now biologically inactive.

1.3 Biosynthesis

Benzoisochromane quinones are essentially polyketides and their biosynthesis involves a series of decarboxylative condensation reactions between small carboxylic acids and malonate using enzyme complexes. The highly reactive intermediate produced is then further processed through a set of intramolecular cyclisation, elimination, redox and group transfer reactions to generate the highly functionalized natural product.[33] The biosynthetic mechanism of *Streptomyces* pyranonaphthoquinone antibiotics is proposed to follow a polyketide pathway, similar to fatty acid biosynthesis in which the carbon backbone arises from the condensation of acetate units derived from acetyl-CoA or malonyl-CoA.[33-36] The cyclisation of the polyketide intermediates is achieved through

intermolecular aldol condensations. The biosynthesis of actinorhodin **19** is shown in **Scheme 9**.[37]

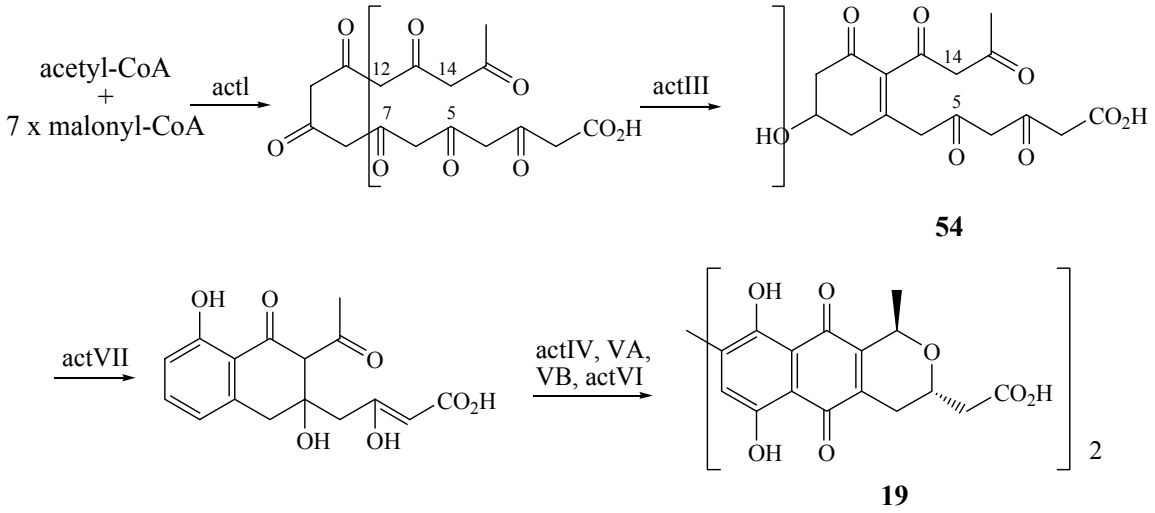

Scheme 9

According to a study on the cyclisation pattern of synthetic oligoketides,[33] the polyketide derived from an acetyl CoA starter unit and seven malonyl CoA extender units undergoes transformation through a regiospecific intramolecular aldol condensation between C-7 and C-12. A second aldolase then forms the bond between C-5 and C-14. It then undergoes aromatisation of the two rings, oxidation to the quinone, hydroxylation and dimerisation to form actinorhodin **19**. The genes present in the biosynthetic pathway are denoted by 'act' in **Scheme 9**.

1.4 Synthetic Strategies Towards Benzoisochromane Quinones

Due to their significant biological activity as well as their interesting and challenging structures, benzoisochromane quinones have received much attention from synthetic chemists. Numerous synthetic methods have been developed and in this chapter some of the different approaches towards their synthesis will be presented.

1.4.1 Syntheses of the Monomeric Benzoisochromane Quinones

1.4.1.1 Biomimetic Approaches

Since much chemical effort has been devoted towards the study of the biosynthesis of polyketide chains, one approach towards the chemical synthesis of benzoisochromane quinones was to mimic the strategy adopted by nature.[38] (±)-Eleutherin **2** and isoeleutherin **3** were synthesized in a biomimetic fashion starting from 2-pyrrolidinylgluterate diester **56** as shown in **Scheme 10**.[39] Tandem attack of two equivalents of the dianion of acetylacetone **55** on ester **56** produced the heptaketide **57**, which underwent a spontaneous cyclisation to form the naphthyl diketone **58**. This was then treated with trifluoroacetic acid to accomplish the cyclisation of the third ring producing the pyran **59**. Catalytic hydrogenation followed by monomethylation, in the absence of light, produced a 9:1 mixture of *cis* and *trans* pyrans **60** and **61**. The mixture of isomers was then oxidized with Fremys salt to afford the quinones **2** and **3**. While the major *cis* isomer was assigned as (±)-eleutherin **2**, isomerisation of **2** in phosphoric acid afforded an equilibrium mixture with mainly the *trans* isomer **3**.

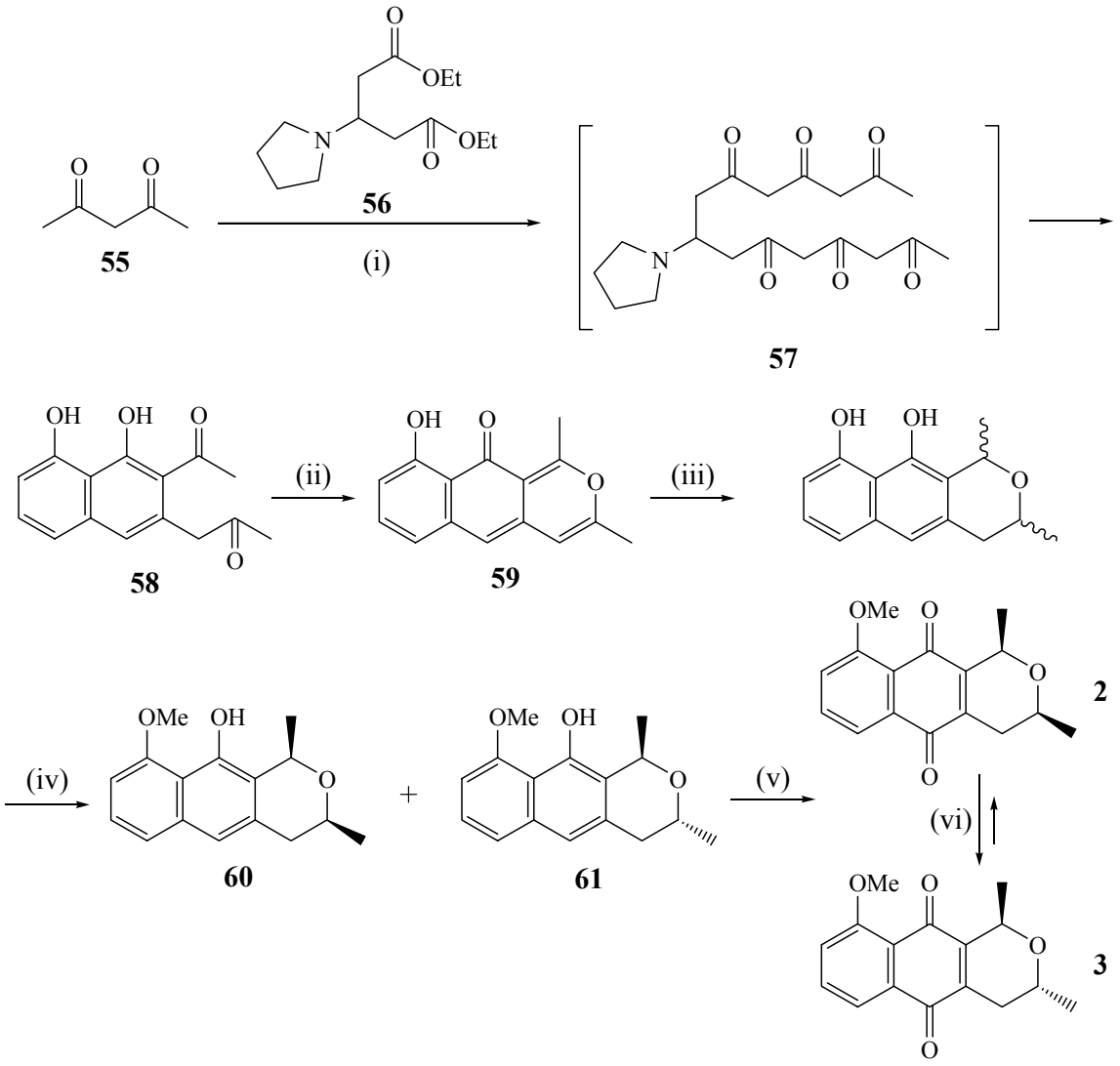

Scheme 10 *Reagents and conditions*: (i) **55**, LDA, THF, -78 °C, then **56**, -35 °C; (ii) EtOH, CF_3CO_2H cat., reflux; (iii) 5% Pd/C, EtOH, H_2, rt; (iv) CH_2N_2, Et_2O; (v) $(KSO_3)_2NO$; (vi) H_3PO_4.

1.4.1.2 Phthalide Annulations

The use of phenylsulphonyl phthalides has been a common method to construct several pyranonaphthoquinone antibiotics.[40] This approach was used by Tatsuta *et al.*[41] in the synthesis of the nanaomycins and kalafungins. (**Scheme 11**). The addition of the lithium *tert*-butoxide generated anion of **62** to the Michael acceptor **63** and gave an intermediate bridged structure which was then transformed to the hydroquinone **64** via concomitant

cleavage of the γ-lactone and loss of the phenylsulfonyl group followed by tautomerism. The free phenols of **64** were then protected as methyl ethers and the product was subjected to sodium borohydride reduction to yield **65** exclusively in the 3,4-*syn* configuration.

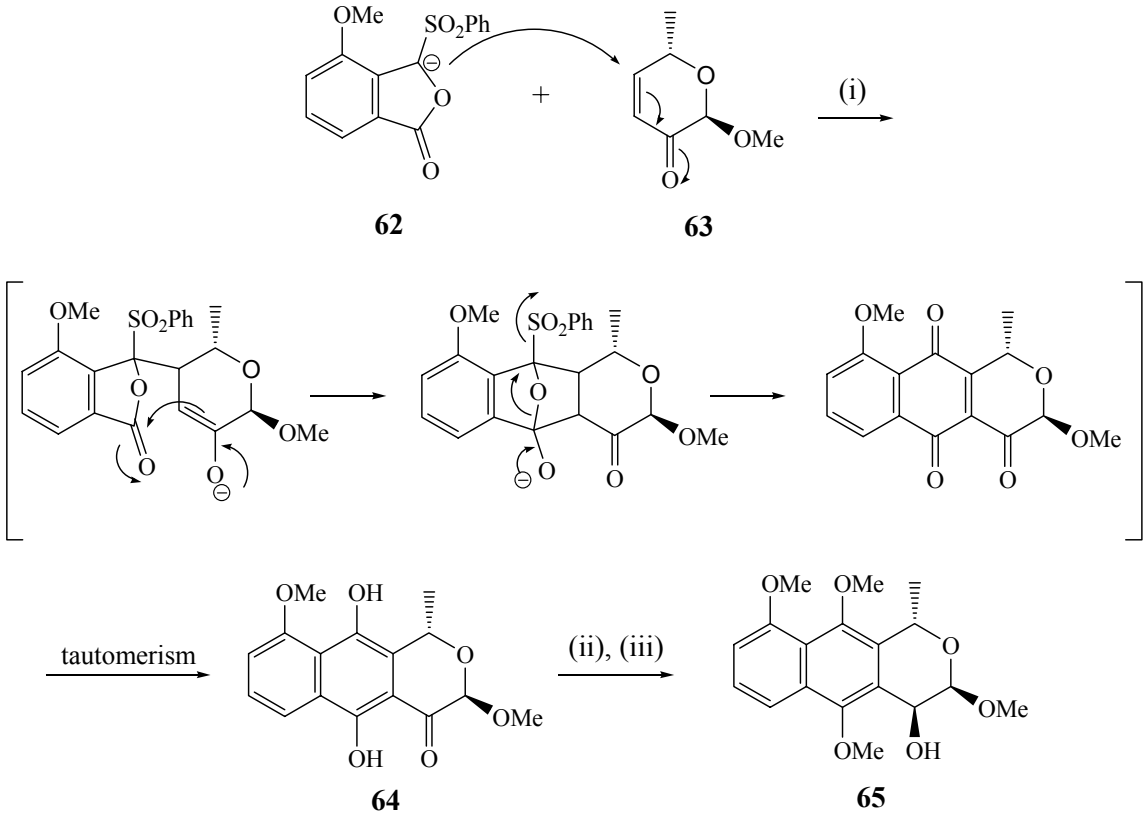

Scheme 11 *Reagents and conditions*: (i) *t*-BuOLi, THF, 80%; (ii) K_2CO_3, $(MeO)_2SO_2$, acetone, 40 °C; (iii) $NaBH_4$, MeOH, 88%.

1.4.1.3 Reductive Mercury(II) Acetate-Mediated Cyclisations

It has been demonstrated by de Koning and co-workers[42] that the oxidative ring closure of benzylic alcohol **66** with mercury(II) acetate, and other subsequent steps affords the isochromanol **69** (**Scheme 12**). Their syntheses relies on the fact that a vinyl substituent is present *ortho* to the benzyl alcohol. The isochromanol **69** was synthesized by first treating **66** with mercury(II) acetate followed by treatment of the resultant mercury(II)

intermediate with oxygen, and then sodium borohydride, to yield a 1:1 mixture of the *cis:trans* alcohols **67**. This alcohol was then oxidized to the corresponding ketone **68** and subsequently reduced to afford only the *cis*-isochroman-4-ol **69.**

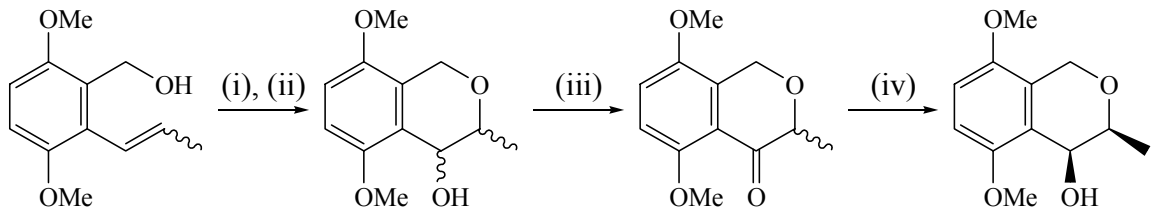

66 **67** **68** **69**

Scheme 12 *Reagents and conditions*: (i) $Hg(OAc)_2$, THF, 15 min; (ii) $NaBH_4$, DMF, O_2, 86%; (iii) PCC, CH_2Cl_2, 74%; (iv) $LiAlH_4$, Et_2O, 80%.

1.4.1.4 Ring Expansions of Substituted Cyclobutanones

Moore and co-workers[43] have proposed a different approach to the synthesis of a quinone nucleus. They have presented a general enantioselective route to lactones such as **75**. The key reaction involved the electrocyclic ring opening of the cyclobutanone to a conjugated ketene, which then underwent thermal ring closure and rearrangement to form quinones or hydroquinones. In the example depicted in **Scheme 13**, treatment of cyclobutanedione **70** with lithiated lactol **71** in ether at −78 °C gave **72** in a 51% yield. Upon thermolysis of this compound in refluxing toluene, **72** was converted into the ketene intermediate **73**. This was followed by a pericyclic rearrangement to result in a ring expanded intermediate, which tautomerised to the isochromane **74**. Treatment of **74** with HCl followed by pyridinium chlorochromate (PCC) oxidation then yielded the quinone lactone **75** in an overall yield of 38%.

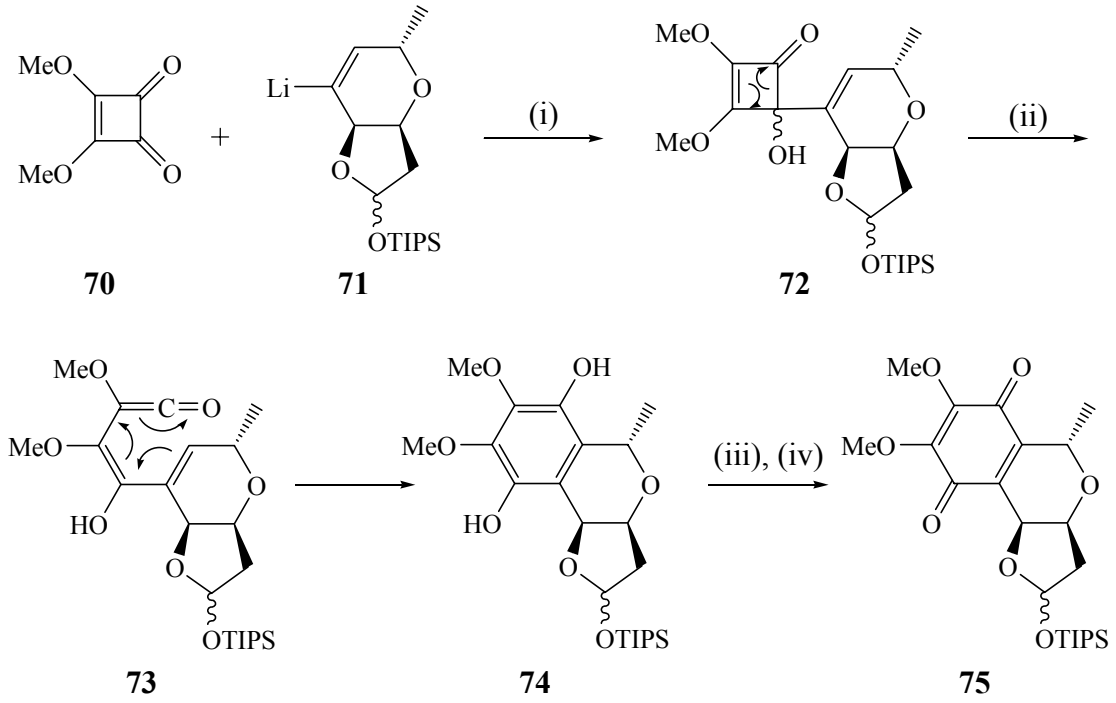

Scheme 13 *Reagents and conditions*: (i) Et_2O, -78 °C; (ii) 110 °C; (iii) HCl; (iv) PCC.

1.4.2 Synthesis of Dimeric Benzoisochromane Quinones

The synthesis of dimeric benzoisochromane quinones from closely related naturally occurring metabolites is an approach that has proved particularly useful. The monomer units of dimeric compounds can also be synthesised however the penultimate coupling step is sometimes not achieved. Consequently these compounds are normally made from pre-existing molecules that carry the required functionality, or by mimicking the process by which they are formed naturally.[40] Some examples of this will be depicted in the next section.

1.4.2.1 Synthesis from other Natural Products

In the synthesis of the enantiomer of actinorhodin **80** by Laatsch[44] (**Scheme 14**) cyclisation, methylation and deacetylation of α-naphthocyclinone **76** produced

deacetylanhydro-α-naphthocyclinone methyl ester **77**, which was then degraded by diazomethane to form naphthol **78** after monomethylation. Oxidative coupling of this monomer **78** then provided the dimer **79**, which was oxidized with cerium(IV) nitrate to afford the dimer **80**, the enantiomer of actinorhodin (**19**).

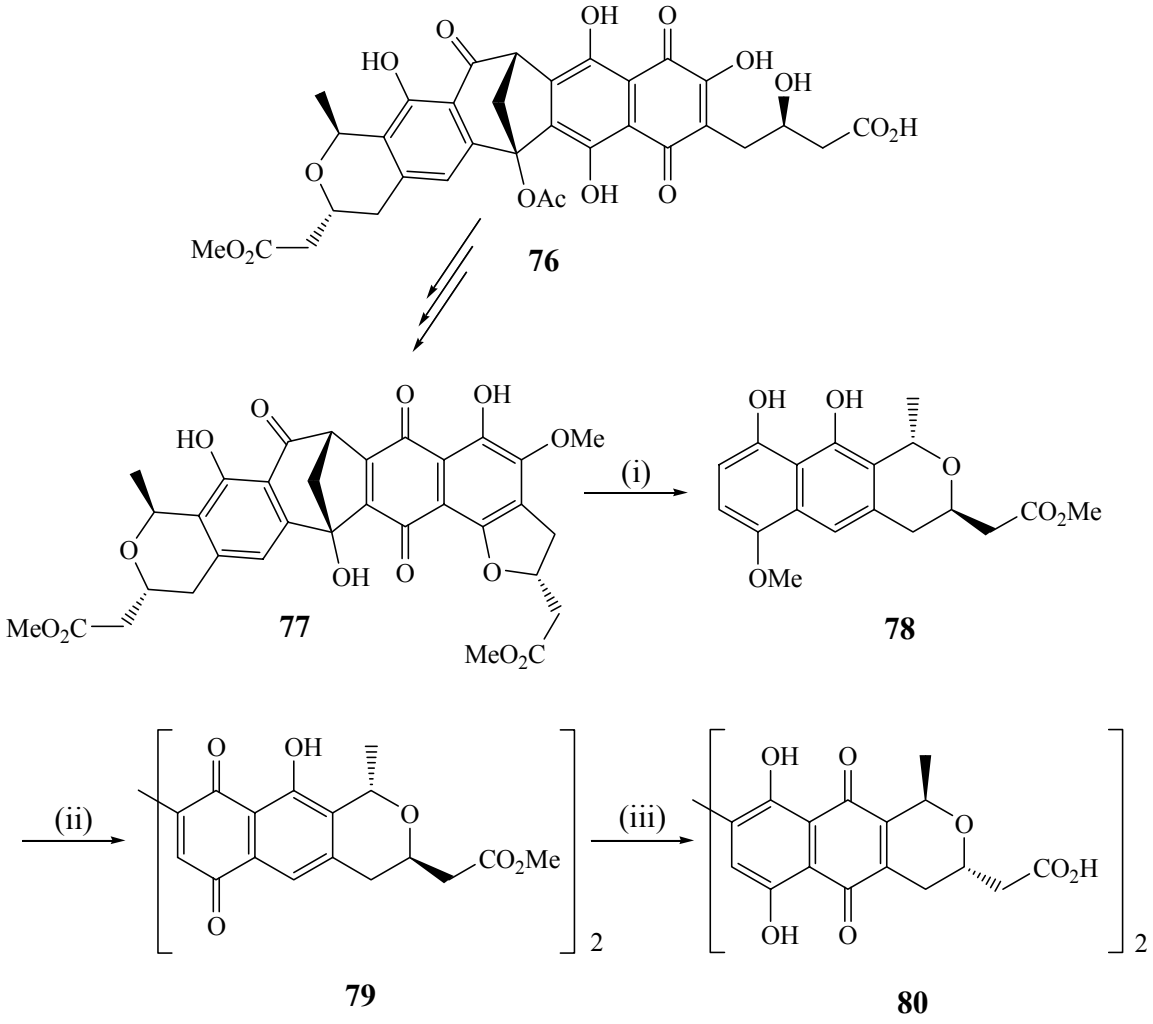

Scheme 14 *Reagents and conditions*: (i) CH_2N_2, CH_2Cl_2, 0 °C; (ii) Ag_2O, Et_3N, $CHCl_3$; (iii) aq. CAN, MeCN.

1.4.2.2 Coupling of Monomer Units

The biosynthetic formation of the protoaphin **83** and protoaphin-*fb* **84** *in vivo* is likely to involve the coupling between the two halves of the molecules. This coupling has been achieved *in vitro*[45] by the heating of quinone A **81** and glucoside B **82** (**Scheme 15**). In this case the glucoside is thought to be utilized as an electron donor and the quinone as the electron acceptor. Self rather than mixed coupling has also been carried out with **81** and **82**.[46]

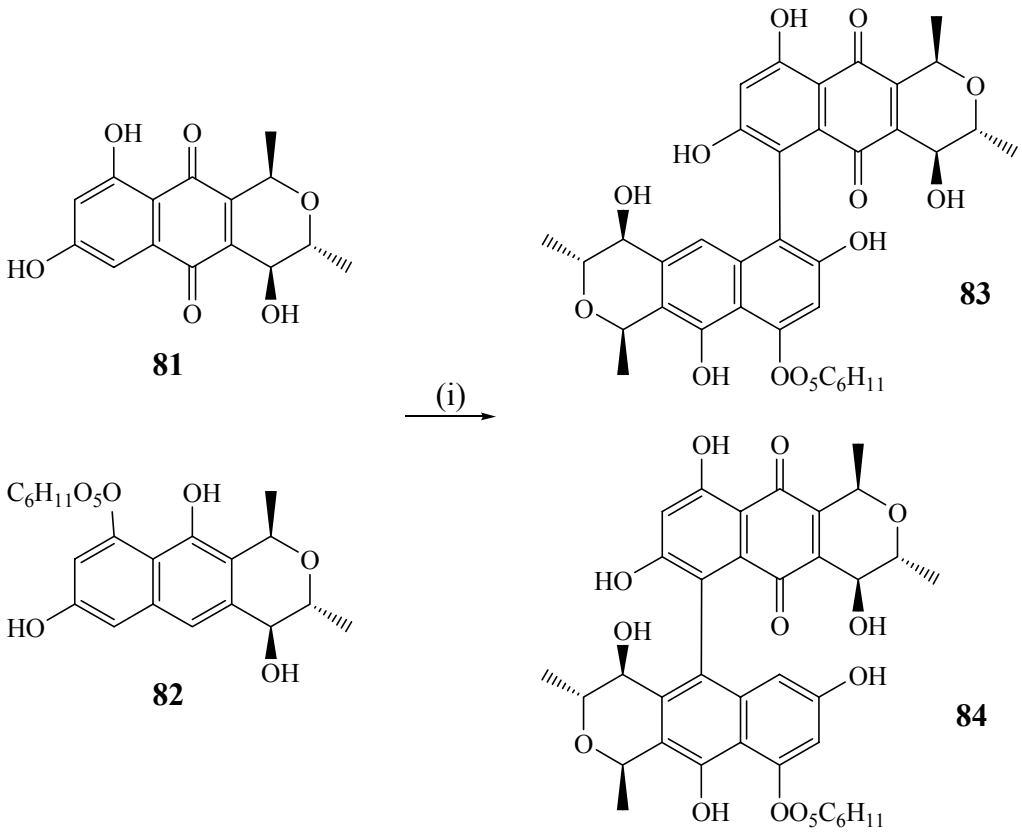

Scheme 15 *Reagents and conditions*: (i) pH 6.6, aq. solution, 80 °C.

1.5 Aims of this Project

The aims of this project have been divided into two sections. Firstly we will aim to develop a novel method for the synthesis of enantiomerically pure isochromanols **85a** and **85b**. These molecules will provide us with a handle for stereoselectively adding substituents to the C-1 and C-3 positions, as found in many naturally occurring pyranonaphthoquinones. With these methods in place, for the second part of this project, we hope to develop synthetic procedures for the synthesis of the naturally occurring cardinalin 3 **23**. (**Figure 13**).

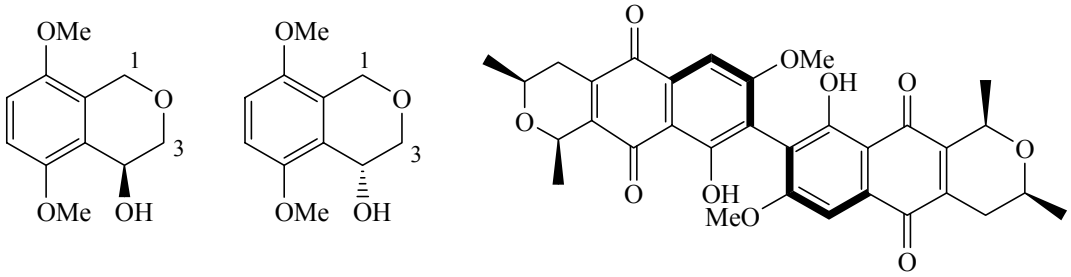

85a **85b** **23**

Figure 13

1.5.1 Synthesis of Enantiomerically Pure Isochromanols

The racemic alcohol **85** can be disconnected, through a hydroboration-oxidation reaction (Section 2.1.2) back to the isochromene **86**, which we plan to synthesize using ring closing metathesis (RCM) (discussed in Section 2.1.1). The precursor for this novel step is the diallyl ether **87** which disconnects back to the benzyl alcohol **88**, which has been previously synthesised at the Wits laboratories.[47] The retrosynthesis is presented in **Scheme 16**.

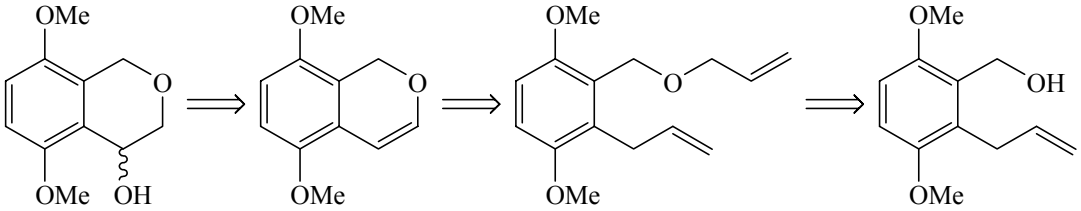

Scheme 16

With the racemic alcohol **85** in hand, it should be possible to separate the two enantiomers, using an enantioselective enzymatic reaction. In order to achieve this, the alcohol **85** will be acetylated to form **89**. A lipase enzyme will then used to de-acetylated one enantiomer of **89** while leaving the other enantiomer untouched (**Scheme 17**). This work is discussed in Section 2.1.3.

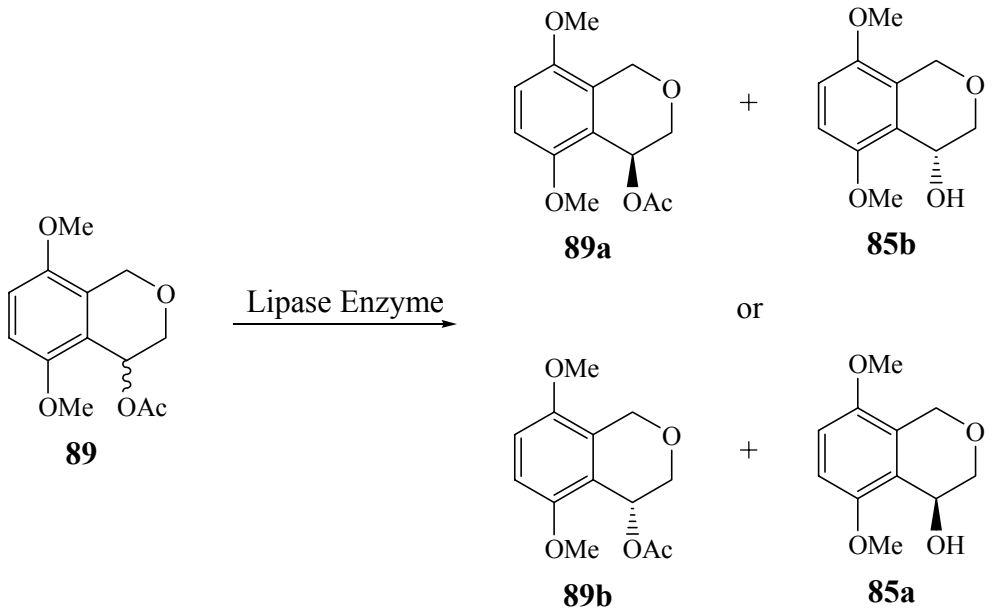

Scheme 17

Finally, the need for enantiomerically pure alcohols **85a** and **85b** in order to add the required methyl groups to positions C-1 and C-3, in a stereoselective manner will be discussed in Chapter 3.

1.5.2 Progress Towards the Synthesis of Cardinalin 3

Previously in our laboratories, the synthesis of the naturally occurring ventiloquinone L **10** was successfully carried out starting from 2,4-dimethoxybenzaldehyde **90** (**Scheme 18** and **19**).[48,49] The readily available starting material **90** was subjected to a Stobbe condensation with diethyl succinate, followed by Friedel-Crafts acylative cyclisation to produce the acetoxynaphthalenecarboxylic acid ethyl ester **91**. Chemoselective phenolic acetate hydrolysis with guanidine produced the naphthol **92**. This product was then subjected to routine allylation to give the ether **93**, which then underwent thermal Claisen rearrangement to yield **94**. The phenol was then protected as the benzyl ether **95** by *O*-benzylation. The aldehyde **97** was produced over two steps, by initially reducing the ester to the primary alcohol **96**, followed by partial re-oxidation with pyridium chlorochromate.

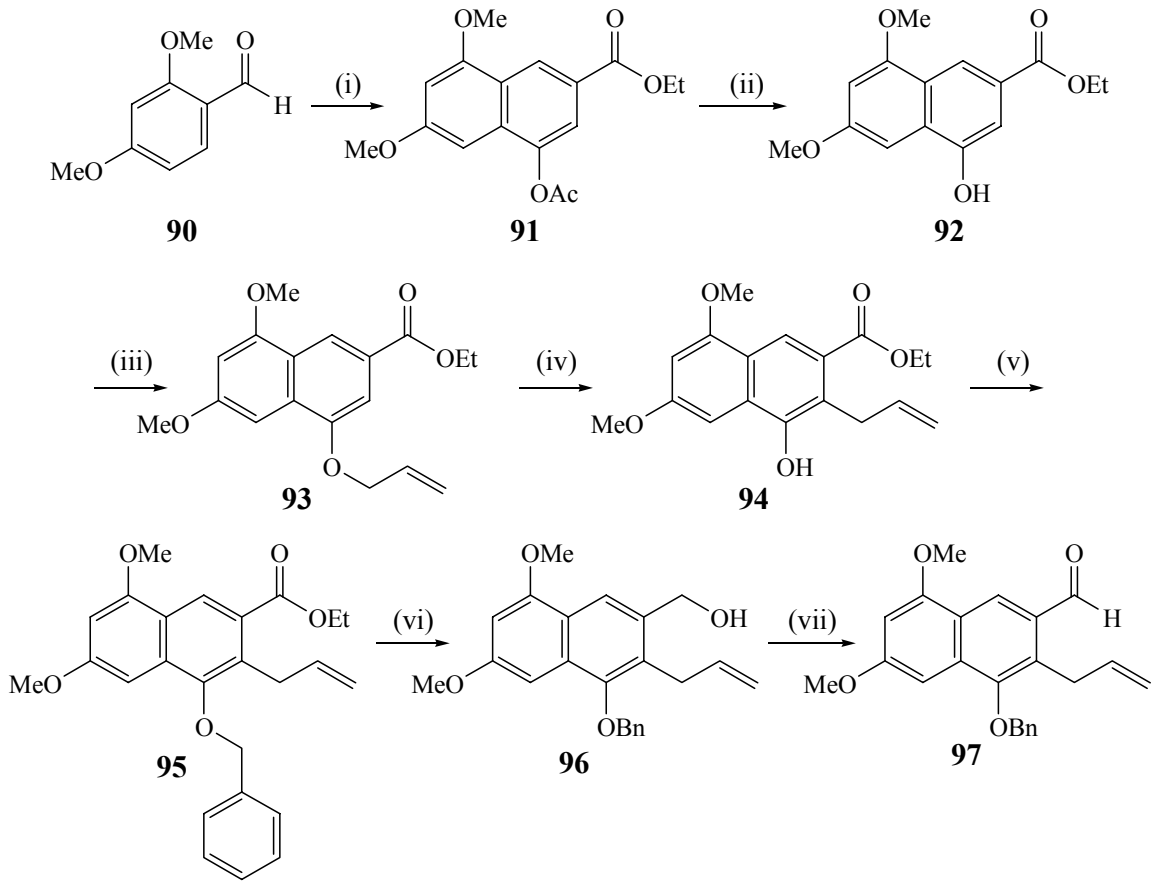

Scheme 18 *Reagents and conditions*: (i) (a) Diethyl succinate, ^{t}BuOH, KO^{t}Bu, reflux, 2 h; then (b) NaOAc, Ac_2O, 140 °C, 2 h, 77%; (ii) guanidine, EtOH, CH_2Cl_2, rt, 1 h, 95%; (iii) K_2CO_3, allyl bromide, acetone, reflux, 16 h, 99%; (iv) DMF, 170 °C, 12 h, 75%; (v) K_2CO_3, BnCl, KI, acetone, reflux, 18 h, 100%; (vi) $LiAlH_4$, THF, 0 °C→rt, 18 h, 95%; (vii) PCC-Al_2O_3, CH_2Cl_2, rt, 8 h, 78%.

Treatment of the aldehyde **97** with methylmagnesium iodide gave the desired alcohol **98**. This alcohol **98** was subjected to Wacker oxidation to produce to isochromene **99**. Catalytic hydrogenation of **99** over palladium on charcoal resulted in reduction of the enol ether as well as hydrogenolysis of the benzyl group in the one step to give predominately the *cis* isochromanol **100**. Pure *rac-cis* **100** was dissolved in DMF and treated with oxygen gas under salcomine catalysis to give the desired quinone; the literature reported 7-methoxyeleutherin **101**. Selective cleavage of the C-8 methyl ether with boron trichloride gave the desired target *rac*-ventiloquinone L **10**.

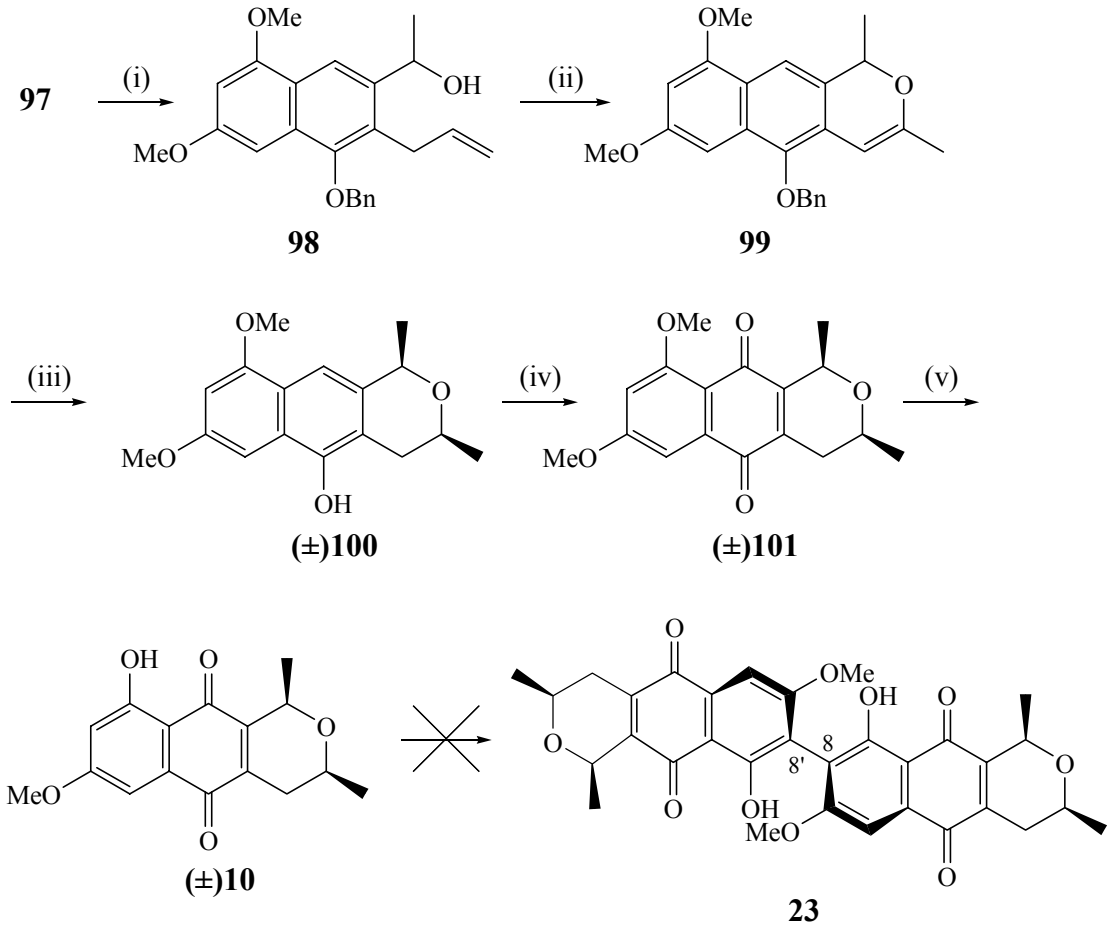

Scheme 19 *Reagents and conditions*: (i) MeMgI, Et_2O, THF, 0 °C→rt, 18 h, 95%; (ii) $PdCl_2$(cat), $CuCl_2$, H_2O, DMF, O_2, rt, 3 h, 92%; (iii) Pd-C(cat), H_2(500 kPa), CH_2Cl_2, dioxane, rt, 48 h, 45% (for 3:1 *cis:trans* mixture); (iv) Salcomine(cat), DMF, O_2, rt, 18 h, 90%; (v) BCl_3, CH_2Cl_2, -78 °C, 70%.

Ventiloquinone L **10** is the monomer of the naturally occurring cardinalin 3 **23**. On completion of the synthesis of **10**, numerous methods were employed to attempt "dimerising" the molecule to give **23**, however they were all unsuccessful. In this project, we hoped to make progress towards the synthesis of **23** using this overall synthetic methodology but with different tactics. Therefore in our synthesis we commence with the formation of the final C8-C8′ biaryl axis of **23** as a first step and then continue with the planned synthesis in a bi-directional manner. The retrosynthesis of cardinalin 3 **23** (**Scheme 20**), following the developed methodology disconnects to the bis-

acetoxynaphthalenecarboxylic acid ethyl ester **105,** which is derived from the Stobbe condensation of the diformylated biphenyl **104**. This molecule can be further disconnected to the tetramethoxy biphenyl **103** which is synthesised from the homocoupling of commercially available 1,3 dimethoxybenzene **102.**

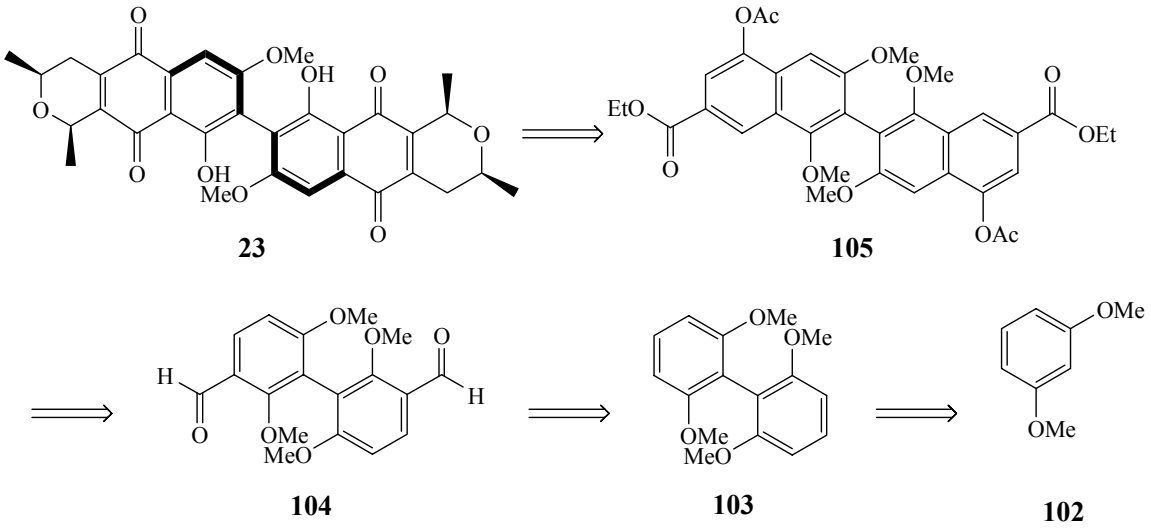

Scheme 20

Although the complete synthesis was not achieved in this project, we believe that the final steps for formation of the pyran ring of cardinalin 3 **23**, can be achieved utilising enzymes as well as arene chromium tricarbonyl complexes (discussed in Chapter 3) for the stereoselective addition of the C-1 and C-3 methyl substituents.

CHAPTER 2: RESULTS AND DISCUSSION: PART A

2.1 Synthesis of the Allyl Ether 87

Using well documented methodology, the synthesis of the diallyl ether **87** could be easily achieved from commercially available 2,5-dihydroxybenzoic acid **106**. The retrosynthesis of our synthetic strategy is shown below in **Scheme 21**. The allyl ether **87** could be disconnected to the benzyl alcohol **88** through a retro *O*-allylation. The benzyl alcohol **88** was disconnected to the ether **109**. It could be obtained from the reduction of the ester moiety of **109**. The ether **109** was disconnected to the unprotected **108** through a retro-methylation. The *C*-allylated **108** was a result of a regioselective Claisen rearrangement of **107**. Finally **107** was disconnected to the readily available **106** through a double *O*-allylation.

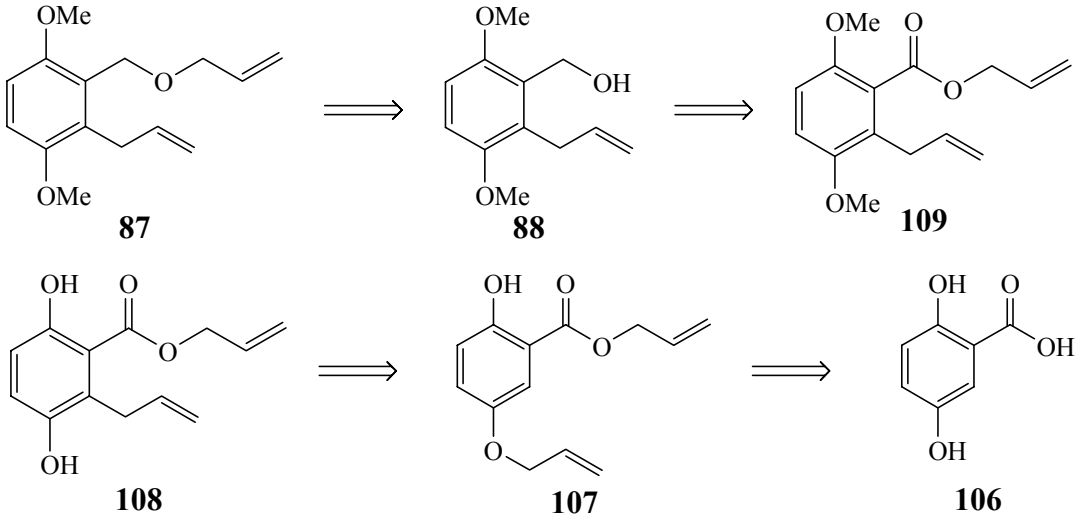

Scheme 21

Our synthesis began with the treatment of 2,5-dihydroxybenzoic acid **106,** in a 1 molal solution in acetone, with 2.2 equivalents each of potassium carbonate and allyl bromide, under reflux conditions (**Scheme 22**). These dilute conditions were found to be optimal for the synthesis of the desired diallylated product **107**. The carboxylic acid proton should

be the most acidic proton, with a pK_a of approximately 5 and hence allyl ester formation should be completed first. The phenolic protons have a pK_a of about 10. The phenol *ortho* to the acid, however, is not only more sterically crowded, but is also expected to display hydrogen bonding, being in close proximity to the carbonyl, thus hindering the formation of the 2-allyl ether. The desired compound **107** was obtained in a yield of 92%.

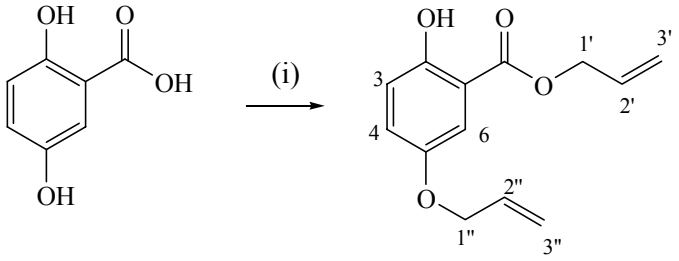

106 **107**

Scheme 22 *Reagents and conditions*: (i) K_2CO_3, allyl bromide, acetone, Δ, 24 h, 92%.

A prominent singlet at δ 10.35 in the ^{1}H NMR spectrum of **107**, was clear evidence of the hydrogen-bonded 2-hydroxy group. The desired diallylated species, also revealed the typical splitting pattern in the aromatic region consistent with a 1,2,4-aromatic trisubstitution pattern. The doublet furthest downfield was assigned to 6-H, as it is the most deshielded aromatic proton due to the electron withdrawing effects of the carbonyl group as well as the anisotropic effects of the carboxylate group. The doublet clearly showed *meta* coupling to 4-H with *J*=3.1 Hz. The doublet of doublets, assigned to 4-H, showed *ortho* and *meta* coupling to 3-H and 6-H respectively, with coupling constants of *J*=9.1 and 3.1 Hz respectively. It is expected further downfield than 3-H due to the electron withdrawing mesomeric effect of the carboxylate at the *para* position. The signal for 3-H showed only *ortho* coupling to 4-H with *J*=9.1 Hz. It was most upfield, being the most strongly influenced by the shielding effect of the electron donating *ortho* phenol substituent of **107**. The ether and ester methylene protons were observed as two doublets at δ 4.50 and δ 4.85 with coupling constants of *J*=5.3 and 5.7 Hz respectively.

Claisen rearrangement of the diallylated compound was then achieved by heating the compound in the absence of solvent at 170 °C for 24 hours. Although there are two *ortho* positions available (C-6 and C-4) for the pericyclic [3,3] sigmatropic shift, at completion of the reaction there was only a single product, shown by TLC analysis. This was confirmed to be the desired, more sterically hindered hydroquinone **108** in an 86% yield. It has previously been shown[50,51] that electron-withdrawing substituents, in this case an ester, favour Claisen-migration to the position *ortho* to them. It has further been suggested that strong internal hydrogen bonding as shown in **107**, confers a naphthalenoid character on the molecule.[50] The arrangement resembles that of 2-allyloxynaphthalene **110**, which gives 1-allyl-2-naphthol **111** exclusively on Claisen rearrangement **(Scheme 23)**.

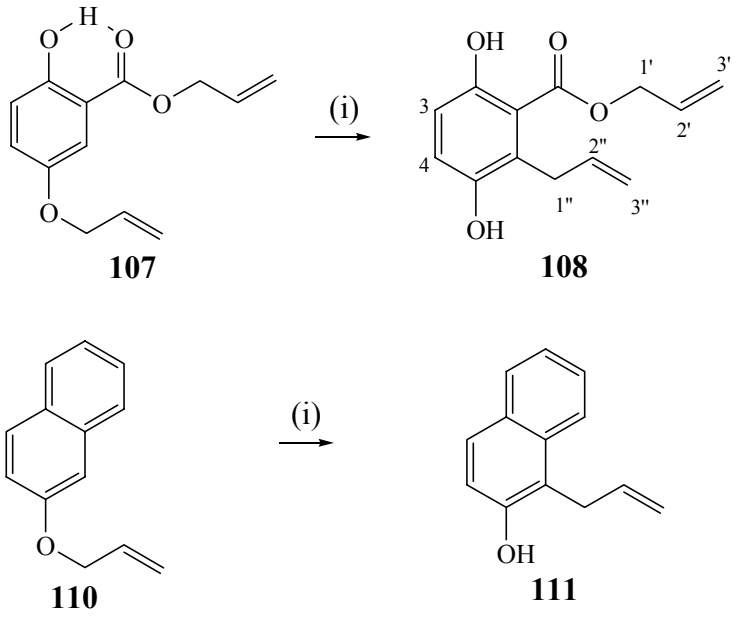

Scheme 23 *Reagents and conditions* (i) 170 °C, 24 h.

The rearrangement of the allyl substituent *ortho* to the ester was unequivocally confirmed by the NMR spectroscopic data. The aromatic region of the ^{1}H NMR spectrum was simplified by the disappearance of the doublet at δ 7.36 for the 6-H of **107**. Instead it now contained only 2 doublets, integrating for 1 proton each, at δ 6.99 and δ 6.82, showing a

typical *ortho* relationship with coupling constants of *J*=8.9 Hz. Further confirmation that the *O*-allyl group was now a *C*-allyl substituent was evident in the upfield shift of the allyl methylene carbon signal from δ 69.6 to δ 32.4 in the ^{13}C NMR spectrum. All other signals in both the ^{1}H and ^{13}C NMR spectra were in line with expectations.

The free hydroquinone **108** was then protected as its bis(methyl)ether **109**, by treatment of **108** with potassium carbonate and dimethyl sulfate, in acetone, under reflux conditions. The yellow mixture initially turned purple-brown, indicative of the phenoxide formation. It finally became light brown in colour when the methylation was complete. Analysis by TLC showed a characteristic purple spot corresponding to the protected hydroquinone **109** (**Figure 14**). The excess dimethylsulfate was quenched by the addition of an aqueous ammonia solution and finally purified by column chromatography to produce **109** in an 82% yield. The disappearance of the phenolic signals was complemented by two new singlets at δ 3.78 and δ 3.77, integrating for 3 protons each, indicating the presence of the two methoxy groups. Methylation was further confirmed by the disappearance of the O-H stretch at 3424 cm^{-1} in the IR spectrum of **109**.

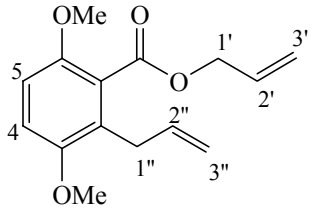

109

Figure 14

The ester **109**, was then subjected to reduction by lithium aluminium hydride in THF to afford the alcohol **88** in 93% yield (**Figure 15**). The signals for the allylic ester protons were no longer present in the ^{1}H NMR spectrum of **88**. A new singlet at δ 4.71 was assigned to the benzylic protons on the hydroxyl-bearing carbon. A broad signal at δ 2.30 was characteristic of the proton of the alcohol group. This was further confirmed by a broad IR spectral band at 3416 cm^{-1} for the hydroxyl O-H stretch. The ^{13}C NMR

spectrum of the starting material **109**, showed a signal for an ester at δ 167.4, was no longer present in the ^{13}C NMR spectrum for the alcohol **88**. Instead a signal for the benzylic carbon was evident at δ 55.8.

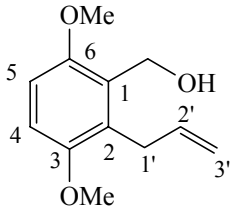

88

Figure 15

O-Allylation of the alcohol **88** was smoothly achieved by stirring a THF solution of **88** in the presence of sodium hydride and allyl bromide at reflux for 24 hours. TLC analysis of the reaction mixture showed a single spot with R_f= 0.59, as opposed to the much lower R_f = 0.32 for the alcohol with a 20% EtOAc/hexane eluent. The oil contaminant from the sodium hydride reagent was removed by gradually increasing the eluent polarity from hexane to 20% EtOAc/hexane on a silica gel column. The formation of **87** was confirmed by the absence of the benzylic hydroxy proton signal in its ^1H NMR spectrum, as well as the additional signals at δ 6.03-5.89, 5.32-5.16 and 4.03 clearly showing that an *O*-allyl substituent was attached to the benzylic alcohol (**Figure 16**).

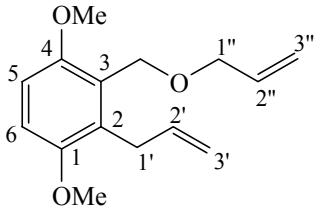

[87]

Figure 16

With the allyl ether **87** in hand, we are now ready to form our model isochromene system **86**, utilising RCM with the Grubbs second generation ruthenium catalyst as well as ruthenium mediated isomerisation as shown in the retrosynthesis in **Scheme 24**.

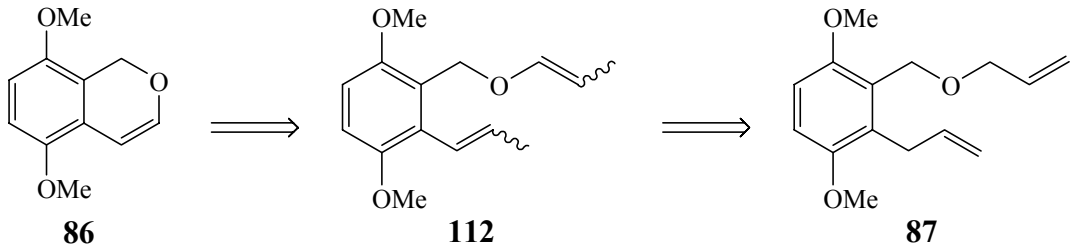

86 **112** **87**

Scheme 24

2.1.1 The Synthesis of Benzo-Fused Isochromene Systems

As previously described, numerous other methods have been developed in forming isochromene systems. Our aim was to synthesise our desired isochromene **86**, by utilizing the metal catalyzed transformation known as ring closing metathesis (RCM).

2.1.1.1 Oxygen Heterocycle Formation by Ring Closing Metathesis

The fundamental discovery that the *in situ* generation of catalysts from certain transition metal salts and main group alkylating agents, not only promote polymerisation of olefins, but can also effect the mutual alkylidene exchange reaction of alkenes, has evolved into a highly prosperous field of research.[52] This transformation was awarded the Nobel Prize in Chemistry to Grubbs, Shrock and Chauvin in 2005. It involves the cleavage and formation of double bonds, as depicted in **Scheme 25**, and has become a popular method for the assembly of cyclic alkenes.[52] This synthetic approach is generally referred to as "alkene metathesis".

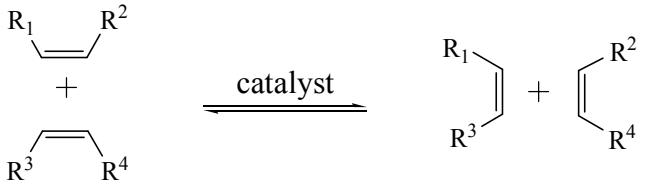

Scheme 25

Extensive research in the field of organometallic chemistry has lead to the discovery of a new generation of metal alkylidene complexes, which have proved to be reasonably oxygen and moisture tolerant, thermally stable, high performing catalysts.[53] Among the most popular and versatile catalysts, are the ruthenium carbene complexes such as **113** (**Figure 17**), introduced by Grubbs and co-workers,[54] which have become well embraced tools for advanced organic synthesis.

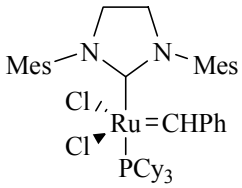

113

Figure 17

The generally accepted mechanism of metathesis reactions, as proposed by Chauvin[55] consists of a sequence of formal [2+2] cycloadditions/cycloreversions involving alkenes, metal carbenes and metallocyclobutane intermediates. A generalised catalytic cycle, involving a Grubbs-type metathesis catalyst (with ruthenium being the metal), is shown in **Scheme 26**.

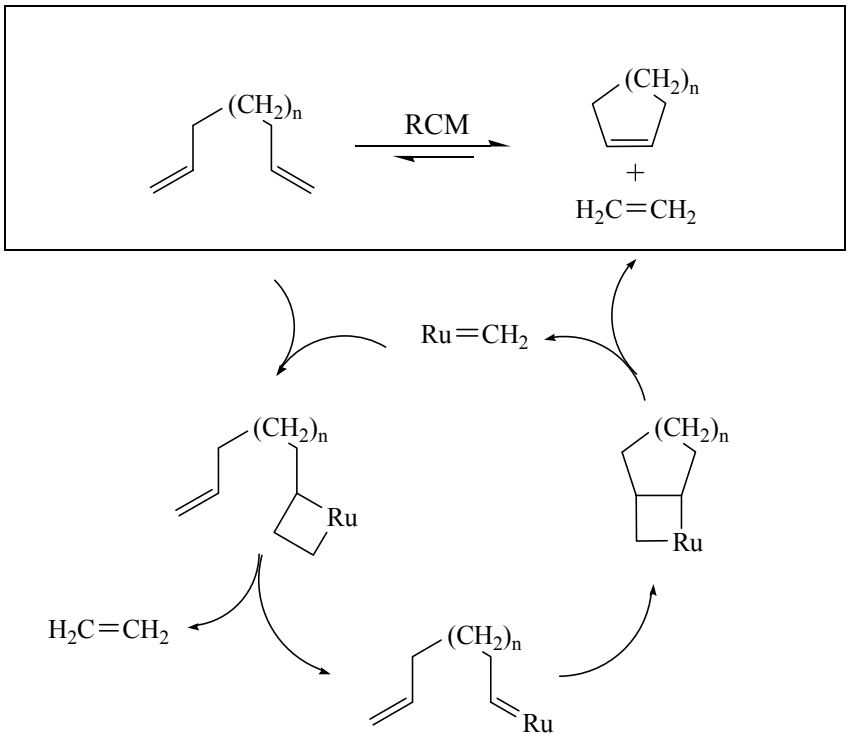

Scheme 26

Although the individual steps leading to the overall transformation are reversible, the equilibrium is often directed by thermodynamic effects.[52] If, as shown in the general cycle, one of the olefin products of the reaction is volatile (ethene), the desired cycloalkene will accumulate in the reaction mixture.

Examination of our model isochromene **86**, shows that it could be possible to assemble this product using the RCM reaction as shown in the retrosynthesis below (**Scheme 27**). The target compound must however be made from the conjugated alkene **112**. Therefore as the first step we needed to make **112** from **87** before attempting the RCM reaction.

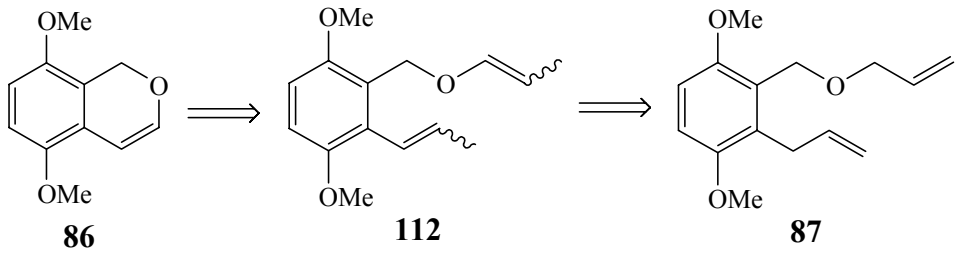

Scheme 27

2.1.1.2 Ruthenium-Mediated Isomerisation

Previously, in our laboratories, various methods for the isomerisation of terminal alkenes to internal alkenes have been attempted.[47] Initially, using methodology demonstrated by de Koning and co-workers[42] selective conversion of the *C*-allylic group was achieved, while preserving the *O*-allylic functionality **114**. This would afford a seven-membered heterocycle starting from the precursor **87**. However **114** failed to undergo the desired RCM to yield **115**. (**Scheme 28)**

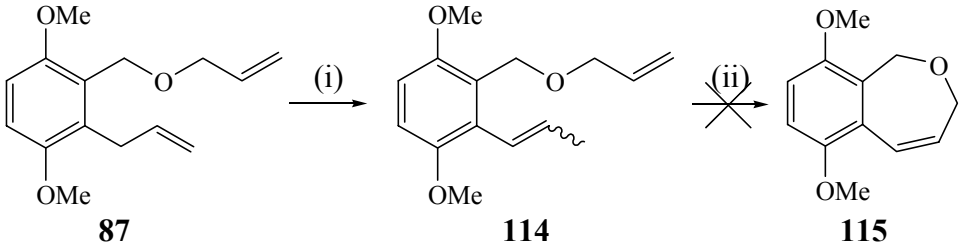

Scheme 28 *Reagents and conditions*: (i) KO^{t}Bu, DMF, rt, 16 h, 81%[47]; (ii) toluene, Grubbs II cat. **113**, 70 °C, 24 h.

Another method attempted, was the synthesis of a vinyl ether, using the catalytic method developed by Ishii and co-workers[56] (**Scheme 29).** Benzyl alcohol **116** was heated in toluene at reflux with vinyl acetate and either sodium acetate or sodium carbonate as the base, in the presence of the iridium catalyst, bis(cyclooctadienyliridium (II) chloride) for

ten hours to afford **117**.[47] This methodology however, proved fruitless for the conversion of **88** to the corresponding vinyl ether **108.**

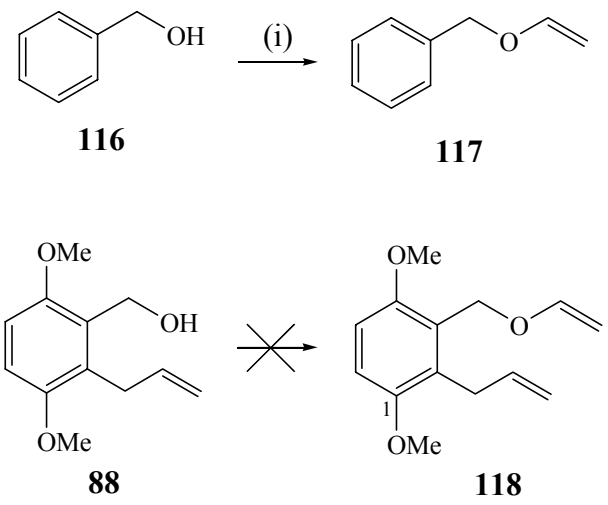

Scheme 29 *Reagents and conditions*: (i) $[Ir(cod)Cl_2]_2$, Na_2CO_3, toluene, 100 °C, 94%.

Thus, in order to afford our desired vinyl ether, a different approach was attempted in this MSc. Ruthenium-mediated catalysis has, in addition to RCM, also gained popularity for the isomerisation of terminal alkenes to internal alkenes. Examples of this type of isomerisation reactions coupled with RCM have recently been published by our group,[57-59] and the ruthenium isomerisation catalyst of choice, compound **119** (**Figure 18**), has been extensively studied[60,61] and found to be particularly robust.

$[RuClH(CO)(PPh_3)_3]$

119

Figure 18

Our diallyl ether **87** was then subjected to a two step/one pot procedure, by adding 0.5 mol% of the isomerisation catalyst **119** to the ether **87** under solvent-free conditions, followed by heating the mixture to 90 °C for 3 hours. The expected isomerised intermediate was not isolated as *in situ* isomerisation followed by the addition of Grubbs

II catalyst **113** has been shown to result in higher yields of the ring closed product in some of our other projects. The Grubbs II catalyst **113**, in dry, degassed toluene was then added, and the resulting solution was cooled down to 70 °C and left stirring for 24 hours (**Scheme 30**).

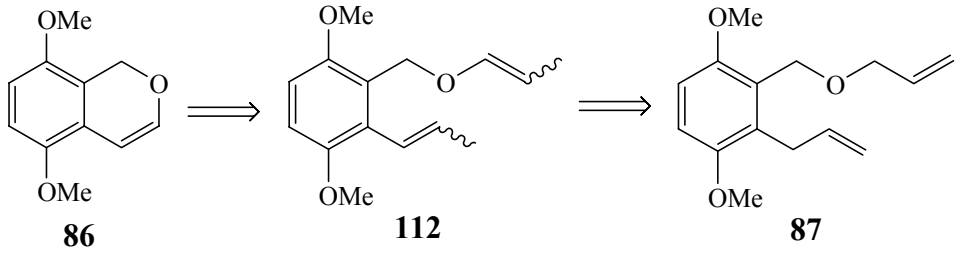

Scheme 30 *Reagents and conditions*: (i) Ru isom. cat., **119**, 90 °C, 3 h; (ii) toluene, Grubbs II cat. **113**, 70 °C, 24 h, overall yield 85%.

The ^{1}H NMR spectrum of the isochromene **86** formed was greatly simplified compared to that of the allyl ether **87**. Most notable was the disappearance of the various multiplets for the *O*- and *C*-allyl substituents. The singlet for the two benzylic protons was shifted downfield from δ 4.57 to δ 5.11. In addition, the proton 4-H gave rise to a signal at δ 6.56, as expected for a vinyl proton. In the ^{13}C NMR spectrum similarly we noted the disappearance of 4 signals depicting the loss of butene. The new signals for C-4 and C-3 were now found at δ145.6 and δ 99.4 respectively, as expected for vinyl ether alkene protons. Additional proof for the formation of the ring closed product was found from high resolution mass spectroscopy which gave a molecular ion of *m/z* 192.0797. The isochromene **86** required a mass of 192.0786.

2.1.2 The Synthesis of Isochroman-4-ol by Hydroboration-Oxidation

Hydroboration reactions are versatile and commonly used reactions in synthetic organic chemistry for the reduction of almost any non-aromatic carbon-carbon multiple bond. In addition, oxidation of the borane-substrate intermediate to yield alcohols has been well documented.[62,63] With the introduction of various chiral alkyl boranes, stereoselective

reduction of multiple bonds are also possible. Since the chiral hydroboration-oxidation reaction on this particular substrate has been previously attempted with no success,[64] we decided to continue with the achiral route producing the racemic product **85** (**Scheme 31**), which we wished to then subject to an alternative, novel method in order to separate the enantiomeric benzylic alcohols.

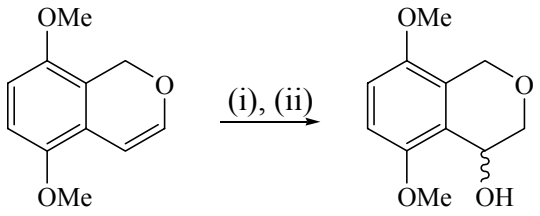

86 **(±)85**

Scheme 31 *Reagents and conditions:* (i) Borane-methyl sulfide complex, THF, 0 °C → rt; 2 h; (ii) NaOH, H_2O_2, 24 h.

The racemic benzylic alcohol **85** was produced as expected by treating a tetrahydrofuran solution of the isochromene **86** with the achiral borane-methyl sulfide complex followed by oxidation of the resulting mixture with aqueous sodium hydroxide and hydrogen peroxide. Spectroscopic analysis confirmed unequivocally that *rac*-**85** was produced. The vinyl proton signal at δ 6.56 in the ^{1}H NMR spectrum was no longer observed. The two benzylic methylene protons were now non-equivalent and appeared as two doublets at δ 4.85 and δ 4.51 with geminal coupling constants of J=16.0 Hz. The splitting patterns for 4-H and 3-H were now more complicated. The signal for 4-H shifted upfield to δ 4.79 from δ 6.56. The signal for 3-H shifted from a doublet at δ 6.04 to two doublet of doublets at δ 4.08 and δ 3.78. In addition the new 4-hydroxyl signal was observed as a broad singlet at δ 2.88. The notable features in the ^{13}C NMR spectrum were the shifts of the signals for C-4 (δ 145.6 to δ 60.3) and C-3 (δ 99.4 to δ 70.3). The IR spectrum showed a prominent broad band at 3447 cm^{-1} for the hydroxyl stretch. The mass spectrum showed a molecular ion at *m/z* 210.0904 consistent with the formula $C_{11}H_{13}O_4$ (calculated 210.0892) thus further confirming the formation of the racemic alcohol **85**.

2.1.3 Enantiomeric Discrimination

We have previously discussed the benefits of transition metal catalysts in our ring closing step, which has become a common tool used by synthetic organic chemists. Another increasingly popular synthetic tool, from another related field of science, which has become increasing useful is biocatalysis.[65] We wished to use this methodology in order to separate the two enantiomeric benzylic alcohols of **85**.

2.1.3.1 Introduction into Biocatalysis

Living cells are capable of carrying out a huge range of enzyme-catalysed chemical transformations, some of which have little or no precedence in synthetic organic chemistry.[66] Enzymes are remarkable catalysts, which are capable, not only of accepting a wide range of substrates, but also of exhibiting high chemo-, regio- and enantioselectivity.[67] It is due to these remarkable catalytic properties that there is an increasing interest in elucidating and exploiting these biological catalysts in organic synthesis. These giant macromolecules, possess a highly complex three dimensional structure arising from the spontaneous folding of a polypeptide chain, which is a linear sequence of amino acid building blocks joined together by amide linkages. It is this complex structure which affords high enantioselectivity in the reactions catalysed. The price and availability of enzymes has also significantly decreased over the past few years, also making them more economically attractive catalysts.

The part of the enzyme's complex tertiary structure, which is responsible for carrying out the chemical reaction, is known as the 'active site'. It is usually a hydrophilic cleft or cavity which contains an array of amino acid side chains which bind to the substrate. Since this active site is chiral, it is naturally only able to bind to one enantiomer of the substrate. This high substrate selectivity is the hallmark of enzyme catalysis.[66] The one application of enzymes that we have chosen to explore is their use in resolving racemic mixtures of alcohols into their optically active components by making use of the enzyme lipase.

2.1.3.2 Transesterification Reactions with the Enzyme Lipase

Lipases are fat-soluble enzymes which play an important role in food digestion. They assist in the breakdown of fats, oils and lipid content in foods by hydrolyzing the ester functional groups. The lipase enzyme can also function in the opposite direction, that is, in the presence of an appropriate acyl donor; it can also acetylate the chiral alcohol. This transfer of functionality is referred to as transesterification. Since enzymes function stereospecifically and we intended to take advantage of this useful property to separate the two enantiomers of our racemic alcohol. The enzyme will acetylate one enantiomer of the alcohol to the corresponding acetate, while leaving the other enantiomer untouched. This will then facilitate the easy separation of the enantiomerically pure products. Deacetylation of the racemically prepared acetate as well will result in hydrolysis of one enantiomer and the other enantiomer unreacted. This thus provides us with an enzymatic method for the resolution of our enantiomers. The racemic acetate **89** was prepared for this purpose.

2.1.3.3 The Synthesis of Isochromen-4-yl Acetate 89

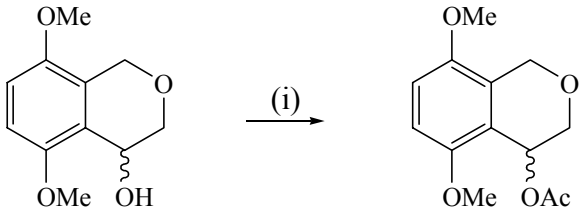

(±)-85 **(±)-89**

Scheme 32 *Reagents and conditions*: (i) Ac_2O, NEt_3, DMAP, THF, 3 h, 70%.

The conversion of the alcohol **(±)-85** to the acetate **(±)-89** was easily achieved in a yield of 70% by reacting a solution of the alcohol **(±)-85** in THF with acetic anhydride and triethylamine and a catalytic amount of 4-dimethylaminopyridine (**Scheme 32**). There was a large shift in the R_f of the product on a silica gel TLC plate as compared to the starting material (0.34 to 0.80 in 50% EtOAc/hexane). Spectroscopic data confirmed the

complete conversion of the alcohol. The most prominent change in the ^{1}H NMR spectrum was the absence of the broad hydroxy signal at δ 2.88 and new singlet, integrating for three protons at δ 2.09 confirming the presence of the methyl group of the acetate group attached. The signal for 4-H was shifted downfield (δ 4.79 to δ 5.93) due to further deshielding. All other signals were in line with expectations. The ^{13}C NMR spectrum showed two new signals. The new ester carbonyl signal was found at δ 170.6 and the new CO*C*H_3 signal appeared at δ 21.2. All the other signals were as expected. The result of the high resolution mass spectrometry gave a molecular ion of *m/z* 252.0999 (Calculated for $C_{13}H_{16}O_5$: *m/z* 252.0998).

With the racemic acetate **(±)-89** in hand we were now in a position for the enzymatic reaction. It was however necessary to determine the most suitable enzyme for the enantioselective conversion, as well as the optimal reaction conditions. This is discussed in the next section.

2.1.3.4 Initial Lipase Screening

There are an enormous amount of commercially available lipases, each one optimal for a specific substrate. They are available as different preparations, for example, in liquid buffers or adsorbed onto solid supports. Each enzyme functions optimally at certain temperature as well as with specific solvent systems and at optimal pH levels. In order to facilitate the testing of various commercially available enzymes and reaction conditions a range of substrates **120-127** with similar structures to our molecule of interest, isochromanol **85** were either purchased or produced in one step (reduction/acetylation) from suitable starting material. They are listed below in **Figure 19**.

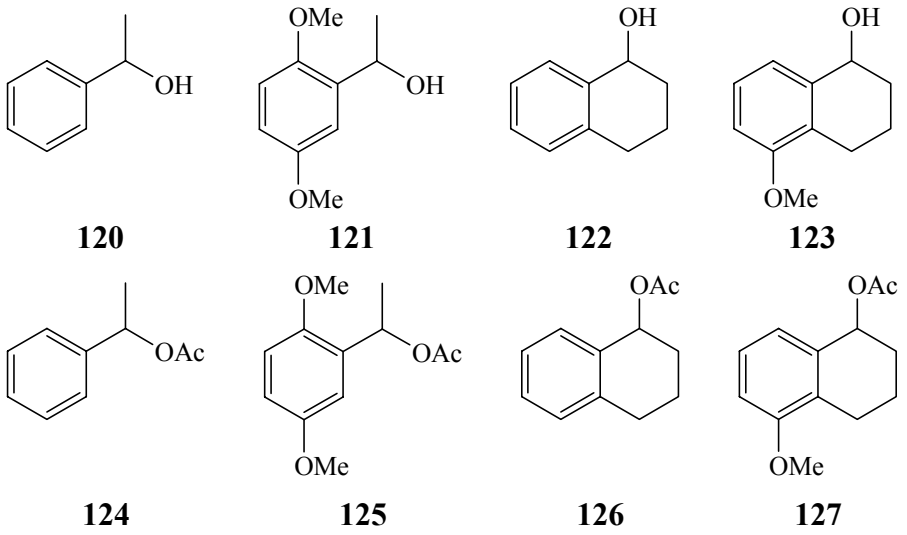

120 **121** **122** **123**

124 **125** **126** **127**

Figure 19

The initial screening involved the testing of a range of forty enzymes which are capable of facilitating the transformation. The five benzylic alcohol substrates (**85** and **120-123**) were subjected to an enzyme assisted acetylation reaction with the acyl donor, vinyl acetate, while the five acetate substrates (**89** and **124-127**) were subjected to an enzyme assisted hydrolysis reaction. This initial screening was done in isopropyl alcohol as the solvent and the buffer system employed was tris (hydroxymethyl)amino methane (Tris), which functioned at pH 8. With all the necessary reagents added, the reaction was allowed to proceed for two hours at 37 °C. due to the small scale of the reaction (mirolitre reactions), the confirmation of conversion was accessed by TLC analysis of the reaction mixture. From this general screening, five positive enzymes that performed well across the range of substrates were then selected. The list of the enzymes utilized in the screening procedure as well as the results obtained are given in Appendix A3.

With the range of possible suitable enzymes narrowed down, it was now possible to assess various reaction conditions. This was done by altering the solvent used. Dioxane, *tert*-butylmethyl ether and toluene were tested for each substrate-enzyme combination. In addition to this, a corresponding reaction set was simultaneously run but with the addition of a detergent, sodium deoxycholate, in order to assess the effect on the enzyme

efficiency. From this run we were able to determine that our substrates functioned best with toluene as the solvent and in the absence of a detergent. The most favorable enzyme that performed well throughout the various reactions was identified as Novozyme 525, a commercial lipase from *Candida antarctica*. The de-acetylation reaction was chosen as the more favourable, less expensive alternative to the acetylation, which required a relatively expensive acyl donor, vinyl acetate. This screening process is summarized in **Figure 20**.

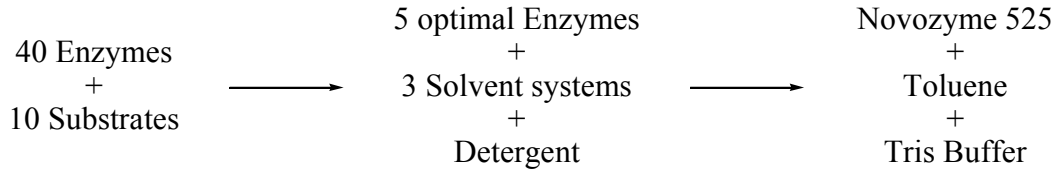

Figure 20

With this enzyme in hand, a few more tests were run at varying temperatures and time intervals. Once again the chosen enzyme functioned well and proved to be resilient at both low and high temperatures (0 °C up to 40 °C).

In the next section we will briefly discuss the proposed mechanism of action of the enzyme, before commencing on the enantioselective reaction of our substrate **(±)-89**.

2.1.3.5 Mechanisms of the Lipase Enzyme

Several members of the family of lipase enzymes contain the amino acid serine **128** (**Figure 21**) in their active sites. It is a polar amino acid, with a hydroxyl side chain. Due to this side chain, the enzyme-substrate interaction probably involves hydrogen bonding.

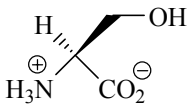

128

Figure 21

The following mechanistic considerations are based on the *Candida antartica* lipase B (CALB), for which numerous molecular modeling studies have been done.[68] The active site in CALB contains the catalytic triad serine-histidine-aspartate, which are common to all serine hydrolyses. As we can see in **Scheme 33**, the serine amino acid of the active site of the enzyme makes use of hydrogen bonding in its interaction with the substrate, forming a tetrahedral intermediate. The reason for the high enantioselectivity of the enzyme towards chiral secondary alcohols is due to the fact that the active site also contains a small cavity called the stereospecificity pocket in which the secondary alcohols have to orientate one substituent during catalysis.[69]

The transesterification then occurs by forming a covalent acyl enzyme and the release of the secondary alcohol. In the presence of water, the reaction will not be reversed and the alcohol will not be re-acetylated. Reaction of the enzyme with the alcohol and vinyl acetate, as the solvent, will form the same covalent acyl enzyme and transfer the acetate group from the acyl donor onto the alcohol. The enantioselectivity is determined by the steric requirements of the stereospecificity pocket.

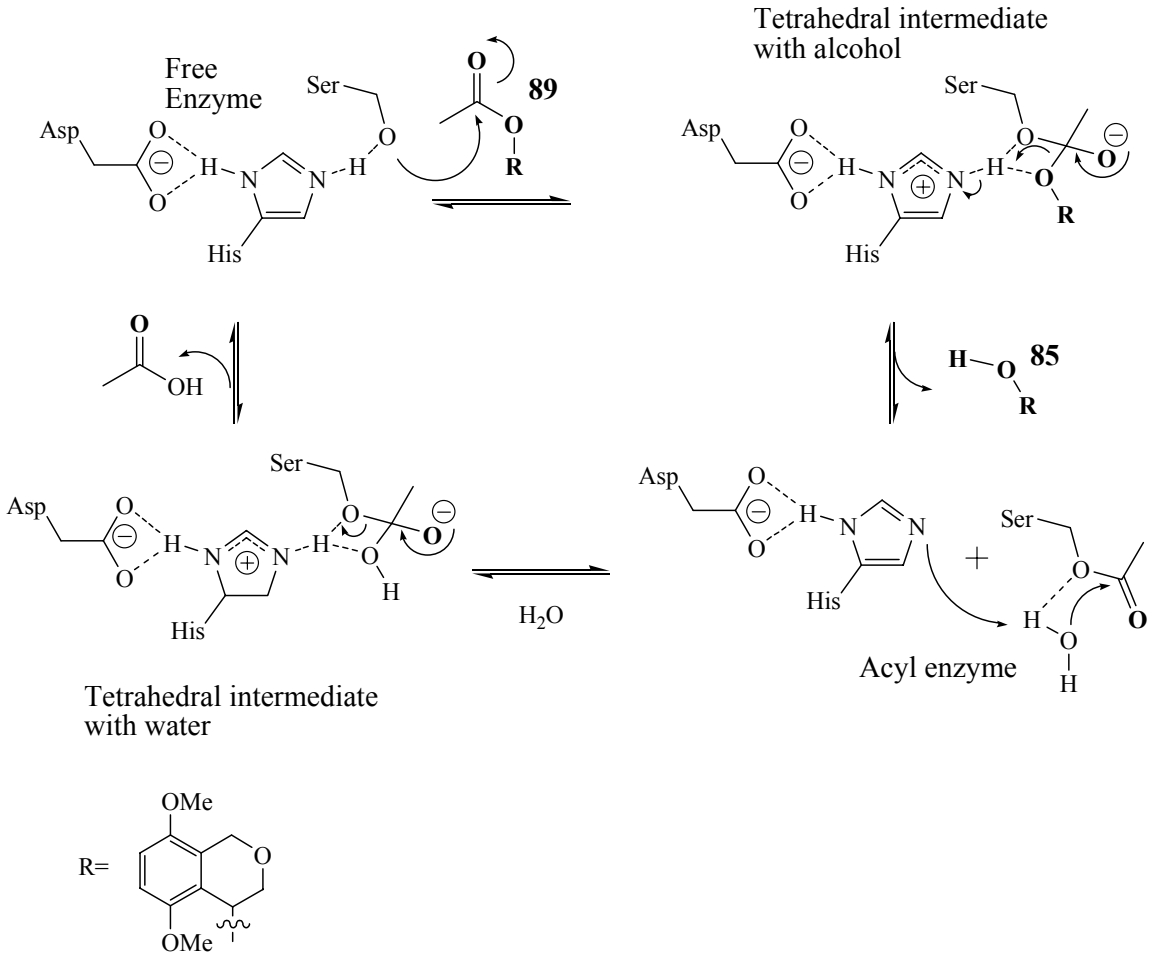

Scheme 33

Before commencing with the enzymatic resolution of the alcohol **(±)-85** and acetate **(±)-89** substrates, we needed to confirm that the enantiomeric ratio of our racemic mixtures was 50:50. This was achieved using a reverse phase high performance liquid chromatography (HPLC) Chiralcel OD column, with hexane and isopropyl alcohol (80:20) as our eluent. As expected, we can see from the HPLC chromatograms of the two substrates, **Figure 22** and **Figure 23** for the isochroman-4-ol **(±)-85**, and the isochromen-4-yl acetate **(±)-89**, respectively, that we have a 1:1 racemic mixture of the two enantiomers of each substrate. Both chromatograms show a common contaminant in both the samples with a retention time of around 4.47.

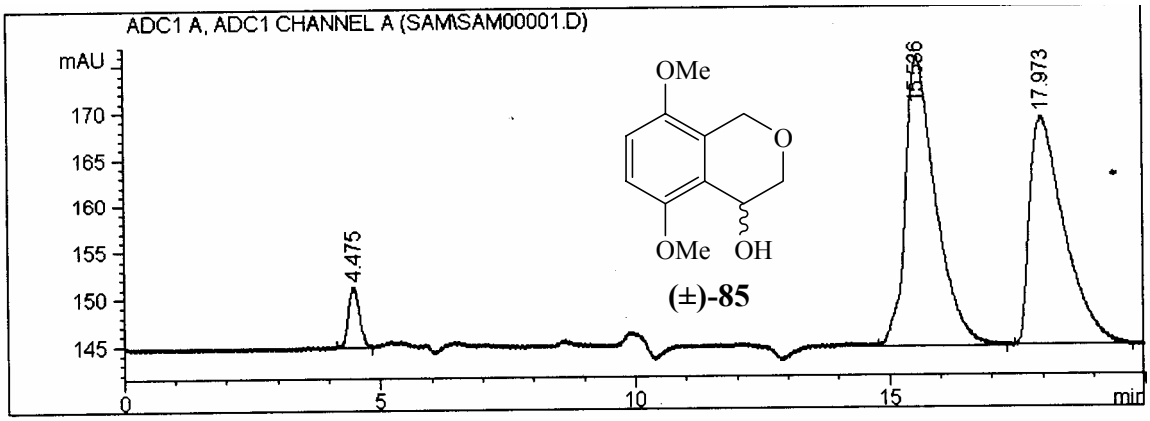

Peak #	RetTime [min]	Type	Width [min]	Area [mAU*s]	Height [mAU]	Area %
1	4.475	BB	0.2295	97.02997	6.33986	3.8238
2	15.536	BB	0.5788	1285.73181	30.73542	50.6681
3	17.973	BB	0.6682	1154.79346	24.32492	45.5081
Totals :				2537.55524	61.40020	

Figure 22

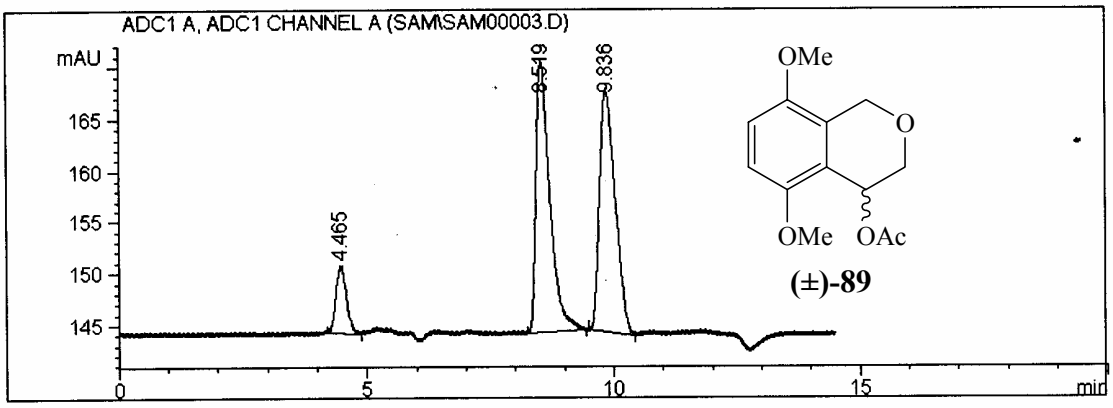

Peak #	RetTime [min]	Type	Width [min]	Area [mAU*s]	Height [mAU]	Area %
1	4.465	BB	0.2265	97.48974	6.46135	8.5713
2	8.519	BB	0.2938	520.67096	26.53168	45.7775
3	9.836	BB	0.3297	519.23322	23.55395	45.6511

Figure 23

2.1.3.6 Resolution of (+)-Isochroman-4-ol and (–)-Isochromen-4-yl Acetate

Our initial approach involved the deacetylation of our racemic acetate **(±)-89**. This was regarded as a simpler option since no acyl donor was required and the commercial enzyme utilised, Novozyme 525, was available in a buffered solution of the lipase enzyme. Any water present would not affect the hydrolysis process. Since there was no readily available information of the liquid preparation of the enzyme, it was also necessary to prepare a buffer solution for the optimum activation and functioning of the enzyme. The buffer solution employed was that of tris (hydroxymethyl)amino methane (Tris HCl) buffer, which maintained the suspension at a pH of 7.5. The acetate was dissolved in a minimal amount of toluene and to this was added the buffer solution, followed by the enzyme suspension. The reaction mixture was stirred for 2 hours at room temperature. Completion of the reaction was confirmed by normal phase HPLC on a C18 column, which showed a 50% conversion of the starting material to what we hoped would be one specific enantiomer of the alcohol. The organic phase was then extracted with EtOAc and dried. The products were analysed using reverse phase HPLC under the same conditions as above in order to determine the enantiomeric ratio. This is shown in **Figure 24**.

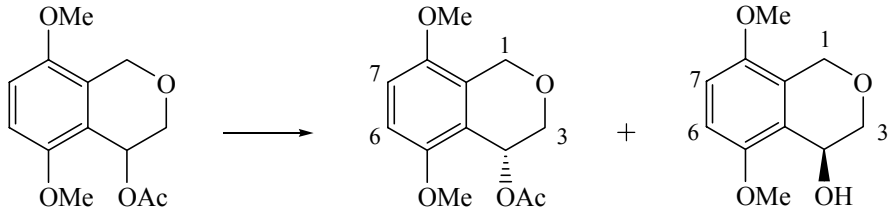

(±)-89

(-)-89
or opposite
enantiomer

(+)-85
or opposite
enantiomer

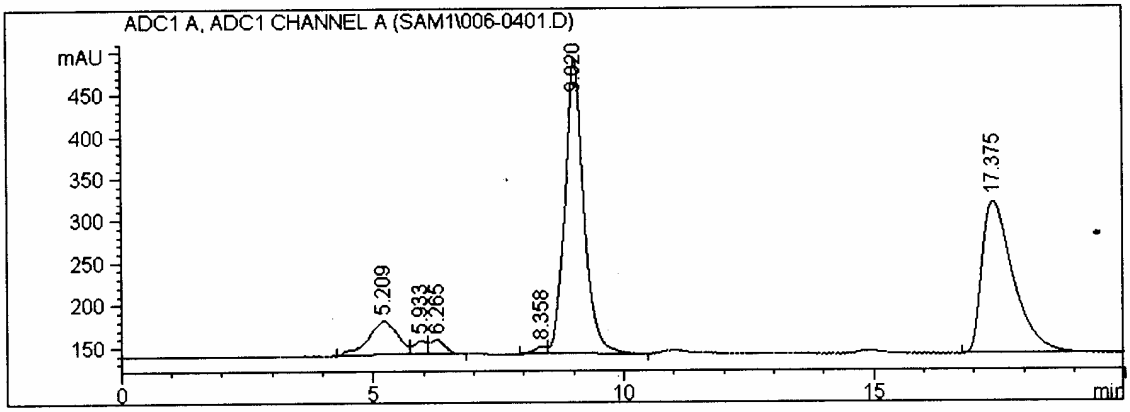

Peak #	RetTime [min]	Type	Width [min]	Area [mAU*s]	Height [mAU]	Area %
1	5.209	BV	0.5320	1663.53625	40.25893	8.5034
2	5.933	VV	0.2441	290.74759	16.05595	1.4862
3	6.265	VV	0.2836	355.23572	16.94279	1.8158
4	8.358	BV	0.2356	165.01167	9.46703	0.8435
5	9.020	VV	0.3797	9235.79883	350.69000	47.2103
6	17.375	BB	0.6502	7852.77539	180.11496	40.1407

Figure 24

On comparison of the reaction mixture chromatogram **Figure 24** with that of the substrate chromatograms **Figure 22** and **23**, we can see that only one enantiomer of the acetate was hydrolysed to what we presumed to be the corresponding chiral benzylic alcohol, while the other enantiomer remained unreacted. The enantiomeric ratio of the alcohol was determined to be greater than 98% from the ratio of the area under the peaks.

The products from the reaction mixture were separated using silica gel column chromatography, to give us the single enantiomers of the acetate **(–)-89** (30%) and the

alcohol **(+)-85** (33%). The ^{1}H and ^{13}C NMR spectra of the enriched enantiomers of **85** and **89** matched that of the racemic counterparts identically. A 1% solution of each compound in chloroform was prepared in order to measure the optical rotation. The unreacted isochromen-4-yl acetate **89**, gave an optical rotation of $[\alpha]_D$= –93.0 and the enantioselectively hydrolysed isochroman-4-ol **85**, showed an optical rotation of $[\alpha]_D$= +28.0.

The (+)-alcohol **(+)-85** was then chemically acetylated using the same procedure as that subjected to the racemic alcohol. The product **(+)-89** obtained in 81% yield was similarly purified and analysed to confirm the acetylation. This product was then also analysed for optical rotation and found to give an optical rotation of $[\alpha]_D$= +72.0.(c= 1 in $CHCl_3$). While the direction of rotation of light was in line with expectations, the value was not. This may be due to several contributing factors of concentration, temperature etc which greatly affect the sensitivity of the polarimeter.

Similarly the enriched (–)-acetate **(–)-89** was subjected to a deacetylation, using potassium carbonate in methanol. The reaction was established to be complete by TLC. It was purified and analysed spectroscopically to confirm the conversion to **(–)-85** in a yield of 82%. Analysis on the polarimeter of a 1% solution in $CHCl_3$ gave a reading of $[\alpha]_D$= –41.0. Once again we have obtained a correct value for the direction of rotation of light, i.e. the opposite to the other optical isomer, however the value is different probably due to the same reasons outlined above.

CHAPTER 3: CONCLUSIONS AND FUTURE WORK: PART A

3.1 Enantiomeric Resolution of Isochroman-4-ol 85

The main aim of this project was the synthesis of the racemic benzylic alcohol **85**, and its resolution into its stereoisomers with the use of biocatalysis. The racemic alcohol was synthesised over seven steps from the commercially available 1,5-dihydroxybenzoic acid **106** (**Scheme 34**). The synthesis commenced with the diallylation of starting material **106** to produce **107** in a 92% yield. This product was the subjected to thermal Claisen rearrangement to produce the hydroquinone **108** in 86%. Methylation to protect the phenols then resulted in **109** in 82%. This was followed by lithium aluminium hydride reduction of the ester to yield the benzyl alcohol **88** in 93% yield. The benzyl alcohol was then allylated to the allyl ether **87** in a 91% yield.

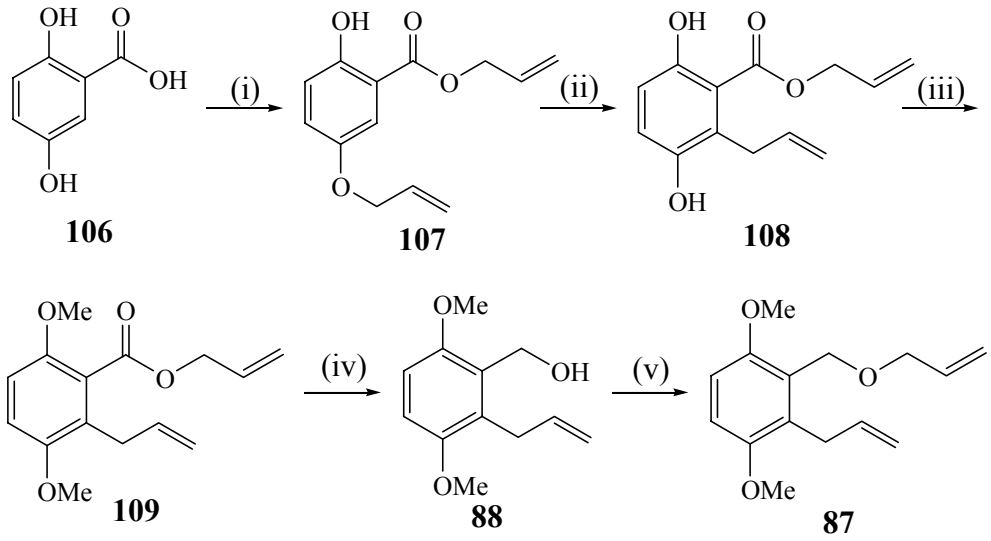

Scheme 34 *Reagents and conditions*: (i) K_2CO_3, allyl bromide, acetone, Δ, 24 h, 92%; (ii) 170 °C, 18 h, 86%; (iii) K_2CO_3, Me_2SO_4, acetone reflux, 24 h, 82%; (iv) $LiAlH_4$, THF, 40 °C, 2 h, 93%; (v) allyl bromide, NaH, THF, reflux, 24 h, 91%.

With the allyl ether in hand, the formation of the isochromene was accomplished over two steps with the ruthenium mediated isomerisation and ring closing metathesis (RCM)

reaction in a one pot/two step synthesis. The overall yield for this novel step was 85% (**Scheme 35**). Therefore the overall yield for this seven step procedure is an excellent 47%. With the conditions for this transformation optimised, it can now be extended to the ring closing of other analogous substrates for example for the formation of C-1 substituted isochromenes e.g. from **129** to **130** (**Scheme 36**).

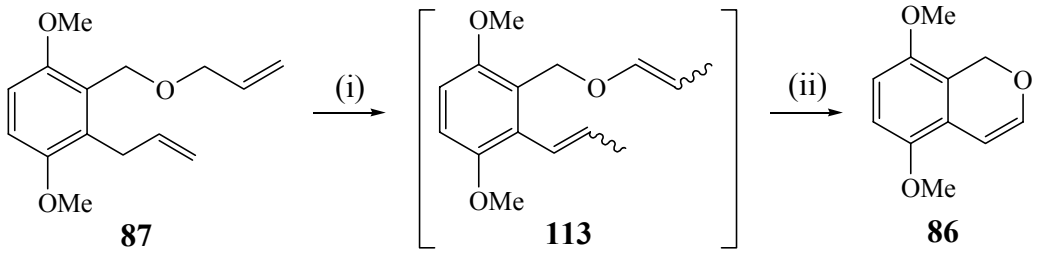

87 **113** **86**

Scheme 35 *Reagents and conditions*: (i) Ru isom. cat., **118**, 90 °C, 3 h; (ii) toluene, Grubbs II cat. **112**, 70 °C, 24 h, overall yield 85%.

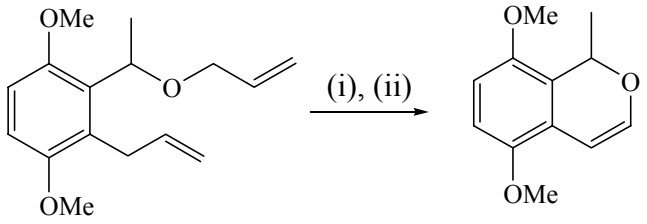

129 **130**

Scheme 36

The isochromene **86** was then converted to our desired isochromanol **85** using the hydroboration reaction followed by oxidation. The achiral borane reagent used, a borane-methyl sulfide complex, gave us a 1:1 racemic mixture of the alcohol **85** in a 84% yield. This alcohol was then converted to the acetate **89** under standard procedures to obtain **89** in a yield of 70% (**Scheme 37**).

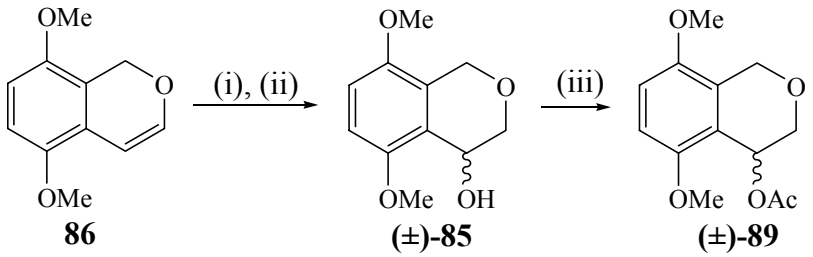

86 **(±)-85** **(±)-89**

Scheme 37 *Reagents and conditions*: (i) Borane-methyl sulfide, THF, 0 °C→rt, 2 h; (ii) NaOH, H_2O_2, 24 h, 84%; (iii) Ac_2O, NEt_3, DMAP, THF, 3 h, 70%.

The lipase enzyme, Novozyme 525 was then used to hydrolyse the (+)-enantiomer of our acetate **(±)-89** producing the corresponding (+)-alcohol **(+)-85**, while leaving the (–)-acetate **(–)-89** unreacted (**Scheme 38**).

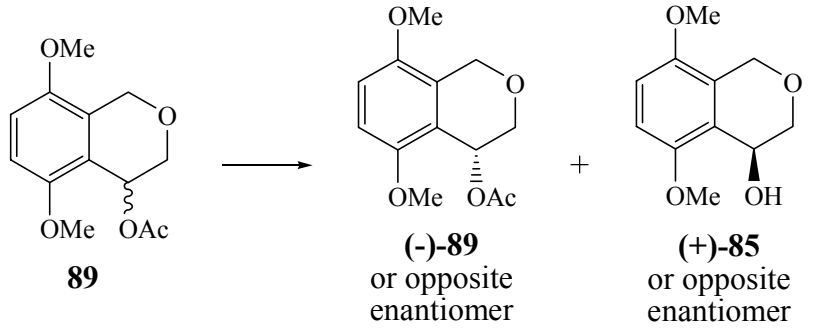

89 **(-)-89** or opposite enantiomer **(+)-85** or opposite enantiomer

Scheme 38 *Reagents and conditions*: (i) toluene, buffer soln (pH 7.5), lipase enzyme, 2 h, 33% (+)-**85**, 30% unreacted (–)-**89**.

We were then able to chemical convert our enantiomerically pure (+)-isochromanol **(+)-85** to the corresponding (+)-acetate **(+)-89** in a yield of 81%; as well as the (–)-acetate **(–)-89** to the (–)-alcohol **(–)-85** in a yield of 82% while retaining the stereochemistry.

The next crucial step will be the derivatisation of the optically active alcohols **(+)-** and **(–)-85** in order to obtain crystal structures of the molecules and thus assign their absolute configuration according to the Cahn-Ingold-Prelog rules. Thereafter we will try to

introduce substituents at the C-1 and C-3 positions of the isochromanol nucleus (**Figure 25**) using arene-tricarbonyl complexes as outlined below.

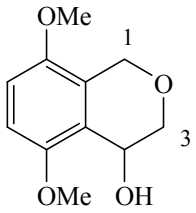

85

Figure 25

3.2 The Chemistry of Arene-Tricarbonylchromium Complexes

It has been found that that the $Cr(CO)_3$ moiety, when attached to an arene ligand, is able to facilitate transformations that the free arene ligand is incapable of.[70] Some of these novel properties are summarised in **Figure 26.**

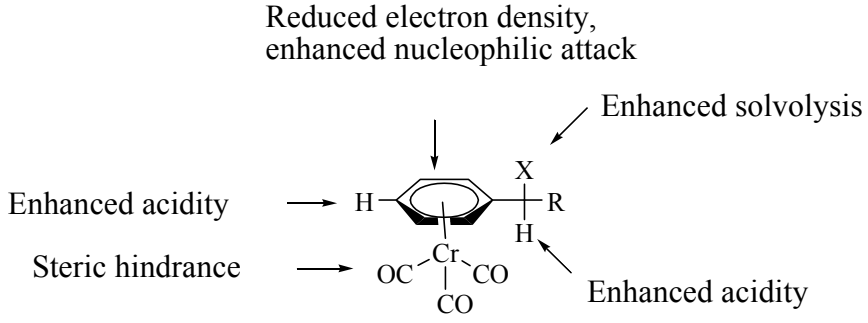

Figure 26

The arene-$Cr(CO)_3$ complexed carbanions are stabilized at the benzylic position,[71] and regio- and stereo-selective products can be obtained *via* the benzylic carbanions depending on the orientation of the $Cr(CO)_3$ to the arene.[72]

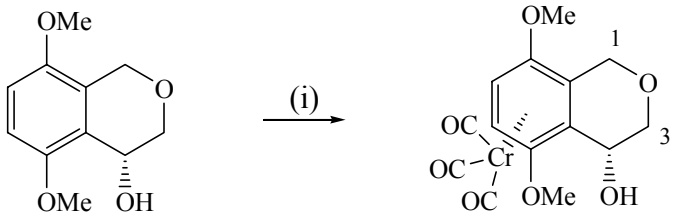

85 **131**

Scheme 39 *Reagents and conditions*: (i) $[Cr(CO)_6]$, *n*-Bu_2O/heptane/THF (1:1:0.1), Argon, 120 °C, 36 h.[73]

Moreover on complexing to the arene ligand in our case the isochromanol **85**, the $Cr(CO)_3$ should complex on the same side as the enantiomerically pure benzylic alcohol function thus forming the single diastereomer **131** (**Scheme 39**). Due to the steric hindrance of the metal complex one face of the molecule is shielded and therefore substituents can now be added to the C-1 and C-3 positions in a stereoselective manner.

For the addition of substituents to both these positions we envisage oxidation of the secondary alcohol **131** to the ketone **132**. The chiral information is now stored as a chiral planar complex. Then by using a suitable base to abstract the acidic protons from both the desired C-1 and C-3 positions, we should be able to access these positions from the opposite face of the chromium tricarbonyl tripod to produce **133** followed by **134**. Furthermore, reduction of the ketone should also proceed in a similar stereoselective manner to finally give us, after decomplexation of the $Cr(CO)_3$ moiety, the compound **135**, with stereo defined substituents in the C-1, C-3 and C-4 positions. This strategy is depicted in **Scheme 40**.

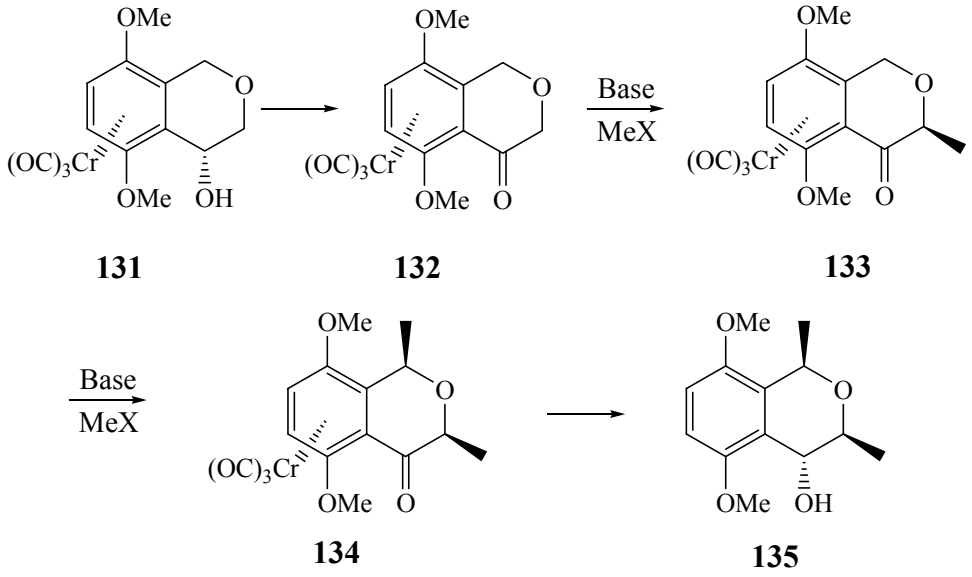
OMe
O
(OC)3Cr
OMe
OH
131
OMe
O
(OC)3Cr
OMe
O
132
Base
MeX
OMe
O
(OC)3Cr
OMe
O
133
Base
MeX
OMe
O
(OC)3Cr
OMe
O
134
OMe
O
OMe
OH
135

Scheme 40

CHAPTER 4: RESULTS AND DISCUSSION: PART B

At this point we decided to start with the other part of the MSc. i.e. the construction of the biaryl naphthalene portion of the cardinalin 3 **23** nucleus (**Figure 27**).

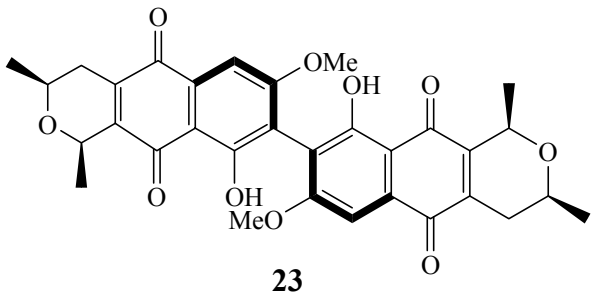

23

Figure 27

4.1 Synthesis of the Biaryl Axis

Biaryls are available through the coupling of the aryl halide with an excess of copper at elevated temperatures. This classic transition metal mediated dimerisation is well known as the Ullmann reaction.[74]

4.1.1 The Ullmann Reaction

There is a universal acceptance that the formation of biaryl axis in the Ullmann reaction involves the interaction of an aryl copper species with an aryl halide, although the mode of coupling is controversial.[75] The mechanism may involve the formation of σ or π complexes with the halogen atom, polarizing the bond. The metal may also undergo oxidation and subsequent reduction to afford the coupled product through either one electron transfers or electron pair processes.[76]

While the actual mechanism of the copper mediated homo-coupling of aryl halides has not been entirely elucidated, it has been proposed that the Ullmann type reactions

proceeds through a cycle, and in one proposed mechanism, a copper(I) compound **137** formed from the lithiated species **136**, forms the active species which is then postulated to undergo oxidative addition with the second equivalent of the aryl halide **138** to form a Cu(III) species **139**. This is followed by reductive elimination and the formation of the aryl-aryl carbon bond in compound **103**.[77] This cycle is depicted in **Scheme 41** with our molecule of interest **138**, and the aryl cuprate **137**, as our Cu(I) species.

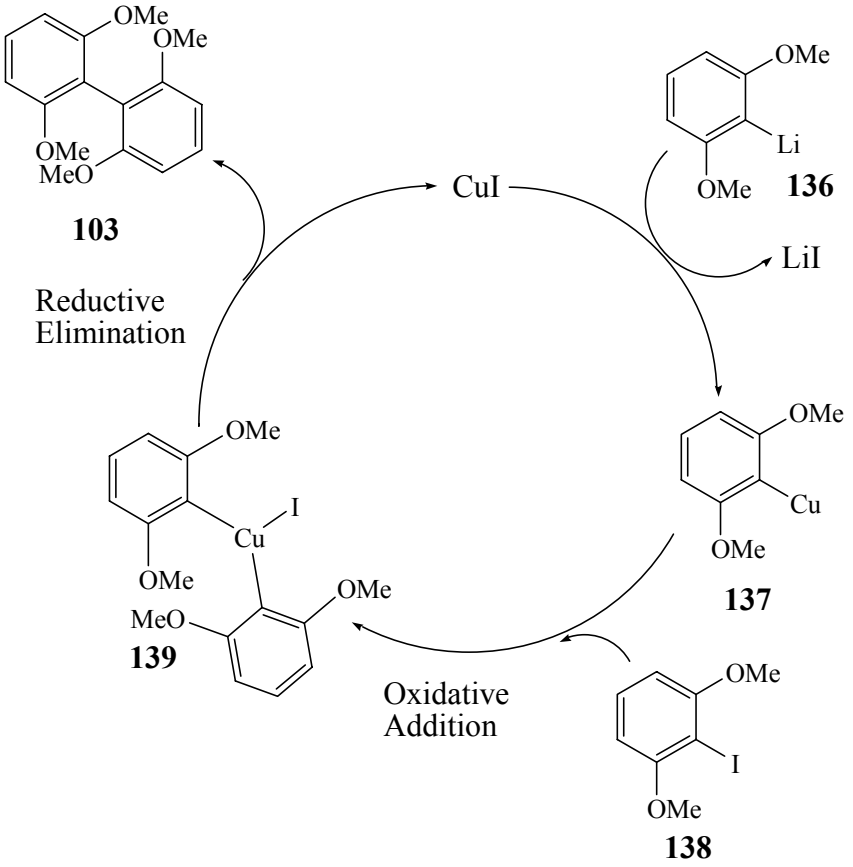

Scheme 41

There are various known modifications of the Ullmann reaction. The approach used in this project was the coupling of a preformed aryl copper intermediate with an aryl halide.[78] Our aryl halide of choice was iodo-1,3-dimethoxybenzene **138**. The ease of halogen displacement from an aromatic ring is generally I>Br>Cl>F.[79] This is opposite to the trend observed in uncatalysed aromatic nucleophilic substitution reactions.[80]

Our synthesis of the one partner of the Ullmann reaction, 2-iodo-1,3-dimethoxybenzene, **138**, began with the lithiation of 1,3-dimethoxybenzene **102** at 0 °C, giving a milky white solution. This was followed by the addition of a solution of iodine in tetrahydrofuran. The completion of the reaction was clearly visible by the appearance of the darker halogen colour, once all the aryl lithium intermediate **136** had reacted. The product was extracted from the reaction mixture and recrystallised from a dichloromethane-ethanol mixture to yield 93% of the desired aryl halide **138** (**Scheme 42**).

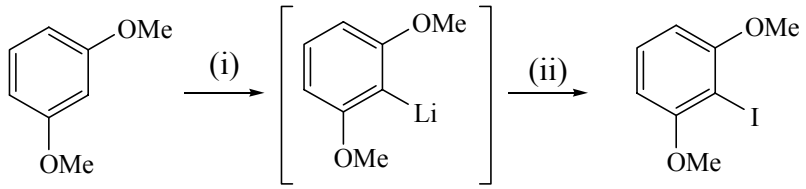

102 **136** **138**

Scheme 42 *Reagents and conditions*: (i) *n*-BuLi, THF, 0 °C, 1 h; (ii) I_2, THF, rt, 1h, 93%.

Spectroscopic data unequivocally confirmed the identity of the molecule **138**. The ^{1}H NMR spectrum was highly simplified due to the C_2 axis of symmetry of the molecule. The aromatic region contained two signals, a triplet integrating for one proton, 5-H, and a doublet integrating for the two equivalent protons, 4-H and 6-H. Both signals had coupling constants of J=8.3 Hz, indicative of *ortho* coupling. The absence of a singlet in the aromatic region for 2-H confirmed that substitution of the proton with our halide had indeed taken place. The other signal in the spectrum was a singlet at δ 3.89, integrating for six protons, assigned to the methoxy groups. There were only five signals in the ^{13}C NMR spectrum due to the symmetry of the molecule. All the signals were in line with expectations. The aromatic CO signals were further downfield at δ 158.4, followed by C-5 and ArC-I and finally C-4 and C-6. The signal for the methoxy carbons were found at δ 56.1. Strongest confirmation for the aromatic iodide compound **138** was received from the high resolution mass spectrum. The molecular ion was found at *m/z* 263.9654, and the molecule $C_8H_9IO_2$ required M^+ 263.9647.

The formation of the aryl copper intermediate **137** similarly began with the lithiation of 1,3-dimethoxybenzene **102** at 0 °C. This was followed by the addition of copper(I) iodide to facilitate the transmetallation at room temperature. This intermediate **137** was not isolated and characterized. The iodated aryl compound **138**, dissolved in pyridine, was then added and the resultant mixture was heated at reflux for 72 h. It has previously been found that the addition of potential ligands for the copper(I) atom, like pyridine, was found to enhance the rate of halogen exchange.[81] This may play a role in the ease of displacement of the halogen from the aryl halide by the copper compound in the oxidative addition step. After an acid workup, the extracted crude material was recrystallised from a dichloromethane-ethanol mixture to yield the desired 2,2′,6,6′-tetramethoxy-1,1′-biphenyl **103**, (**Scheme 43**) in 93% yield. The Ullmann reaction has been found to proceed faster with aryl halides that are substituted in the *ortho* position with groups that contain lone pairs of electrons, regardless of whether they are electron donating or electron withdrawing.[82]

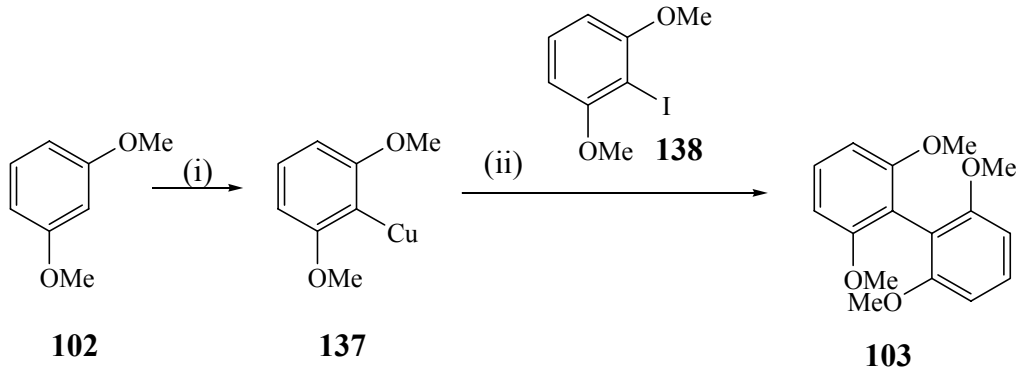

Scheme 43 *Reagents and conditions*: (i) *n*-BuLi, CuI, 0 °C, 3 h; (ii) **138**, pyridine, reflux, 72 h, 93%.

The ^{1}H NMR spectrum as well as the ^{13}C NMR spectrum, while giving all the signals as expected, was not very useful in confirming the synthesis of the biaryl axis. This was due to the fact that once again we have formed a symmetrical molecule, with two C_2 axis of symmetry, which resulted in minimal signals in both spectra. Moreover the aromatic ring of **103** has the same substitution pattern as the iodated precursor **138** therefore giving

similar carbon and hydrogen signals, with slight shifts in the δ values. Confirmation of the formation of the dimer therefore came from the high resolution mass spectrum, which showed a molecular ion of *m/*z 274.1198. ($C_{16}H_{18}O_4$ requires M^+ 274.1205).

Another popular alternative for the homocoupling of aryls is through the use of palladium catalysis in the Suzuki coupling of the arylboronic acids with aryl halides.[83] Palladium salts are however more expensive than copper salts and require the use of various sophisticated ligands such as phosphines, and have a higher toxicity. Although there have been numerous advances in this protocol, some substrates still give a poorer yield when compared to the Ullmann dimerisation.[84] Although in some cases steric hindrance does inhibit Ullmann coupling, the effect is more pronounced in Suzuki couplings.[85] The Ullmann reaction has therefore remained the reaction of choice for large scale syntheses.[86] This alternative was also investigated and is discussed in the next section.

4.1.2 The Suzuki Coupling Reaction

In order to explore both alternatives of the biaryl coupling reactions, the boronic acid of 1,3-dimethoxybenzene was prepared by once again lithiating the substrate, 1,3-dimethoxybenzene **102**, at the 2 position and then reacting this intermediate with trimethyl borate. The new borate formed was then acidified in order to form the desired boronic acid, **139**. (**Scheme 44**)

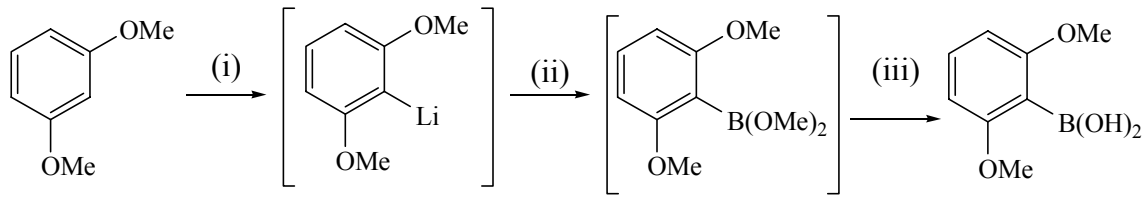

102 **139**

Scheme 44 *Reagents and conditions*: (i) *n*-BuLi, THF, 0 °C, 1 h; (ii) $B(OMe)_3$, 0 °C, 18 h; (iii) HCl.

Once again the number of protons in the ^{1}H NMR spectrum are halved due to the C_2 axis of symmetry of **139**. The ^{1}H NMR spectrum of the boronic acid closely resembled that of the previous halide as well as the biphenyl, but with an additional singlet at δ 7.22 integrating for the two new protons of the boronic acid group. The ^{13}C NMR spectrum also closely resembled the previously synthesized iodo complex **138**, with one key difference; the C-2 carbon was now attached to an electropositive boron atom and was no longer deshielded to a large extent. This signal in the ^{13}C NMR spectrum shifted upfield to δ 55.8, as opposed to δ 112.6 for the C-2 attached to iodine in **138**. The result of the high resolution mass spectrometry gave a molecular ion of *m/z* 182.0761 (Calculated for $C_8H_{11}BO_4$: *m/z* 182.0750). For the Suzuki coupling reaction, the aryl halide used was once again the iodide **138**, simply because it was readily available to us.

The Suzuki coupling reaction proceeds through a catalytic cycle in which a carbon-carbon bond is formed between the carbon of **139** bearing the boronic acid and the carbon of **138** bearing the halide. The reaction makes use of a palladium catalyst, in this case, tetrakis(triphenylphosphine)palladium(0) [$Pd(PPh_3)_4$] **140** to effect the transformation. In this mechanism, the boronic acid **139** needs to be activated with a base to form **143**. This activation enhances the polarisation of the organic ligand, to facilitate the transmetallation. The catalytic cycle is depicted in **Scheme 45**.[87] The reaction begins by the oxidation of the Pd(0) catalyst **140** with the aryl halide **138** to give a Pd(II) intermediate **141**. This Pd(II) complex then undergoes a transmetallation with the base-activated boronic acid, expelling the aryl group onto the Pd to form **144**. The base activation of the boronic acid adds a nucleophile into the low lying orbitals of the boron, hence forming a borate **143**. Reductive elimination follows to give the coupled product **103** with a new carbon-carbon bond as the biaryl axis.

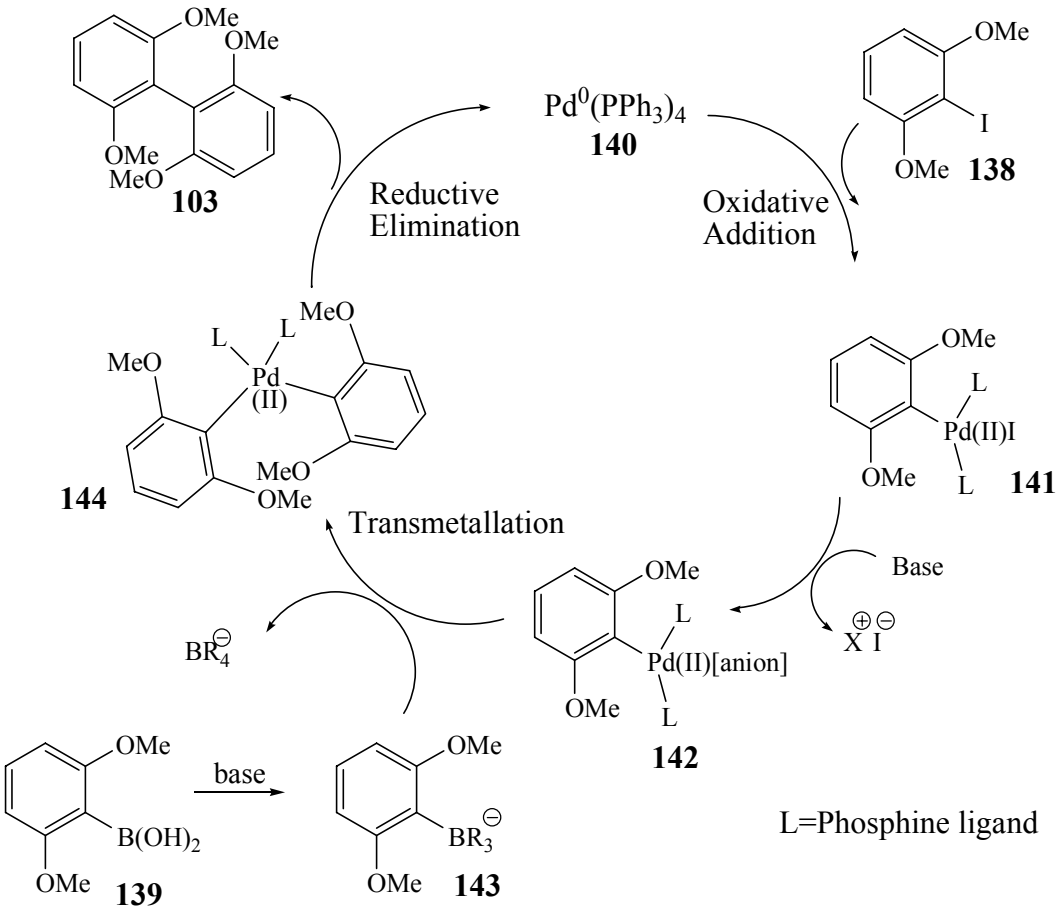

Scheme 45

In the formation of our biaryl axis, using $Pd(PPh_3)_4$ as our catalyst and aqueous sodium carbonate as our base, we were able to obtain our dimer **103** in a yield of 54% from the coupling of **138** and **139**. This was significantly lower than that of the previous procedure and therefore not a viable alternative for the start of our linear synthesis. Falck and co-workers[84] were able to improve this yield to 75% through the homocoupling of the boronic acid using Ag_2O and catalytic $CrCl_2$ in THF under mild conditions (65 °C for 10-12 h). This procedure too would thus fail to compete with the classic Ullmann approach.

4.2 The Synthesis of the Dicarbaldehyde 104

The next step in our synthesis was the formylation of our biphenyl precursor **103**. The classic formylation reaction published by Vilsmeier and Haack in 1927[88] makes use of the salt **147**, formed from formamides and acid chlorides to formylate aromatic compounds, the most common being dimethylformamide (DMF) **145** and phosphoryl chloride ($POCl_3$) **146**. The salt **147** reacts with the substrate in an electrophilic substitution reaction yielding an iminium salt **148**, which is then hydrolysed to the aldehyde **104** (**Scheme 46**).

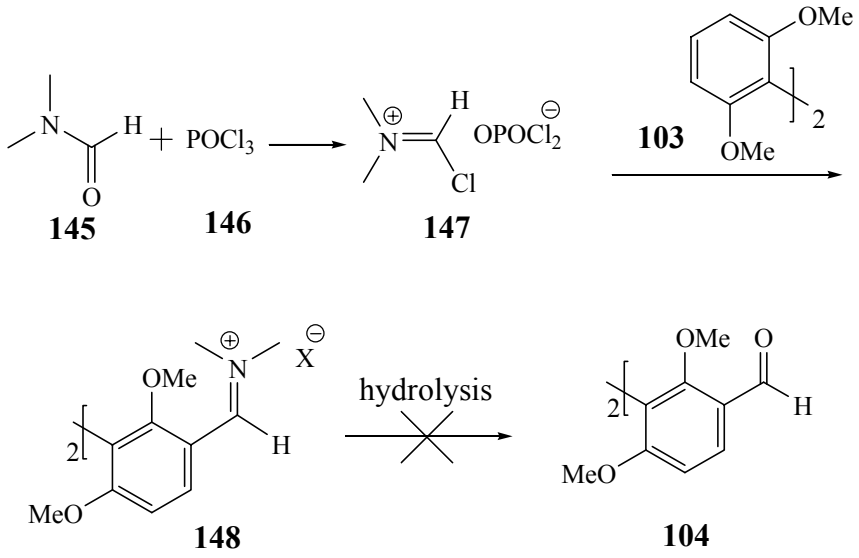

Scheme 46

This classic reaction however failed to yield our desired dicarbaldehyde **104**, even after refluxing for more than 9 days. The phosphoryl chloride **146** was substituted by trifluoromethanesulphonic anhydride, in the hope of forming a more reactive iminium salt for our less activated aromatic compound,[89] but still with no success

We then attempted a variant of the Vilsmeier-Haack reaction, the Rieche formylation, first described by Gross *et. al*[90] which involves the titanium-mediated formylation of sterically hindered aromatics. The reaction makes use of dichloromethyl methyl ether in

the presence of titanium(IV) chloride. The reaction could take place through the following proposed mechanism shown in **Scheme 47**.[91] The substitution takes place at the *ortho* position to form our desired **104**. The regioselectivity of the reaction can be explained in terms of the coordination of the titanium atoms with the oxygen atoms of the methoxy groups forming the intermediate **149** which results in **150**. This coordination not only favours the desired regioselectivity, but also increases the electrophilicity of the dichloromethyl methyl ether and thus the rate of the reaction.[91]

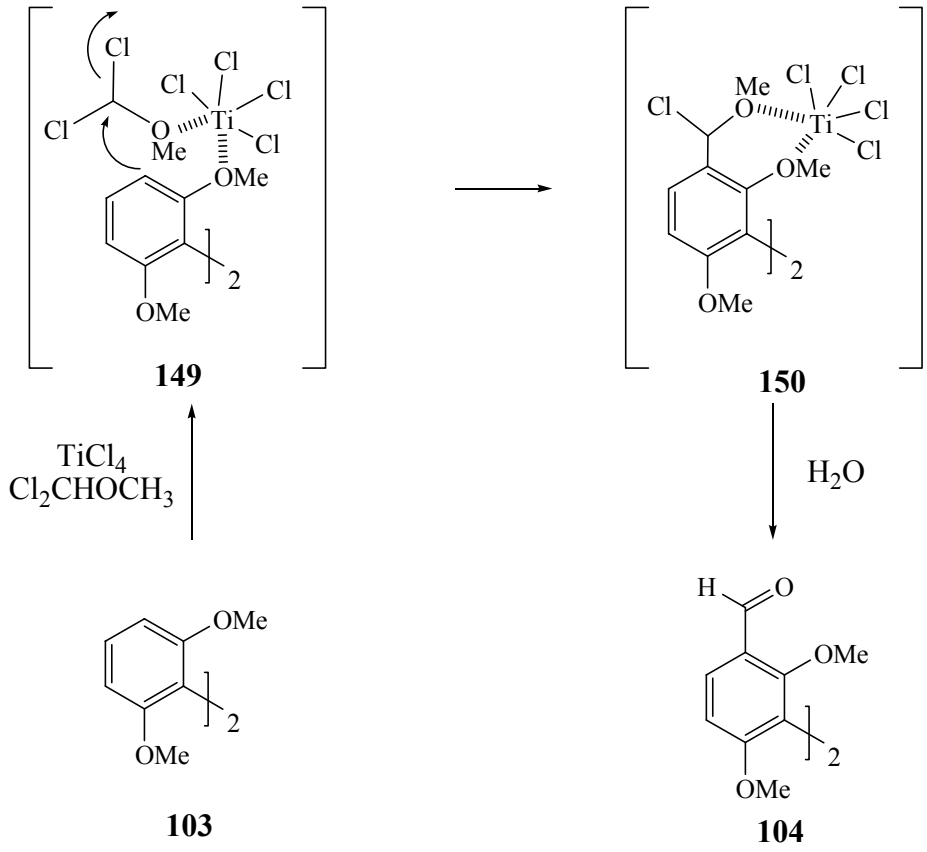

Scheme 47

For our desired diformylation, four equivalents of $TiCl_4$ were added to a solution of our tetramethoxy biphenyl **103** in dry dichloromethane. The clear solution immediately changed to a bright orange colour. The reaction mixture was then cooled to −78 °C and

2.8 equivalents of the dichloromethyl methyl ether was added. The solution then darkened to brown. After a reaction time of 1 h, the reaction mixture was poured over ice and acidified with aqueous HCl to produce a bright pink organic phase. The reaction mixture was extracted with organic solvent and the residue was purified by silica column chromatography to produce our desired dicarbaldehyde **104**, in an excellent yield of 95% (**Figure 28**).

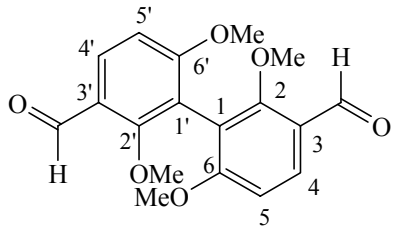

104

Figure 28

Spectroscopic analysis of the compound in hand confirmed that we had indeed accomplished the formylation reaction at both the desired *ortho* positions. The ^{1}H NMR spectrum had a new signal at δ 10.17 for the two equivalent aldehyde groups. The aromatic region now changed from a doublet integrating for four protons and a triplet integrating for two protons to two doublets integrating for two protons each. Both the signals exhibited coupling constants of *J*=8.8 Hz, indicative of an *ortho* relationship. The signals for the methoxy groups were found at δ 3.76 and δ 3.52. The number of signals were again an indication of the two C_2 symmetries of the molecule. The new signals for the aldehyde groups were found in the ^{13}C NMR spectrum at δ 188.8. The signals for C-2 and C-6 were now found at δ 163.5 and δ 162.7. Similarly the signals for C-3 and C-5 were also separated, appearing at δ 123.1 and δ 107.1. The signals for the equivalent methoxy substituents were found at δ 63.0 and δ 56.1. The formula $C_{18}H_{18}O_6$ required a molecular ion of *m/z* 330.1103 and the parent ion on our high resolution mass spectrum was found at *m/z* 330.1093.

The 2,2',6,6'-tetramethoxy[1,1′-biphenyl]-3,3′-dicarbaldehyde **104** was recrystallised from a dichloromethane-ethanol mixture and the white crystals afforded (mp. = 151-155 °C) were subjected to single crystal X-ray diffraction analysis. The information obtained is summarised in Appendix A4. From our structure we can clearly see the two C_2 axis of symmetry of our molecule. Due to the steric effect of the tetrasubstitution of the methoxy groups, the two benzene rings are orientated perpendicular to each other. Also the methyls of the methoxy groups *para* to the formyl groups are planar with respect to the ring, whereas with the substituents *ortho* to the aldehydes, the methyl group of the methoxy, lies out of this plane as shown in **Figure 29**.

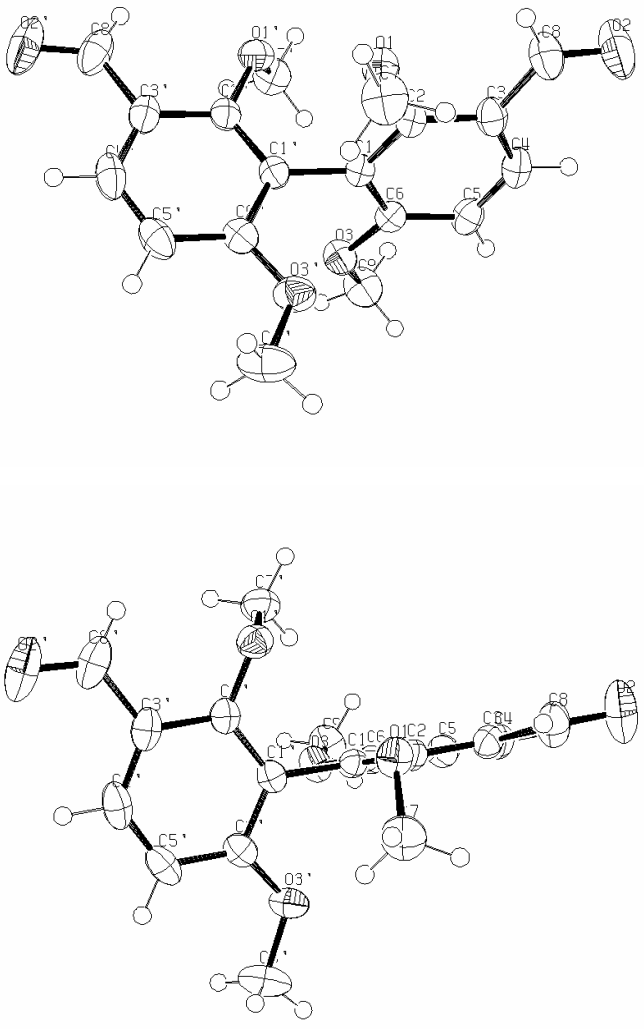

Figure 29

With our diformylated biphenyl **104** in hand we are now able to continue with our planned bi-directional synthesis as per the methodology developed for the synthesis of the naturally occurring monomer, ventiloquinone L.[48]

4.3 The Synthesis of the Bis-acetoxynaphthalenecarboxylic Acid Ethyl Ester 105

The synthesis of the dimer of the acetoxynaphthalenecarboxylic acid ethyl ester **105**, was achieved through the Stobbe condensation followed by a Friedel-Crafts acylative cyclisation of **104** (**Scheme 48**).

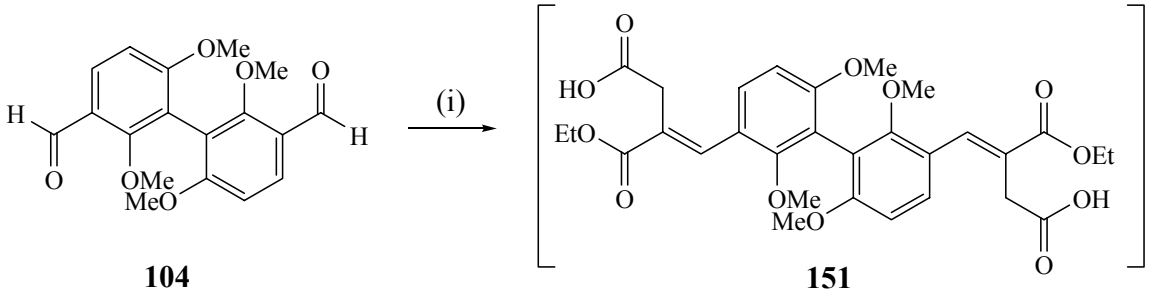

104 **151**

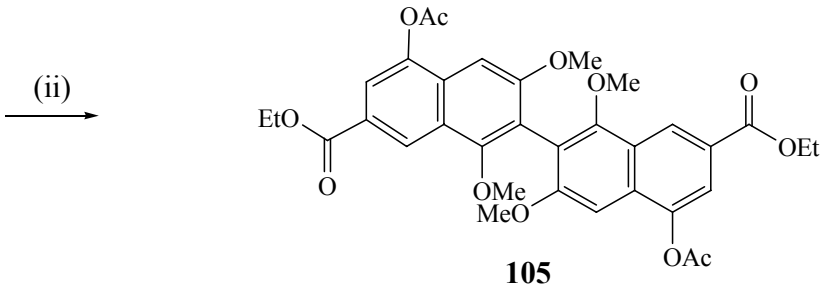

105

Scheme 48 *Reagents and conditions*: (i) Diethyl succinate, ^{t}BuOH, KO^{t}Bu; (ii) NaOAc, Ac_2O.

The Stobbe condensation is the reaction of aldehydes or ketones with an ester of succinic acid to form alkylidenesuccinic acids (e.g. **151**).[92] For our desired product we made use of diethyl succinate and the base employed was potassium *t*-butoxide to form **152**. The success of the reaction and the specificity of the succinic ester is associated with the

juxtaposition of a carbethoxyl group for the ring formation in **154** as shown in **Scheme 49** below, which is then cleaved by an alkoxide to form the unsaturated half ester **151**.

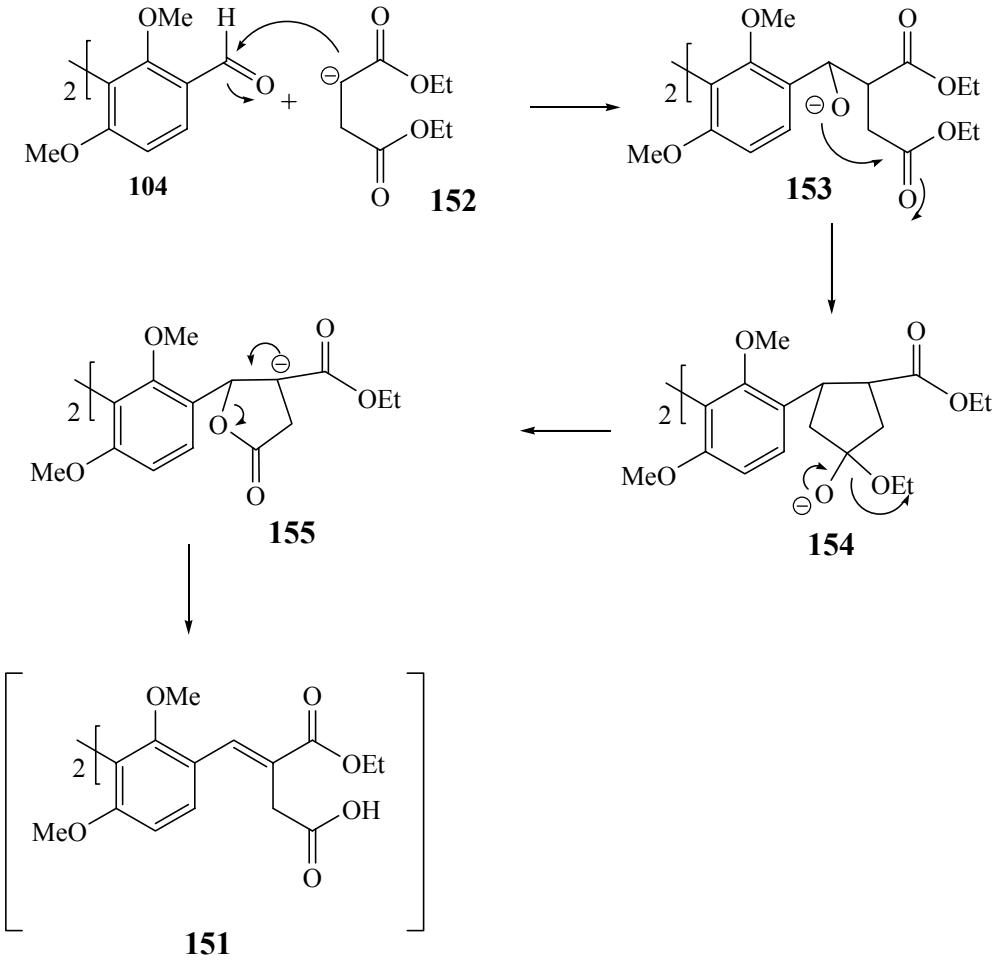

Scheme 49

The alkylidene acid **151**, which was isolated and used without further purification, can now undergo a cyclodehydration. This is possible due to the appropriate stereochemical configuration of the aryl group being *cis* to the $-CH_2COOH$ group.[92] Our cyclisation was achieved using sodium acetate and acetic anhydride to give us the bis-acetate **105** (**Figure 30**). This is effectively a Friedel-Crafts acylative cyclisation reaction. The bright yellow product **105**, was produced in an overall yield of 60% over the two steps.

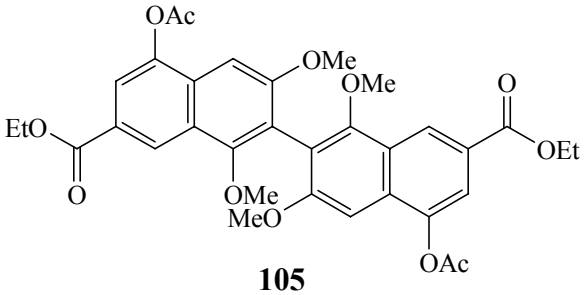

105

Figure 30

The confirmation of the success of the cyclisation was unequivocally displayed in the ^{1}H NMR spectrum of **105**. There was no longer a signal for the aldehyde proton present, and the aromatic region was now occupied by 3 singlets for protons 1-H, 3-H and 5-H. The presence of the ethyl group was confirmed by the expected typical splitting pattern of a quartet (at δ 4.43) and triplet (at δ 1.42), integrating for 2 and 3 protons respectively. There was a substantial increase in the number of signals in the ^{13}C NMR spectrum on the conversion of the dialdehyde **104** into diarylnaphthalene **105**. The new carbonyl signals for the acetate and the ester groups were found at δ 169.4 and δ 166.2 respectively. In addition there were now three aromatic hydrogen bearing carbon signals at δ 123.9, δ 118.9 and δ 94.9. The aromatic region of the spectrum now also contained five signals for carbons bearing no hydrogens. The signal for the methyl group of the acetate was found at δ 21.0 and the signals for the carbons of the ethyl group were at δ 61.1 and δ 14.4. The high resolution mass spectrum of the molecule $C_{34}H_{34}O_{12}$ was found at *m/z* 634.2038. The required mass was calculated to be *m/z* 634.2051.

As the research of both Part A and Part B was relatively successful, this work will be continued in a PhD study.

CHAPTER 5: CONCLUSIONS AND FUTURE WORK: PART B

5.1 Progress towards the Synthesis of Cardinalin 3 23

Based on the synthesis of ventiloquinone L **10** (**Chapter 1, Schemes 18 and 19**), we were able to disconnect the molecule **23** back to the tetra-substituted biphenyl **103** which already has the C8-C8′ biaryl axis of cardinalin 3 **23** in place (**Scheme 50**).

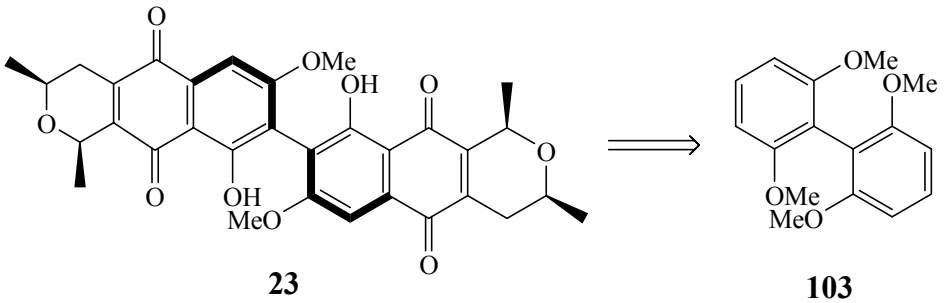

23 **103**

Scheme 50

5.1.1 Biaryl Bond Formation

The formation of the C8-C8′ biaryl bond was accomplished *via* two alternative routes. In the Suzuki coupling reaction, the iodo-complex **138** was coupled to the boronic acid **139** (**Scheme 51**), however the yield of this reaction was a disappointing 54%.

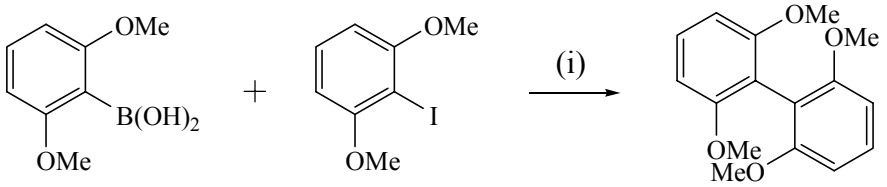

139 **138** **103**

Scheme 51 *Reagents and conditions*: (i) $Pd(PPh_3)_4$, DME, aq. Na_2CO_3, 18 h, 54%.

The coupling was also attempted using the conditions of the classic Ullmann reaction. This route proved far more rewarding as the biphenyl **103** was obtained in a yield of 93%. Here the iodo-aryl **138** was coupled to the cuprate halide **137**, which was synthesised *in situ* from 1,3-dimethoxybenzene (**Scheme 52**).

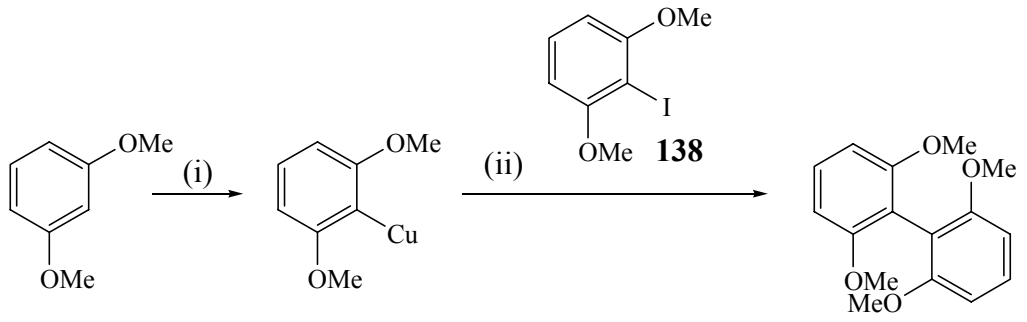

Scheme 52 *Reagents and conditions*: (i) *n*-BuLi, CuI, 0 °C, 3 h; (ii) **138**, pyridine, reflux, 72 h, 93%.

5.1.2 Formation of the Bis-naphthalene 105

Diformylation of **103** was achieved with the Rieche formylation procedure in a yield of 95%, and this product **104** was subjected to Stobbe condensation followed by an intramolecular Friedel-Crafts acylation to give us the bis-naphthalene **105** (**Scheme 53**) in an acceptable yield of 60% over the two steps.

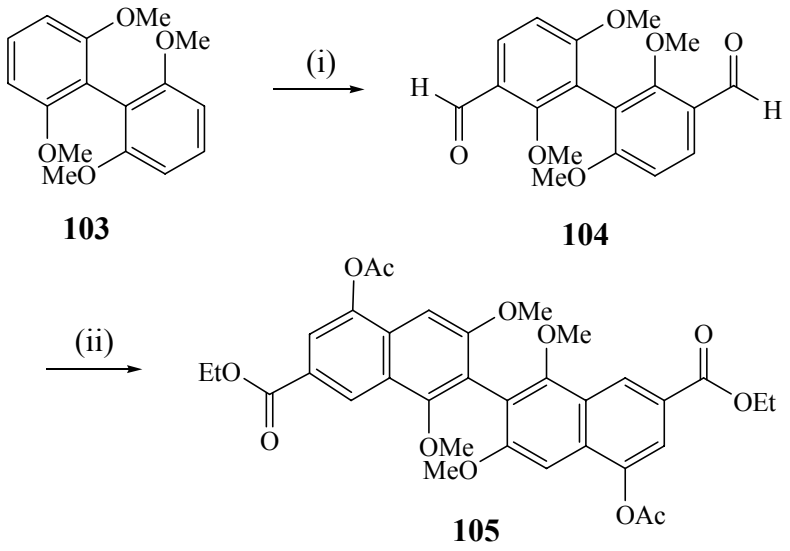

Scheme 53 *Reagents and conditions*: (i) $TiCl_4$, Cl_2CHOCH_3, CH_2Cl_2, −78 °C→ 0 °C, 2 h, 95%; (ii) (a) diethyl succinate, ^{t}BuOH, KO^{t}Bu; (b) NaOAc, Ac_2O, 60%.

With the molecule **105** in hand we can now, for future work, continue towards the synthesis of cardinalin 3 **23**, using the methodology developed for the synthesis of ventiloquinone L **10**.[48] In addition on formation of the 1,3-dimethyl pyran ring we will be able to now use the methodogy developed on utilising enzymes, and following this, then use the arene-tricarbonyl complex chemistry to our advantage to hopefully introduce substituents at the C-1 and C-3 positions in a stereoselective manner onto the pyran nucleus (**Scheme 54**).

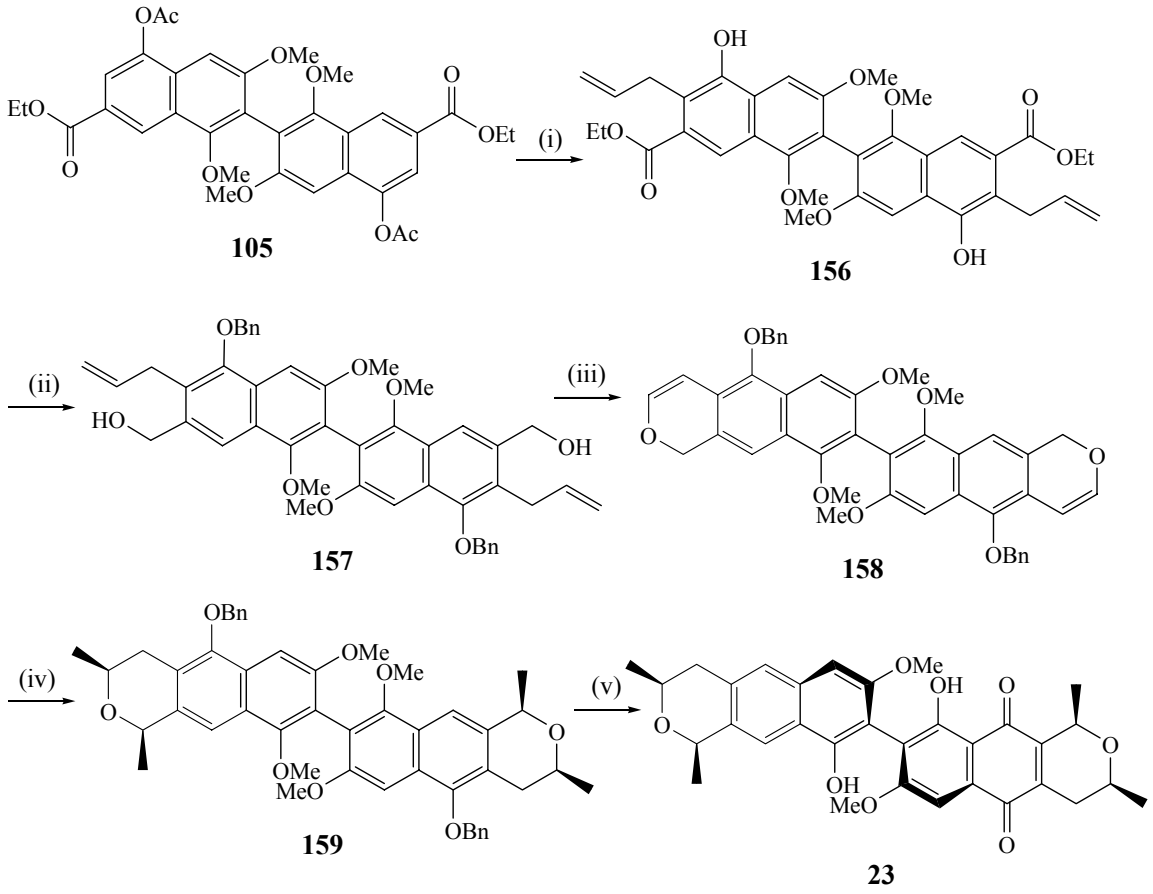

Scheme 54 (i) Acetate hydrolysis, *O*-allylation, Claisen rearrangement; (ii) benzylation, reduction of ester; (iii) *O*-allylation, isomerisation and RCM; (iv) hydroboration, enzymatic enantiomeric resolution, chromium complexation, stereo-selective methylation, de-oxygenation of benzylic alcohol; (v) de-benzylation, salcomine oxidation, selective demethylation.

CHAPTER 6: EXPERIMENTAL PROCEDURES

6.1 General Experimental Procedures

6.1.1 Purification of Solvents and Reagents

All solvents used for reactions and preparative chromatography were distilled prior to use. Where necessary, they were also dried by standard methods as recommended by Perrin *et al.*[93] Tetrahydrofuran, was distilled from the sodium benzophenone ketyl radical; dichloromethane, and triethylamine from calcium hydride and toluene from sodium. Chloroform was dried from passage through basic alumina (ICN Adsorbentien, ICN Alumina Super I). Where necessary, solvents were stored over activated molecular sieves (4 Å) under a nitrogen atmosphere. Potassium *tert*-butoxide was sublimed prior to use. Unless otherwise noted, other reagents were obtained from commercial sources and used without further purification.

6.1.2 Chromatographic Separations

The R_f values quoted are for analytical thin layer chromatography (TLC) on aluminium-backed Macherey-Nagel Alugram Sil G/UV_{254} plates pre-coated 0.25 mm silica gel 60, detection by UV-absorption. Preparative column chromatography was carried out on both wet- and dry-packed columns using Macherey-Nagel Kieselgel 60 silica gel 60 (particle size 0.063-0.200 mm) as the adsorbent. Mixtures of EtOAc and hexane were used as the mobile phase.

High performance liquid chromatography (HPLC) was carried out on a Hewlett Packard Series 1050 system, with a Chiralcel OD reverse phase column.

6.1.3 Spectroscopic and Physical Data

All melting points were obtained on a Reichert hot-stage microscope, and are uncorrected.

^{1}H NMR (nuclear magnetic resonance) spectra were recorded on a Bruker AVANCE 300 (300.13 MHz) or a Bruker 400 (400.13 MHz) spectrometer. Spectra were recorded in deuterated chloroform ($CDCl_3$) and chemical shifts are reported in parts per million downfield from tetramethylsilane, the internal standard; coupling constants are given in Hertz. Splitting patterns are designated as "s", "d", "t", "q" and "m"; these symbols indicate "singlet", "doublet", "triplet", "quartet" and "multiplet" respectively. NMR data are reported as follows: chemical shift (integration of signal, description of signal, coupling constant(s) where applicable, assignment).

^{13}C NMR (^{1}H decoupled) spectra were recorded on a Bruker AVANCE 300 (75.47 MHz) or Bruker DRX 400 (100.63 MHz) spectrometer. Spectra were recorded in deuterated chloroform ($CDCl_3$) and chemical shifts are reported in parts per million relative to the central signal of deuterated chloroform, taken as δ 77.00.

IR (infrared) spectra were recorded on a Bruker IFS-25 Fourier Transform spectrometer or on a Bruker Vector-22 Fourier Transform spectrometer. Liquid samples were recorded as thin films between sodium chloride plates, while solid samples were recorded as solutions in chloroform in sodium chloride cells. The signals were reported on the wavenumber scale (ν/cm^{-1}). Signals were designated as "s", "m", "w" and "br"; these symbols indicate "strong", "medium", "weak" and "broad" respectively. IR spectra data were reported as follows: wavenumber (intensity, assignment).

High resolution mass spectra were recorded on a Kratos MS 9/50, VG 70E MS or a VG 70 SEQ mass spectrometer.

Optical rotations were measured on a Jasco DIP 3-70 instrument at 22 °C at the sodium D line, and $[\alpha]_D$ values are given in $deg.cm^2.g^{-1}$.

6.1.4 Crystal Structure Solution and Refinement

Intensity data were collected at 20 °C on a Bruker SMART 1K CCD area detector diffractometer with graphite monochromated Mo K_α radiation (50 kV, 30 mA). The collection method involved ω-scans of width 0.3 °. Data reduction was carried out using the program *SAINT+* and absorption corrections were made using the program *SADABS.*[94] The crystal structure was solved by direct methods using *SHELXTL.*[95] Non hydrogen atoms were first refined isotropically followed by an anisotropic refinement by full matrix least squares calculations based on F^2 using *SHELXTL*. Hydrogen atoms were positioned geometrically and allowed to ride on their respective parent atoms. Diagrams and publication material were generated using SHELXTL and PLATON.[96]

6.1.5 Other General Procedures

The term "*in vacuo*" refers to the removal of solvent by rotary evaporation, followed by removal of the residual solvent at oil pump pressure (*ca.*0.1-1 Torr) at ambient temperature until constant mass was achieved.

6.2 Experimental Procedures Related to Part A

6.2.1 Synthesis of Allyl 5-(allyloxy)-2-hydroxybenzoate 107

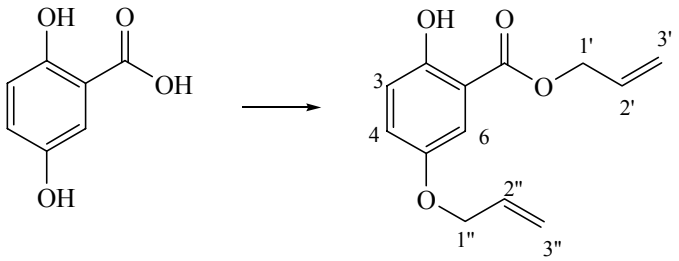

106 **107**

Potassium carbonate (11.94 g, 85.8 mmol, 2.2 equiv.) was added to a clear yellow solution of 2,5-dihydroxybenzoic acid (6.01 g, 39.0 mmol) in acetone (600 cm^3), in a 2 litre quickfit conical flask fitted with a condenser. The resulting mixture was heated to 30 °C, while stirring under nitrogen. Allyl bromide (7.43 cm^3, 10.38 g, 85.8 mmol, 2.2 equiv.) was then slowly added to the solution by syringe. The resulting mixture was heated at reflux for 24 h, during which time it became a thick white paste. The reaction mixture was cooled, filtered through celite and the acetone then removed *in vacuo*. The residue was purified by silica gel column chromatography (20% EtOAc/hexane) to yield the diallylated product, as white needle-like crystals (8.42 g, 92%). $\mathbf{R_f}$ = 0.72 (20% EtOAc/hexane); **mp.** 43-45 °C, (lit[97] 43.5-44.5 °C); **IR** ($CHCl_3$): $\nu_{max}(cm^{-1})$ = 3440 (s, br, OH), 1649 (s, C=O), 1614 (s, C=C); **^{1}H NMR** (300 MHz, $CDCl_3$): δ_H = 10.35 (1H, s, O*H*), 7.36 (1H, d, *J*=3.1, 6-H), 7.11 (1H, dd, *J*=9.1, *J*=3.1, 4-H), 6.92 (1H, d, *J*=9.1, 3-H), 6.11-5.97 (2H, ddt, *J*=12.5, *J*=5.5, *J*=1.6, 2′ and 2″-H overlapped), 5.46-5.43 (2H, m, 3′-H), 5.35-5.27 (2H, m, 3″-H), 4.85 (2H, d, *J*=5.7, 1′-H), 4.50 (2H, d, *J*=5.3, 1″-H); **^{13}C NMR** (75 MHz, $CDCl_3$) δ_C = 169.5 (*C*=O), 156.3 (C-2), 151.0 (C-5), 133.2 (C-2″), 131.5 (C-2′), 124.6 (C-6), 118.9 (C-4), 118.5 (C-3), 117.7 (C-3″), 113.5 (C-3′), 111.9 (C-1), 69.6 (C-1″), 65.8 (C-1′).

6.2.2 Synthesis of Allyl 2-allyl-3,6-dihydroxybenzoate 108

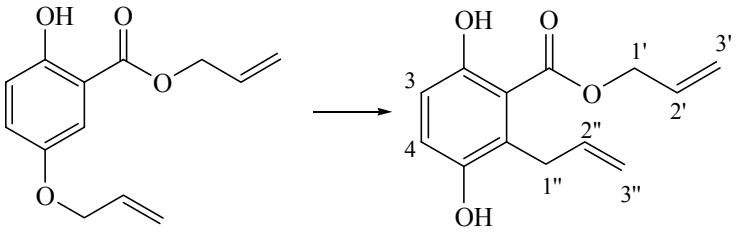

107 **108**

In a 50 cm^3 RB flask equipped with a reflux condenser, neat allyl 5-(allyloxy)-2-hydroxybenzoate (11.81 g, 50.4 mmol) was heated at 170 °C for 18 h, under a nitrogen atmosphere. The white powder melted to first form a yellow oil and then a deep orange liquid that became a black viscous oil. This was allowed to cool before purifying by silica gel column chromatography (5 →10 →20% EtOAc/hexane) to afford allyl 2-allyl-3,6-dihydroxybenzoate as an viscous orange oil (10.14 g, 86%). $\mathbf{R_f}$ = 0.45 (20% EtOAc/hexane); **IR** (film): $\nu_{max}(cm^{-1})$ = 3424 (s, br, OH), 1664 and 1610 (s, C=C); **^{1}H NMR** (300 MHz, $CDCl_3$): δ_H = 10.34 (1H, s, 2-O*H*), 6.99 (1H, d, *J*=8.9, 4-H), 6.82 (1H, d, *J*=8.9, 3-H), 6.09-5.93 (2H, m, 2′ and 2′′-H overlapped), 5.45-5.32 (2H, m, 3′-H), 5.11-5.02 (2H, m, 3′′-H), 4.86 (2H, m, 1′-H), 3.74 (2H, d, *J*=5.8, 1′′-H); **^{13}C NMR** (75 MHz, $CDCl_3$) δ_C = 170.5 (*C*=O), 156.1 (C-2), 147.3 (C-5), 136.3 (C-2′), 131.2 (C-2′′), 126.4 (C-6), 123.4 (C-4), 119.7 (C-3), 116.6 (C-3′), 115.5 (C-3′′), 112.9 (C-1), 66.5 (C-1′), 32.4 (C-1′′).

6.2.3 Synthesis of Allyl 2-allyl-3,6-dimethoxybenzoate 109

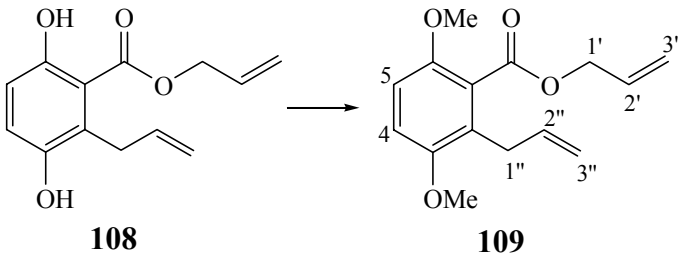

108 **109**

In a 100 cm^3 RB flask fitted with a condenser, potassium carbonate (8.50 g, 61.0 mmol, 2.5 equiv.) was added to a clear yellow solution of allyl 2-allyl-3,6-dihydroxybenzoate (5.70 g, 24.4 mmol) in acetone (100 cm^3), The solution was stirred at rt until it turned purple brown. Dimethyl sulfate (5.80 cm^3, 7.70 g, 61.0 mmol, 2.5 equiv.) was then added by syringe and the resulting mixture was refluxed for 24 h. The crude reaction mixture, which was light brown in colour, was filtered through celite and the acetone was removed *in vacuo*. Once the residue cooled, diethyl ether (300 cm^3) was added. The ether layer was washed with a 10% aqueous ammonia solution (300 cm^3) until frothing stopped. The aqueous layer was thoroughly extracted with diethyl ether and dichloromethane. The organic extracts were combined and dried with anhydrous $MgSO_4$ before filtering through celite. The solvent was removed *in vacuo*. After purification by silica gel column chromatography (20% EtOAc/hexane) allyl 2-allyl-3,6-dimethoxybenzoate was obtained as a clear yellow oil (5.26 g, 82%). $\mathbf{R_f}$ = 0.47 (20% EtOAc/hexane); **IR** (film): $\nu_{max}(cm^{-1})$ = 1731 (s, C=O), 1638 and 1598 (m, C=C); **^{1}H NMR** (300 MHz, $CDCl_3$): δ_H = 6.84 (1H, d *J*=9.0, 4-H), 6.75 (1H, d, *J*=9.0, 5-H) 6.07-5.83 (2H, m, 2′ and 2′′ overlapped), 5.45-5.26 (2H, m, 3′-H), 5.02-4.95 (2H, m, 3′′-H), 4.82 (2H, d, *J*=5.8, 1′-H), 3.78 (3H, s, OC*H*$_3$), 3.77 (3H, s, OC*H*$_3$), 3.35 (2H, d, *J*=6.3, 1′′-H); **^{13}C NMR** (75 MHz, $CDCl_3$) δ_C = 167.4 (C=O),151.6 (C-6), 150.2 (C-3), 135.9 (C-2′′), 131.9 (C-2′), 127.1 (C-1), 125.1 (C-2), 118.6 (C-4), 115.3 (C-5), 112.4 (C-3′), 109.8 (C-3′′), 65.8 (C-1′) 56.4 (6-OCH_3), 56.2 (3-OCH_3), 31.7 (C-1′′).

6.2.4 Synthesis of (2-Allyl-3,6-dimethoxyphenyl)methanol 88

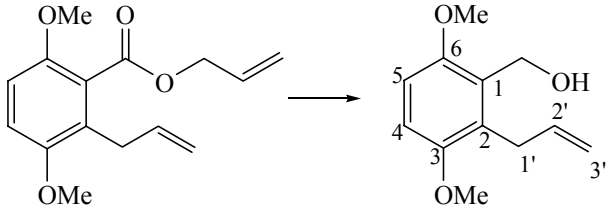

109 **88**

In a 250 cm^3 two neck RB flask, allyl 2-allyl-3,6-dimethoxybenzoate (5.20 g, 20.0 mmol) was dissolved in THF (250 cm^3). The solution was cooled to 0 °C and lithium aluminium

hydride (1.52 g, 40.0 mmol, 2 equiv.) was added slowly. The resulting suspension was heated to 40 °C and stirred for 2 h. The mixture was cooled to 0 °C again before a 10% aqueous hydrochloric acid solution (10%, 20 cm^3) was slowly added. The aqueous layer was extracted with diethyl ether (4 × 50 cm^3) and dichloromethane (3 × 50 cm^3). The organic extracts were combined and dried with anhydrous $MgSO_4$ before filtering through celite. The solvent was removed *in vacuo* and the residue was purified by silica gel column chromatography (20% EtOAc/hexane) to afford (2-allyl-3,6-dimethoxyphenyl)methanol as a light yellow oil (3.89 g, 93%). $\mathbf{R_f}$ = 0.32 (20% EtOAc/hexane); **IR** (film): $\nu_{max}(cm^{-1})$ = 3416 (s, br, OH), 1637 and 1598 (s, C=C); **^{1}H NMR** (300 MHz, $CDCl_3$) δ_H = 6.77 (2H, dd, *J*=8.9, 4-H and 5-H), 6.04-5.91 (1H, m, 2′-H), 5.00-4.88 (2H, m, 3′-H), 4.71 (2H, s, Ar-C*H*$_2$-O), 3.83 (3H, s, OC*H*$_3$), 3.78 (3H, s, OC*H*$_3$), 3.54 (2H, d, *J*=5.8, 1′-H), 2.30 (1H, s, O*H*); **^{13}C NMR** (75 MHz, $CDCl_3$) δ_C = 152.3 (C-6), 151.8 (C-3), 137.4 (C-2′), 128.8 (C-1), 128.3 (C-2), 114.7 (C-3′), 110.7 (C-4), 108.8 (C-5), 57.5 (O*C*H$_3$), 56.3 (O*C*H$_3$), 55.8 (Ar-*C*H$_2$-O), 29.9 (C-1′).

6.2.5 Synthesis of 2-Allyl-3-allyloxymethyl-1,4-dimethoxybenzene 87

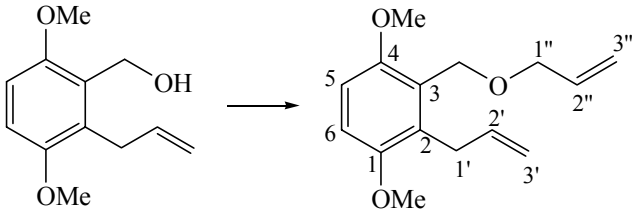

88 **87**

In a 250 cm^3 quick fit conical flask, fitted with a condenser, (2-allyl-3,6-dimethoxyphenyl)methanol (2.70 g, 13.0 mmol) and allyl bromide (1.35 cm^3, 1.88 g, 16.0 mmol, 1.2 equiv.) were dissolved in dry THF (100 cm^3). Sodium hydride (50-55% in oil, 1.87 g, 39.0 mmol, *ca.* 3 equiv.) was added and the solution was refluxed for 24 h under a nitrogen atmosphere, while stirring. Workup was done by adding water (100 cm^3) and then extracting the material with diethyl ether (4 × 50 cm^3). The organic layers were combined, dried with anhydrous $MgSO_4$, filtered through celite and the solvent removed

in vacuo. The residue was purified by silica gel column chromatography by using hexane as the initial eluent to remove the oil from the sodium hydride and then 20% EtOAc/hexane to afford 2-allyl-3-allyloxymethyl-1,4-dimethoxybenzene as a clear yellow oil (2.95 g, 91%). $\mathbf{R_f}$ = 0.59 (20% EtOAc/hexane); **IR** (film): $\nu_{max}(cm^{-1})$ = 1638 and 1595 (m C=C); **^{1}H NMR** (300 MHz, $CDCl_3$) δ_H = 6.81 (1H, d, *J*=8.9, 6-H), 6.73 (1H, d, *J*=8.9, 5-H), 6.03-5.89 (2H, m, 2′ and 2′′-H overlapped), 5.32-5.16 (2H, m, 3′′-H), 4.96-4.89 (2H, m, 3′-H), 4.57 (2H, s, Ar-C*H*$_2$-O), 4.03 (2H, d, *J*=5.8, 1′′-H), 3.78 (3H, s, OC*H*$_3$), 3.77 (3H, s, OC*H*$_3$), 3.53 (2H, d, *J*=5.9, 1′-H); **^{13}C NMR** (75 MHz, $CDCl_3$) δ_C = 152.9 (C-1), 151.6 (C-4), 137.1 (C-2′′), 135.4 (C-2′), 130.2 (C-3), 125.2 (C-2), 116.9 (C-3′′), 114.4 (C-3′), 111.2 (C-6), 109.4 (C-5), 71.3 (C-1′′), 62.7 (Ar-*C*H$_2$-O), 56.4 (O*C*H$_3$), 56.1 (O*C*H$_3$), 30.3 (C-1′).

6.2.6 Synthesis of 5,8-Dimethoxy-1*H*-isochromene 86

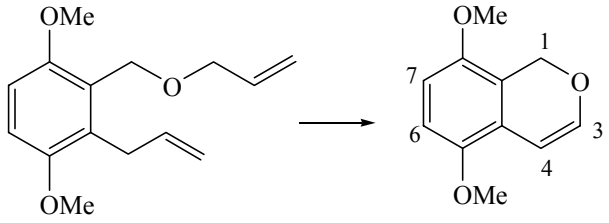

87 **86**

A 100 cm^3 RB flask, equipped with a condenser, was set up under nitrogen. Neat 2-allyl-3-allyloxymethyl-1,4-dimethoxybenzene (2.80 g, 11.3 mmol) was placed in the flask and the isomerisation catalyst, $[RuClH(CO)(PPh_3)_3]$ (54 mg, 0.5 mol%) was added. The mixture was heated for 3 h at 90 °C. In this time the mixture went from light yellow to dark brown. Dry toluene (50 cm^3) and the second generation Grubbs catalyst (48 mg, 0.5 mol%) was then added to the flask and the solution cooled slightly to 70 °C and left at this temperature for 24 h. The material was dried onto silica while removing the solvent *in vacuo*. The material was then purified by silica gel column chromatography (5% EtOAc/hexane) to afford 5,8-dimethoxy-1*H*-isochromene as a yellow resin (1.85 g, 85%). $\mathbf{R_f}$ = 0.42 (5% EtOAc/hexane); **IR** (film): $\nu_{max}(cm^{-1})$ = 1630 and 1581 (s, C=C); **^{1}H NMR**

(300MHz, $CDCl_3$) δ_H = 6.66 (2H, dd, *J*=8.9, 6 and 7-H overlapped), 6.56 (1H, d, *J*=5.8, 4-H), 6.04 (1H, d, *J*=5.8, 3-H), 5.11 (2H, s, Ar-CH_2-O), 3.78 (3H, s, OCH_3), 3.76 (3H, s, OCH_3); **^{13}C NMR** (75 MHz, $CDCl_3$) δ_C = 148.7 (Ar*C*), 147.2 (Ar*C*), 145.6 (C-4), 120.4 (Ar*C*), 116.9 (Ar*C*), 110.1 (Ar*C*H), 109.1 (Ar*C*H), 99.4 (C-3), 62.7 (Ar-*C*H_2-O), 56.0 (O*C*H_3), 55.7 (O*C*H_3); **HRMS**: Found M^+, 192.0797. $C_{11}H_{12}O_3$ requires *M* 192.0786; *m/z* (EI) 192 (M^+, 100%), 177 (78), 149 (16), 134 (7), 121 (10), 106 (5), 91 (10), 77 (10), 63 (5).

6.2.7 Synthesis of 5,8-Dimethoxy-isochroman-4-ol 85

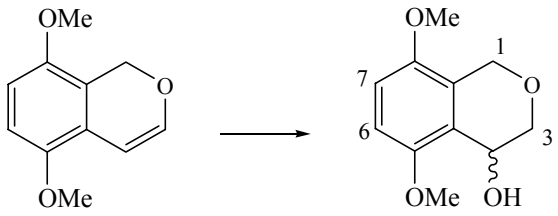

86 **85**

In a 100 cm^3 two neck RB flask equipped with a rubber septum under nitrogen, 5,8-dimethoxy-1*H*-isochromene (1.2 g, 6.24 mmol) was dissolved in dry THF (50 cm^3). The solution was cooled to 0 °C and a borane-methyl sulfide complex (2.0 M in Et_2O, 3.75 cm^3, 7.49 mmol, 1.2 equiv.) was injected by syringe. The reaction mixture was stirred at this temperature for 30 mins, and then at rt for 2 h. The reaction mixture was cooled to 0 °C again and aqueous sodium hydroxide (5 M, 6.24 cm^3, 31.0 mmol, 5 equiv.) followed by aqueous hydrogen peroxide (30% w/w, 7.65 cm^3, 75.0 mmol, 12 equiv.) were added rapidly. The clear solution turned cloudy and frothing was observed. The cloudy reaction mixture was stirred for 24 h before quenching with aqueous hydrochloric acid (5%, 150 cm^3). The organic material was then extracted with diethyl ether (4 × 80 cm^3) and dichloromethane (4 × 80 cm^3). The organic layers were combined, dried with anhydrous $MgSO_4$, filtered through celite and the solvent then removed *in vacuo*. The residue was purified by silica gel column chromatography (50% EtOAc/hexane) to afford the 5,8-dimethoxy-isochroman-4-ol as white flake-like crystals (1.10 g, 84%). $\mathbf{R}_f$ = 0.34 (50%

EtOAc/hexane); **mp.** 96-98 °C; **IR** ($CHCl_3$): $\nu_{max}(cm^{-1})$ = 3447 (w, br, OH), 1606 (s, C=C); **^{1}H NMR** (300MHz, $CDCl_3$) δ_H = 6.72 (2H, m, 6 and 7-H overlapped), 4.85 (1H, d, *J*=16.0, 1-H_a), 4.79 (1H, m, 4-H), 4.51 (1H, d, *J*=16.0, 1-H_b), 4.08 (1H, dd, *J*=12.0, *J*=2.8, 3-H_a), 3.85 (3H, s, OC*H*$_3$), 3.78 (1H, dd, *J*=12.0, *J*=3.1, 3-H_b), 3.76 (3H, s, OC*H*$_3$), 2.88 (1H, s, O*H*); **^{13}C NMR** (75 MHz, $CDCl_3$) δ_C = 151.5 (Ar*C*-O), 149.2 (Ar*C*-O), 125.1 (Ar*C*), 124.7 (Ar*C*), 109.1 (Ar*C*H), 108.3 (Ar*C*H), 70.3 (C-3), 64.3 (C-1), 60.3 (C-4), 55.7 (O*C*H$_3$), 55.5 (O*C*H$_3$); **HRMS**: Found M^+, 210.0904. $C_{11}H_{14}O_4$ requires *M* 210.0892; *m/z* (EI) 210 (M^+, 94%), 180 (100), 165 (49), 151 (7), 134 (9), 120 (10), 107 (7), 91 (12), 77 (13), 65 (7), 51 (8).

6.2.8 Synthesis of 5,8-Dimethoxy-3,4-dihydro-1*H*-isochromen-4-yl acetate 89

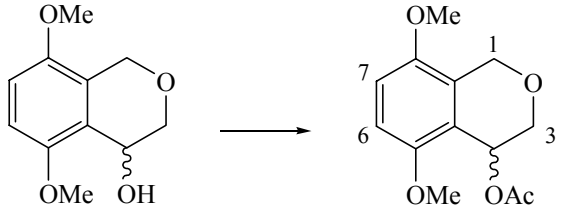

85 **89**

In a 100 cm^3 2 neck RB flask, fitted with a rubber septum, 5,8-dimethoxy-isochroman-4-ol (0.500 g, 2.38 mmol) was dissolved in dry THF (100 cm^3). To this stirred solution was added a catalytic amount of 4-dimethylaminopyridine (DMAP), (29 mg, 0.48 mmol, 10 mol%) followed by acetic anhydride (0.90 cm^3, 19.0 mmol, 4 equiv.), and triethylamine (3.31 cm^3, 47.7 mmol, 10 equiv.). The reaction mixture was stirred at rt for 3 h. The reaction was then quenched with water (50 cm^3). The organic material was then extracted with EtOAc (4 × 80 cm^3). The organic layers were combined, dried with anhydrous $MgSO_4$, filtered through celite and the solvent then removed *in vacuo*. The residue was purified by silica gel column chromatography (30% EtOAc/hexane) to afford the 5,8-dimethoxy-3,4-dihydro-1*H*-isochromen-4-yl acetate as fluffy white crystals (0.42 g, 70%). $\mathbf{R}_f$ = 0.80 (50% EtOAc/hexane); **mp.** 119-121 °C; **IR** ($CHCl_3$): $\nu_{max}(cm^{-1})$ = 1729 (s, C=O), 1646 (s, C=C), 1263 (s, C-O); **^{1}H NMR** (300MHz, $CDCl_3$) δ_H = 6.79 (1H, d, *J*=8.9, 7-H)*, 6.72 (1H, d, *J*=8.9, 6-H)*, 5.93 (1H, m, 4-H), 4.83, (1H, d, *J*=16.1, 1-H_a),

4.48 (1H, d, *J*=16.1, 1-H_b), 4.23 (1H, dd, *J*=12.9, *J*=0.9, 3-H_a), 3.78 (3H, s, OCH_3), 3.77 (3H, s, OCH_3), 3.73 (1H, dd, *J*=12.9, *J*=2.2, 3-H_b), 2.09 (3H, s, COCH_3); **^{13}C NMR** (75 MHz, $CDCl_3$) δ_C = 170.6 (*C*=O), 151.9 (ArC-O), 149.0 (ArC-O), 126.2 (Ar*C*), 120.0 (Ar*C*), 110.2 (Ar*C*-H), 108.5 (Ar*C*-H), 68.7 (C-3), 63.9 (C-1), 62.5 (C-4), 55.8 (O*C*H_3), 55.6 (O*C*H_3), 21.2 (OC-*C*H_3); **HRMS**: Found M^+, 252.0999. $C_{13}H_{16}O_5$ requires *M* 252.0998; *m/z* (EI) 252 (M^+, 29%), 192 (100), 177 (23), 149 (9), 134 (7), 105 (10), 91 (10), 77 (7).

(* interchangeable signals)

6.2.9 General Procedure for the Synthesis of the Alcohol Substrates for Lipase Screening

In a 250 cm^3 RB flask, to a stirred solution of the ketone in methanol (10 cm^3), was added soduim borohydride (1 equiv.). The reaction mixture was stirred for 2 h at rt. Work up was done by adding an aqueous 10% HCl solution (4 cm^3). The organic product was extracted using EtOAc (3 × 10 cm^3). The organic layers were combined, dried over anhydrous $MgSO_4$, filtered and the solvent removed *in vacuo*. The product was purified by silica gel column chromatography (50% EtOAc/hexane) to yield the alcohol.

6.2.9.1 The Synthesis of 1-(2,5-Dimethoxyphenyl) Ethanol 121 [98]

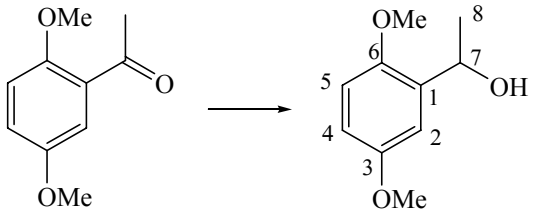

170 **121**

Clear oil (2.2 g, quantitative yield); R_f = 0.38 (30% EtOAc/hexane); **^{1}H NMR** (300 MHz, $CDCl_3$): δ_H = 6.94 (1H, d, *J*=2.8, 2-H), 6.76 (2H, td, *J*=5.8, *J*=8.9, 4-H and 5-H), 5.06 (1H, q, *J*=6.4, 7-H), 3.81, (3H, s, OCH_3), 3.77 (3H, s, OCH_3), 2.73 (1H, s, O*H*), 1.48 (3H, d, *J*=6.5, 8-H); **^{13}C NMR** (75 MHz, $CDCl_3$) δ_C = 153.7 (Ar-*C*O), 150.6 (Ar-*C*O),

134.7 (Ar-*C*), 112.4 (Ar-*C*H), 112.3 (Ar-*C*H), 111.4 (Ar-*C*H), 66.3 (C-7), 55.7 (O*C*H_3), 55.7 (O*C*H_3), 23.0 (C-8).

6.2.9.2 The Synthesis of 5-Methoxy-1,2,3,4-tetrahydronaphthalen-1-ol 123 [99]

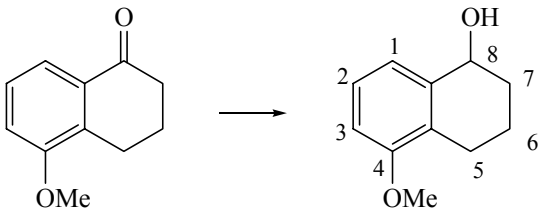

171 **123**

White solid (0.44 g, 87%); R_f = 0.42 (30% EtOAc/hexane); **^{1}H NMR** (300 MHz, $CDCl_3$): δ_H = 7.18 (1H, t, J=7.8, 2-H), 7.05 (1H, d, J=7.6, Ar-CH), 6.75 (1H, d, J= 8.0, Ar-CH), 4.75 (1H, s, OH), 3.81 (3H, s, OCH_3), 2.75 (1H, td, J=5.0, J=8.9, 7-Ha), 2.54 (1H, td, J=6.4, J=13.5, 7-Hb), 1.84 (5H, m, 5-, 6- and 8-H);

6.2.10 General Procedure for the Synthesis of the Acetate Substrates for Lipase Screening

In a 25 cm^3 two neck RB flask, fitted with a rubber septum, the alcohol was dissolved in dry THF (50 cm^3). To this stirred solution was added a catalytic amount of 4-dimethylaminopyridine (DMAP), followed by acetic anhydride (4 equiv.), and triethylamine (10 equiv.). The reaction mixture was stirred at rt for 3 h. The reaction was then quenched with water (25 cm^3). The organic material was then extracted with EtOAc (4 × 50 cm^3). The organic layers were combined, dried with anhydrous $MgSO_4$, filtered through celite and the solvent then removed *in vacuo*. The residue was purified by silica gel column chromatography (30% EtOAc/hexane) to afford the acetate.

6.2.10.1 The Synthesis of 1-Phenylethyl Acetate 124 [100]

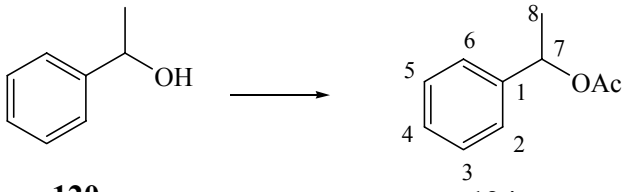

120 **124**

Clear oil (1.07 g, 79%); R_f = 0.67 (30% EtOAc/hexane); **^{1}H NMR** (300 MHz, $CDCl_3$): δ_H = 7.31 (5H, m, Ar-*H*), 5.88 (1H, q, *J*=6.6, 7-H), 2.07 (3H, s, COCH_3), 1.53 (3H, d, *J*=6.6, 8-H); **^{13}C NMR** (75 MHz, $CDCl_3$) δ_C = 170.3 (*C*OCH_3), 141.7 (C-1), 128.5 (Ar-*C*H), 127.8 (Ar-*C*H), 126.1 (Ar-*C*H), 72.3 (C-7), 22.2 (*C*H_3), 21.3 (*C*H_3).

6.2.10.2 The Synthesis of 1-(2,5-Dimethoxyphenyl)ethyl Acetate 125

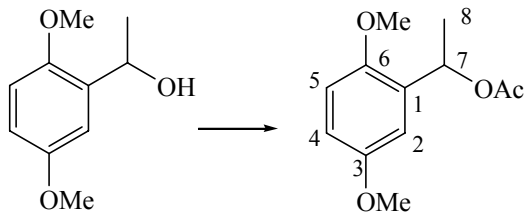

121 **125**

Clear oil (1.12 g, 91%); R_f = 0.53 (30% EtOAc/hexane); **^{1}H NMR** (300 MHz, $CDCl_3$): δ_H = 6.94 (1H, d, *J*=2.6, 2-H), 6.77 (2H, m, 4-H and 5-H), 6.20 (1H, q, *J*=6.5, 7-H), 3.79 (3H, s, OCH_3), 3.77 (3H, s, OCH_3), 2.08 (3H, s, $COCH_3$), 1.46 (3H, d, *J*=6.5, 8-H); **^{13}C NMR** (75 MHz, $CDCl_3$) δ_C = 170.0 (*C*OCH_3), 153.6 (Ar-*C*), 150.1 (Ar-*C*), 131.7 (Ar-*C*), 112.4 (Ar-*C*H), 112.3 (Ar-*C*H), 111.6 (Ar-*C*H), 67.1 (C-7), 56.0 (O*C*H_3), 55.6 (O*C*H_3), 21.2 (*C*H_3), 21.2 (*C*H_3).

6.2.10.3 The Synthesis of 1,2,3,4-Tetrahydronaphthalen-1-yl Acetate 126[101]

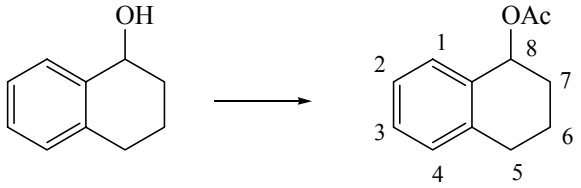

122 **126**

Clear oil (1.11 g, 87%); R_f = 0.64 (30% EtOAc/hexane); **^{1}H NMR** (300 MHz, $CDCl_3$): δ_H = 7.28-7.10 (4H, m, Ar-C*H*), 6.00 (1H, t. *J*=4.1, 8-H), 2.91-2.68 (2H, m, 7-H), 2.07 (3H, s, COCH_3), 2.03-1.75 (4H, m, 5-H and 6-H); **^{13}C NMR** (75 MHz, $CDCl_3$) δ_C = 170.7 (*C*OCH_3), 137.8 (Ar-*C*H), 134.5 (Ar-*C*H), 129.3 (Ar-*C*H), 129.0 (Ar-*C*H), 128.0 (Ar-*C*), 126.0 (Ar-*C*), 69.9 (C-8), 29.0 (*C*H_2), 29.0 (*C*H_2), 21.4 (CO*C*H_3), 18.7 (*C*H_2).

6.2.10.4 The Synthesis of 5-Methoxy-1,2,3,4-tetrahydronaphthlen-1-yl Acetate 126

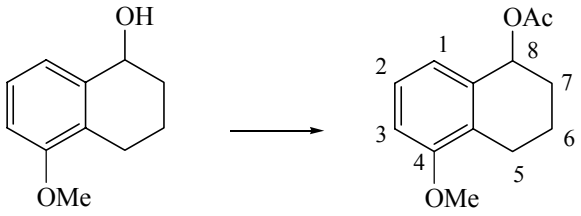

126 **126**

Clear oil (0.22 g 89%); R_f = 0.62 (30% EtOAc/hexane); **^{1}H NMR** (300 MHz, $CDCl_3$): δ_H = 6.23 (1H, t, *J*=7.9, 2-H), 6.89 (1H, d, *J*=7.8, Ar-C*H*), 6.77 (1H, d, *J*=8.1, Ar-C*H*), 5.97 (1H, m, 8-H), 3.82 (3H, s, OCH_3), 2.79-2.58 (1H, m, 7-Ha), 2.50-2.47 (1H, m, 7-Hb), 2.07 (3H, s, COCH_3), 1.97-1.84(4H, m, 6-H and 7-H); **^{13}C NMR** (75 MHz, $CDCl_3$) δ_C = 170.7 (*C*OCH_3), 160.0 (Ar-*C*O), 135.6 (Ar-*C*), 127.0 (Ar-*C*), 126.4 (Ar-*C*H), 121.3 (Ar-*C*H), 109.1 (Ar-*C*H), 70.0 (CH_2), 55.3 (OCH_3), 28.5 (CH_2), 22.7 (CO*C*H_3), 21.4 (C-8), 18.0 (CH_2).

6.2.11 Synthesis of (+)-5,8-Dimethoxy-isochroman-4-ol 85

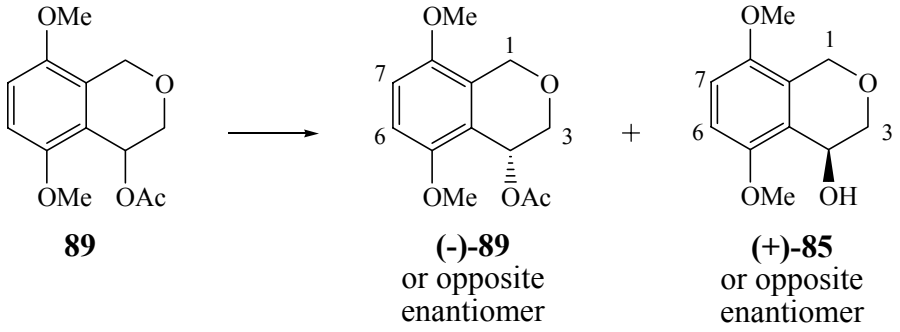

To a stirred solution of the racemic 5,8-dimethoxy-3,4-dihydro-1*H*-isochromen-4-yl acetate (200 mg, 0.79 mmol) in toluene (5 cm^3) was added a buffer solution of tris (hydroxymethyl)amino methane (40 cm^3, 0.1 M, pH 7.5), followed by the lipase enzyme Novozyme 525 (40 cm^3). The reaction mixture was allowed to stir at rt for 2 h. Completion of the reaction was determined by HPLC on a C18 column (70% acetonitrile in H_2O), to show a 50% conversion of the racemic acetate to the alcohol. The reaction mixture was then extracted with EtOAc (3 × 80 cm^3) to isolate the organic products. The organic layers were then combined and dried with anhydrous $MgSO_4$, filtered through celite and the solvent removed *in vacuo*. The enantiomeric excess was determined by HPLC analysis in a Chiralcel OD column (200 × 46 mm) using 20% isopropyl alcohol in hexane as the mobile phase. The crude material was purified by silica gel column chromatography (30% EtOAc/hexane) to give the unreacted (–)-5,8-dimethoxy-3,4-dihydro-1*H*-isochromen-4-yl acetate, $[\alpha]_D$ = – 93.0 (c = 1 in $CHCl_3$), (59 mg, 30%) and the enantioselectively hydrolysed (+)-5,8-dimethoxy-isochroman-4-ol, $[\alpha]_D$ = + 28.0 (c = 1 in $CHCl_3$), (54 mg, 33%). Both products were analysed spectroscopically and characterised as described above.

6.2.12 Synthesis of (–)-5,8-Dimethoxy-isochroman-4-ol 85

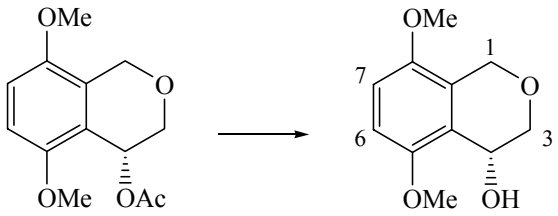

(-)-89
or opposite
enantiomer

(-)-85
or opposite
enantiomer

In a 25 cm^3 RB flask, to a stirred solution of the (–)-5,8-dimethoxy-3,4-dihydro-1*H*-isochromen-4-yl acetate (20 mg, 0.079 mmol) in methanol (2 cm^3), was added potassium carbonate (16.4 mg, 0.119 mmol, 1.5 equiv.). The reaction mixture was stirred for 2 h at rt. Work up was done by adding an aqueous 10% HCl solution (2 cm^3). The organic product was extracted using EtOAc (3 × 5 cm^3). The organic layers were combined, dried over anhydrous $MgSO_4$, filtered and the solvent removed *in vacuo*. The product was purified by silica gel column chromatography (50% EtOAc/hexane) to yield the (–)-alcohol, (13.7 mg, 82%). Optical rotation $[\alpha]_D$ = – 41.0 (c =1 in $CHCl_3$). The product was characterised as described for the racemic alcohol.

6.2.13 Synthesis (+)-5,8-Dimethoxy-3,4-dihydro-1*H*-isochromen-4-yl acetate 89

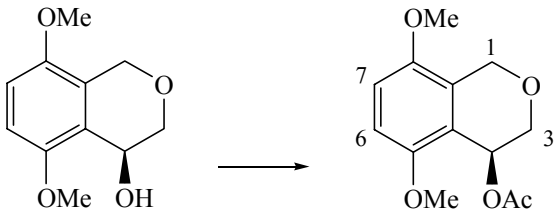

(+)-85
or opposite
enantiomer

(+)-89
or opposite
enantiomer

In a 25 cm^3 two neck RB flask, fitted with a rubber septum, (+)-5,8-dimethoxy-isochroman-4-ol (13.0 mg, 0.062 mmol) was dissolved in dry THF (5 cm^3). To this

stirred solution was added a catalytic amount of 4-dimethylaminopyridine (DMAP), (0.8 mg, 0.006 mmol, 10 mol%) followed by acetic anhydride (0.023 cm^3, 0.25 mmol, 4 equiv.), and triethylamine (0.09 cm^3, 0.62 mmol, 10 equiv.). The reaction mixture was stirred at rt for 3 h. The reaction was then quenched with water (5 cm^3). The organic material was then extracted with EtOAc (4 × 10 cm^3). The organic layers were combined, dried with anhydrous $MgSO_4$, filtered through celite and the solvent then removed *in vacuo*. The residue was purified by silica gel column chromatography (30% EtOAc/hexane) to afford the (+)-5,8-dimethoxy-3,4-dihydro-1*H*-isochromen-4-yl acetate as fluffy white crystals (12.7 mg, 81%). Optical rotation $[\alpha]_D$ = +72.0 (c = 1 in $CHCl_3$). The product was characterised as described for the racemic acetate.

6.3 Experimental Procedures Related to Part B

6.3.1 Synthesis of 2-Iodo-1,3-dimethoxybenzene 120

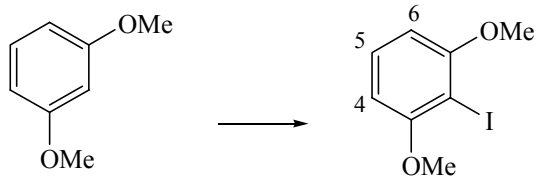

102 **120**

Into a flame dried 250 cm^3 RB flask fitted dropping funnel was placed dry THF (50 cm^3), followed by 1,3-dimethoxybenzene (4.74 cm^3, 5.00 g, 36.2 mmol). The solution was cooled down to 0 °C. Once cooled, the *n*-butyllithium (1.4 M in hexane, 28.4 cm^3, 39.8 mmol, 1.1 equiv.) was slowly added using a dropping funnel. The solution was stirred at 0 °C for 1 h. The dropping funnel was then charged with a solution of iodine (10.10 g, 39.8 mmol, 1.1 equiv.) in THF (70 cm^3). This solution was then added dropwise to the milky white reaction mixture. The end point of the reaction was observed at the appearance of the light brown halogen colour. The resulting solution was stirred for an additional 1 h at rt. Water was then added to the product mixture and the product extracted with CH_2Cl_2. The solvent was removed *in vacuo* and the crude product was recrystallised from dichloromethane-ethanol to give large white crystals of iodo-1,3-dimethoxybenzene (8.84 g, 93%). $\mathbf{R_f}$ = 0.70 (30% EtOAc/hexane); **mp.**= 103-105 °C (lit[102] 104 °C); **IR** ($CHCl_3$): $\nu_{max}(cm^{-1})$ = 1587, 1470 (m, Ar C=C); **^{1}H NMR** (300 MHz, $CDCl_3$): δ_H = 7.26 (1H, t, *J*=8.3, 5-H), 6.50 (2H, d, *J*=8.3, 6-H and 4-H), 3.89 (6H, s, 2 ×O*CH*$_3$); **^{13}C NMR** (75 MHz, $CDCl_3$) δ_C = 158.4 (2 × Ar *C*-O), 128.7 (C-5), 112.6 (Ar*C*-I), 104.5 (C-4 and C-6), 56.1 (2 × O*C*H_3); **HRMS:** Found M^+, 263.9654. $C_8H_9IO_2$ requires *M* 263.9647. *m/z* (EI) 264 (M^+, 100%), 249 (6), 221 (18), 206 (7), 122 (8), 107 (11), 92 (9), 77 (10),51 (8).

6.3.2 Synthesis of 2,2′,6,6′-Tetramethoxy-1,1′-biphenyl 103

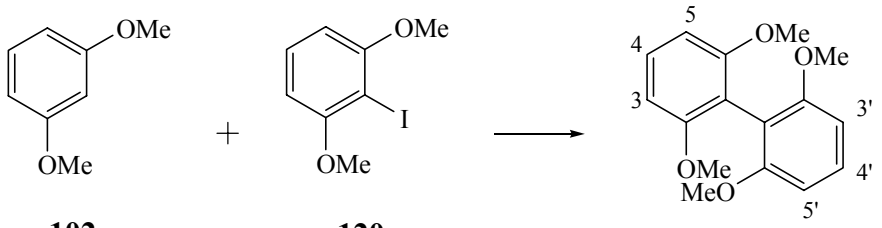

102 **120** **103**

Into a flame dried 250 cm^3 RB flask fitted dropping funnel was placed dry THF (50 cm^3), followed by 1,3-dimethoxybenzene (3.47 cm^3, 3.66 g, 26.5 mmol, 1.1 equiv.). The solution was cooled down to 0 °C. Once cooled, *n*-butyllithium (1.6 M in hexane, 16.56 cm^3, 26.5 mmol, 1.1 equiv.) was slowly added using the dropping funnel. The solution was stirred at 0 °C for 1 h. Copper(I) iodide (5.05 g, 26.5 mmol, 1.1 equiv.), dried overnight in an oven at 110 °C, was added in portions, and the mixture was stirred at rt for another 2 h. The dropping funnel was then charged with a solution of 2-iodo-1,3-dimethoxybenzene (6.36 g, 24.0 mmol) in dry pyridine (50 cm^3). Once added, the dropping funnel was replaced with a condenser, and the mixture was heated under reflux for 72 h. The product mixture was then poured onto ice and acidified with concentrated aqueous HCl (*ca.* 25 cm^3). The product was then extracted with CH_2Cl_2 (3 × 80 cm^3). The organic extracted were then combined, dried with anhydrous $MgSO_4$, and the solvent was removed *in vacuo*. The crude product was recrystallised from dichloromethane-ethanol to give 2,2′,6,6′-tetramethoxy-1,1′-biphenyl (6.12 g, 93%). $\mathbf{R_f}$ = 0.47 (30% EtOAc/hexane); **mp.**= 173-175 °C (lit[78] 175-176 °C); **IR** ($CHCl_3$): $\nu_{max}(cm^{-1})$ = 1587 (ArC=C); **^{1}H NMR** (300 MHz, $CDCl_3$): δ_H = 7.28 (2H, t, *J*=8.3, 3-H and 3′-H), 6.65 (4H, d, *J*=8.3, 3-H, 3′-H, 5-H and 5′-H), 3.71 (12H, s, 4 × OCH_3); **^{13}C NMR** (75 MHz, $CDCl_3$) δ_C = 158.4 (4 × Ar*C*-O), 128.7 (C-4 and C-4′), 112.5 (C-1 and C-1′), 104.4 (C-3, C-3′, C-5 and C-5′), 56.1 (4 × O*C*H_3); **HRMS**: Found M^+, 274.1198. $C_{16}H_{18}O_4$ requires *M* 274.1205; *m/z* (EI) 274 (M^+, 100%), 243 (7), 228 (11), 155 (5), 151 (20), 114 (6), 91 (6).

6.3.3 Synthesis of 2,6-Dimethoxyphenylboronic acid 122

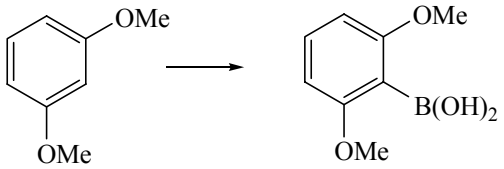

102 **122**

Into a flame dried 250 cm^3 RB flask fitted dropping funnel was placed dry THF (100 cm^3), followed by 1,3-dimethoxybenzene (4.74 cm^3, 5.00 g, 36.2 mmol). The solution was cooled down to 0 °C. Once cooled, the *n*-butyllithium (1.4 M in hexane, 31.1 cm^3, 43.4 mmol, 1.2 equiv.) was slowly added via the dropping funnel. The solution was stirred at 0 °C for 1 h. Trimethyl borate (16.22 cm^3, 15.04 g, 144.7 mmol, 4 equiv.) was then added dropwise via a syringe, at 0 °C. the reaction was stirred for 18 h and allowed to warm up to rt. The mixture was then poured into a large beaker equipped with a stirrer bar. An equivalence of water was added and additional ether (50 cm^3) the mixture was stirred vigorously and the initial pH checked to be basic. 1 M aqueous HCl was then added with stirring, and the pH checked after each addition. This was continued until the mixture was acidic. The organic layer was then extracted using diethyl ether (3 × 100 cm^3). The organic extracts were combined, washed with brine, dried with $MgSO_4$ and filtered. The solution was then concentrated (*ca.* 20 cm^3) by removing the solvent *in vacuo*. Hexane (*ca.* 100 cm^3) was then added to this, resulting in the precipitation of the boronic acid. The solution was cooled in an ice bath and the crystals were then collected by filtration, and washed with cold hexane to afford 2-ethyl-6-methoxyphenylboronic acid (4.65 g, 71%). $\mathbf{R_f}$ = 0.27 (30% EtOAc/hexane); **mp.**= 92-96 °C (lit[103] 100-115 °C); **IR** ($CHCl_3$): $\nu_{max}(cm^{-1})$ = 3474 (br,s, OH), 1650, 1586 (ArC=C); **^{1}H NMR** (300 MHz, $CDCl_3$): δ_H = 7.39 (1H, t, *J*=8.4, 4-H), 7.22 (2H, s, Ar-B(O*H*)$_2$), 6.64 (2H, d, *J*=8.4, 5-H and 3-H), 3.91 (6H, s, 2 × OC*H*$_3$); **^{13}C NMR** (75 MHz, $CDCl_3$) δ_C = 165.4 (2 × Ar*C*-O), 132.9 (C-4), 104.4 (C-3 and C-5), 56.0 (2 × O*C*H$_3$), 55.8 (Ar*C*-B(OH)$_2$); **HRMS:** Found M^+, 182.0761. $C_8H_{11}BO_4$ requires *M* 182.0750; *m/z* (EI) 182 (M^+, 100%), 181 (26), 164 (24), 138 (11), 109 (10), 78 (10), 76 (34).

6.3.4 Synthesis of 2,2′,6,6′-Tetramethoxy-1,1′-biphenyl 103

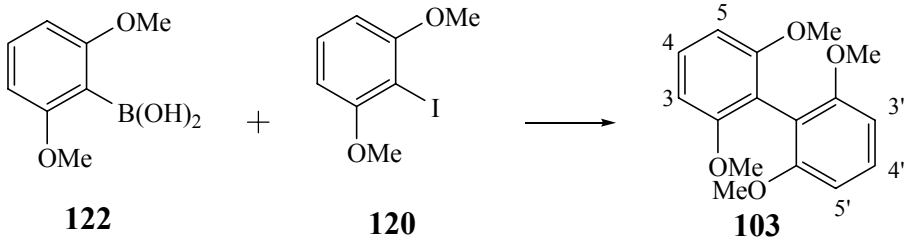

122 **120** **103**

Into a two neck RB flask fitted with a dropping funnel and a condenser (oven dried and under argon) was placed $Pd(PPh_3)_4$ (0.87 g, 0757 mmol, 10 mol%) and 2,6-dimethoxyphenylboronic acid (2.07 g, 11.36 mmol, 1.5 equiv.). The reaction vessel was degassed 5 times and refilled with argon gas. The dropping funnel was then charged with DME (21.0 cm^3) and 2-iodo-1,3-dimethoxybenzene (2.0 g, 7.57 mmol). Argon gas was then bubbled into the dropping funnel by means of a Pasteur pipette and the solution was quickly added to the reaction flask. The dropping funnel was recharged with an aqueous Na_2CO_3 solution (1.8 M, 4.01 g, 21.0 cm^3, 5 equiv.). This solution was similarly degassed for 10 mins and then discharged into the reaction vessel. The two phase mixture was heated to reflux and the yellow reaction mixture was left to reflux for 18 h. During this time the solution became homogenous as the catalyst fully dissolved and a colour change from yellow to pale brown occurred. The reaction mixture was cooled and decanted into a separating funnel. The flask was washed out with EtOAc (*ca* 100 cm^3) and water (*ca* 100 cm^3). After thorough mixing, the organic phase was separated and the aqueous phase was extracted with EtOAc (3 × 80 cm^3). The combined organic fractions were then washed with brine and dried over anhydrous $MgSO_4$. After evaporation of the solvent *in vacuo* the crude material was purified by column chromatography (5 →10 →20% EtOAc/hexane) affording the desired 2,2′,6,6′-tetramethoxy-1,1′-biphenyl (1.41 g, 54%), as the unoptimised yield. The product was characterised as previously described in **Section 6.3.2**.

6.3.5 Synthesis of 2,2',6,6'-Tetramethoxy[1,1′-biphenyl]-3,3′-dicarbaldehyde 104

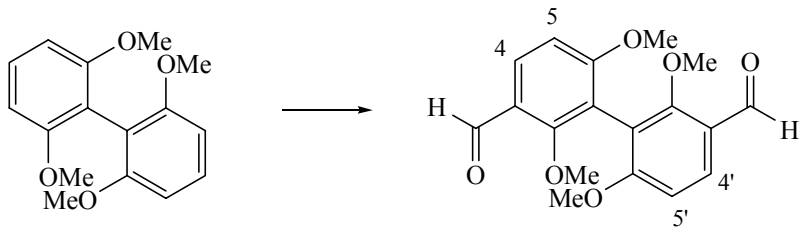

103 **104**

Into a two neck RB flask under argon, fitted with a rubber septum, was added 2,2′,6,6′-tetramethoxy-1,1′-biphenyl (0.70 g, 2.55 mmol) in dry CH_2Cl_2 (50 cm^3). To this solution was added titanium tetrachloride (1.12 cm^3, 1.93 g, 10.2 mmol, 4 equiv.) using a syringe through the septum. The solution immediately changed to an orange colour. The reaction mixture was then cooled down to −78 °C and dichloromethyl methyl ether (0.64 cm^3, 0.82 g, 7.14 mmol, 2.8 equiv.) was then added. The solution changed to a dark brown colour. Stirring at this temperature continued for 30 mins. The resulting solution was then warmed up to 0 °C over 1 h and stirred at this temperature for an additional 15 mins. The product mixture was then poured into a separating funnel containing crushed ice (*ca* 10 g) and aqueous conc. HCl (*ca* 8 cm^3) and shaken vigourously. The organic layer was then separated, washed with water (*ca* 50 cm^3) and brine (*ca.* 50 cm^3). It was then dried over anhydrous $MgSO_4$, filtered and the solvent removed *in vacuo*. The crude material was purified by silica gel column chromatography (40% EtOAc/hexane) to give 2,2',6,6'-tetramethoxy[1,1′-biphenyl]-3,3′-dicarbaldehyde as a white solid (0.80 g, 95%). $\mathbf{R_f}$ = 0.20 (30% EtOAc/hexane); **mp.**= 151-155 °C; **IR** ($CHCl_3$): $\nu_{max}(cm^{-1})$ = 1673 and 1586 (ArC=C); **^{1}H NMR** (300 MHz, $CDCl_3$): δ_H = 10.17 (2H, s, 2 × ArC*H*O), 7.91 (2H, d, *J*=8.8, 4-H and 4′-H), 6.83 (2H, d, *J*=8.8, 5-H and 5′-H), 3.76 (6H, s, 2 × OCH_3), 3.52 (6H, s, 2 × OCH_3); **^{13}C NMR** (75 MHz, $CDCl_3$) δ_C = 188.8 (2 × Ar*C*HO), 163.5 (2 × Ar*C*-O), 162.7 (2 × Ar*C*-O), 130.6 (2 × Ar*C*H), 123.1 (2 × Ar*C*-CHO), 116.4 (2 × Ar*C*), 107.1 (2 × Ar*C*H), 63.0 (2 × O*C*H_3), 56.1 (2 × OCH_3); **HRMS**: Found M^+, 330.1093. $C_{18}H_{18}O_6$ requires *M* 330.1103; *m/z* (EI) 330 (M^+, 79%), 299 (100), 283 (16), 255 (28), 239 (66), 219 (17), 179 (28), 155 (10), 142 (9), 115 (10), 91 (5), 69 (19), 51 (5).

6.3.6 Synthesis of Diethyl [4,4′-diacetoxy-6,6′,8,8′-tetramethoxy-7,7′-binaphthalene]-2,2′-dicarboxylate 105

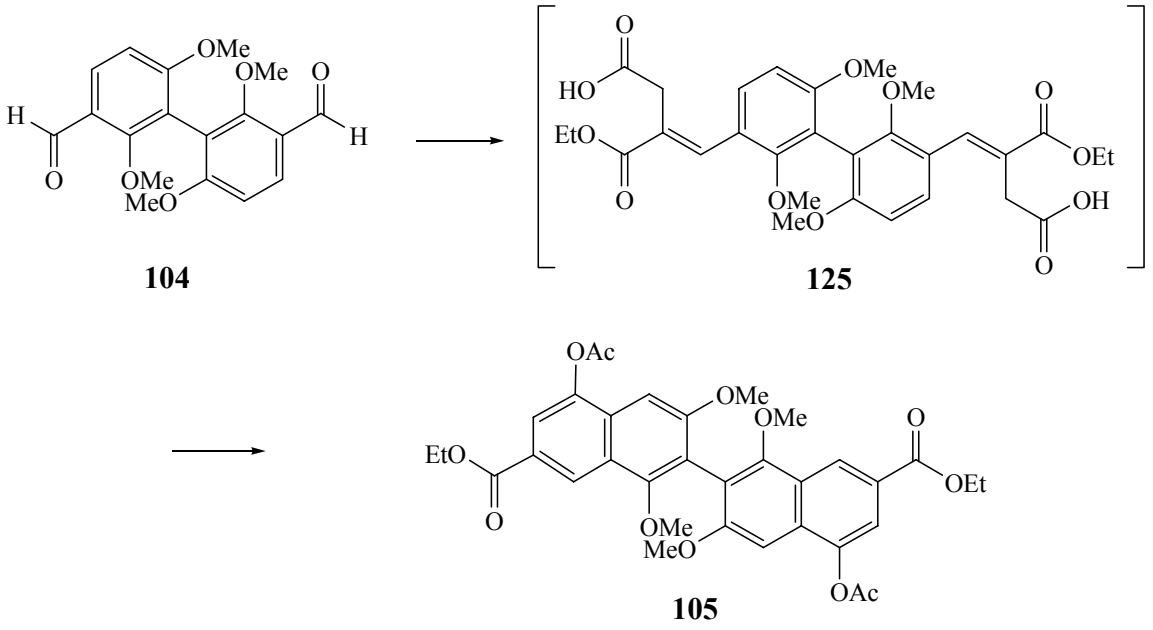

In a two neck RB flask, fitted with a condenser, under argon, 2,2',6,6'-tetramethoxy[1,1′-biphenyl]-3,3′-dicarbaldehyde (1.53 g, 4.63 mmol) and diethyl succinate (2.31 cm^3, 2.42 g, 13.9 mmol, 3 equiv.) were dissolved in dry *t*-butyl alcohol (20 cm^3). To this mixture was slowly added potassium-*t*-butoxide (1.56 g, 13.9 mmol, 3 equiv.). The resulting solution was heated under reflux for 2 h and then allowed to cool down to rt, poured into a separatory funnel containing ice and acidified to pH 3 with aqueous conc. HCl. The product was then extracted with EtOAc (3 × 50 cm^3). The combined organic extracts were then dried over anhydrous $MgSO_4$, filtered, and the solvent removed *in vacuo*. The resultant oil was not purified or characterised, but used immediately in the next step.

In a two neck RB flask, fitted with a condenser, under argon, the Stobbe condensation product from above was dissolved in acetic anhydride (80 cm^3). To this was added anhydrous sodium acetate (1.89 g, 23.2 mmol, 5 equiv.). The mixture was heated at 140 °C for 2 h and then allowed to cool. The acetic anhydride was removed *in vacuo*, water (*ca* 100 cm^3) was added, and the product extracted with CH_2Cl_2 (3 × 100 cm^3). The combined organic extracts were dried over anhydrous $MgSO_4$, filtered and the solvent

removed *in vacuo*. The crude material was purified by silica gel column chromatography (30% EtOAc/hexane) to yield diethyl [4,4′-diacetoxy-6,6′,8,8′-tetramethoxy-7,7′-binaphthalene]-2,2′-dicarboxylate **105** as a bright yellow solid (1.78 g, 60% over two steps). $\mathbf{R_f}$ = 0.17 (30% EtOAc/hexane); **mp.**= >180 °C; **^{1}H NMR** (300 MHz, $CDCl_3$): δ_H = 8.77 (2H, s, 2 × Ar*C*H), 7.87 (2H, s, 2 × Ar*C*H), 7.01 (2H, s, 2 × Ar*C*H), 4.43 (4H, q, *J*=7.1, 2 × OC*H*$_2$CH$_3$), 3.84 (6H, s, 2 × OC*H*$_3$), 3.64 (6H, s, 2 × OC*H*$_3$), 2.51 (6H, s, 2 × COC*H*$_3$), 1.42 (6H, t, *J*=7.1, 2 × OCH$_2$C*H*$_3$); **^{13}C NMR** (75 MHz, $CDCl_3$) δ_C = 169.4 (2 × CH$_3$*C*=O), 166.2 (2 × Ar *C*=OOEt), 159.2 (2 × Ar*C*OCH$_3$), 156.5 (2 × Ar*C*OCH$_3$), 145.7 (2 × Ar*C*), 130.9 (2 × Ar*C*), 125.2 (2 × Ar*C*), 124.7 (2 × Ar*C*), 123.9 (2 × Ar*C*H), 118.9 (2 × Ar *C*H), 117.8 (2 × Ar*C*), 94.9 (2 × Ar*C*H), 61.9 (2 × O*C*H$_3$), 61.1 (2 × OCH$_2$CH$_3$), 55.8 (2 × O*C*H$_3$), 21.0 (2 × C=O*C*H$_3$), 14.4 (2 × OCH$_2$*C*H$_3$); **HRMS**: Found M^+, 634.2038. $C_{34}H_{34}O_{12}$ requires *M* 634.2050; *m/z* (EI) 634 (M^+, 2%), 512 (32), 470 (27), 428 (73), 382 (5), 54 (26), 43 (18).

REFERENCES

1. M. A. Brimble, L. J. Duncalf, and M. R. Nairn, *Nat. Prod. Rep.*, 1999, **16**, 267 and references therein.
2. H. Schmid, T. M. Meijer, and A. Ebnöther, *Helv. Chim. Acta*, 1950, **33**, 1751.
3. H. Schmid and A. Ebnöther, *Helv. Chim. Acta*, 1951, **34**, 561.
4. S. B. Singh, M. G. Cordingley, R. G. Ball, J. L. Smith, A. W. Dombrowski, and M. A. Goetz, *Tetrahedron Lett.*, 1991, **32**, 5279.
5. T. Hanumaiah, D. S. Marshall, B. K. Rao, C. P. Rao, G. S. R. Rao, J. U. M. Rao, K. V. J. Rao, and R. H. Thomson, *Phytochemistry*, 1985, **24**, 2373.
6. S. R. Jammula, S. B. Pepalla, H. Telikepalli, K. V. J. Rao, and R. H. Thomson, *Phytochemistry*, 1991, **30**, 3741.
7. M. E. Bergy, *J. Antibiot.*, 1968, **21**, 454.
8. L. E. Johnston and A. Dietz, *Appl. Microbiol.*, 1968, **16**, 1815.
9. H. Tsujibo, T. Sakamoto, K. Miyamoto, G. Kusano, M. Ogura, T. Hasegawa, and Y. Inamori, *Chem. Pharm. Bull.*, 1990, **38**, 2299.
10. E. L. Rosenfeld and H. E. Laubach, *J. Parisitol*, 1986, **72**, 770.
11. H. Tanaka, Y. Koyama, T. Nagai, H. Marumo, and S. Omura, *J. Antibiot.*, 1975, **28**, 868.
12. J. C. V. Meter, M. Dann, and N. Bohonos, *Antimicrob. Agents Ann.*, 1961, 77.
13. G. A. Ellestad, M. P. Kunstmann, H. A. Whaley, and E. L. Patterson, *J. Am. Chem. Soc.*, 1968, **90**, 1325.
14. G. A. Ellestad, H. A. Whaley, and E. L. Patterson, *J. Am. Chem. Soc.*, 1966, **88**, 4109.
15. A. Nakagawa, N. Fukamachi, K. Yamaki, M. Hayashi, S. Ohisi, B. Kobayashi, and S. Omura, *J. Antibiot.*, 1987, **40**, 1075.
16. J. E. Hochlowski, G. M. Brill, W. W. Andres, S. G. Spanton, and J. B. McAlpine, *J. Antibiot.*, 1987, **40**, 401.
17. N. Tsuji, M. Kobayashi, Y. Wakisaka, Y. Kawamura, M. Mayama, and K. Matsumoto, *J. Antibiot.*, 1976, **29**, 7.
18. H. Brockmann, H. Pini, and O. von Plotho, *Chem. Ber.*, 1950, **83**, 161.
19. D. Ling, L. S. Sheild, and K. L. Reinhart, *J. Antibiot.*, 1986, **39**, 345.
20. M. S. Buchanan, M. Gill, and J. Yu, *J. Chem. Soc., Perkin Trans. 1*, 1997, 919.

21. H. W. Moore, *Science*, 1977, **197**, 527.
22. H. W. Moore and R. Czerniak, *Med. Res. Rev.*, 1981, **1**, 249.
23. A. J. Lin, L. A. Cosby, C. W. Shanksky, and A. C. Sartorelli, *J. Med. Chem.*, 1972, **15**, 1247.
24. J. Oliveira, 'The Synthesis of Isochromanols. Potential Bioreductive Alkylating Agents', PhD, University of the Witwatersrand, Johannesburg, 2000.
25. H. S. Schwartz, J. E. Sodergren, and F. S. Philips, *Science*, 1963, **142**, 1181.
26. V. N. Iyer and W. Szybalski, *Science*, 1964, **145**, 55.
27. B. A. Schweitzer, M. Egholm, and T. H. Koch, *J. Am. Chem. Soc.*, 1991, **114**, 242.
28. M. A. Brimble and M. R. Nairn, *J. Chem. Soc., Perkin Trans. 1*, 2000, 317.
29. C. Cullinane, A. van Rosmalen, and D. R. Phillips, *Biochemistry*, 1994, **33**, 4632.
30. G. Gaudiano, K. Resing, and T. H. Koch, *J. Am. Chem. Soc.*, 1994, **116**, 6537.
31. G. Gaudiano, M. Frigerio, C. Sangsurasak, P. Bravo, and T. Koch, *J. Am. Chem. Soc.*, 1992, **114**, 5546 and references cited therein.
32. S. R. Angle, J. D. Rainier, and C. Woytowicz, *J. Org. Chem.*, 1997, **62**, 5884.
33. D. H. Sherman, M. J. Bibb, T. J. Simpson, D. Johnson, F. Malpartida, M. Fernandez-Moreno, E. Martinez, C. R. Hutchinson, and D. A. Hopwood, *Tetrahedron*, 1991, **47**, 6029.
34. J. N. Collie, *J. Chem. Soc.*, 1907, **91**, 1806.
35. A. J. Birch, *Science*, 1967, **156**, 202.
36. H. G. Floss and J. M. Beale, *Angew. Chem. Int. Ed. Engl*, 1989, **28**, 146.
37. D. O'Hagan, *Nat. Prod. Rep.*, 1992, **9**, 447.
38. T. M. Harris and C. M. Harris, *Tetrahedron*, 1977, **33**, 2159.
39. A. D. Webb and T. M. Harris, *Tetrahedron Lett.*, 1977, 2069.
40. M. A. Brimble, M. R. Nairn, and H. Prabaharan, *Tetrahedron*, 2000, **56**, 1937 and references therein.
41. K. Tatsuta, K. Akimoto, M. Annaka, Y. Ohno, and M. Kinoshita, *Bull. Chem. Soc. Jpn.*, 1985, **58**, 1699.
42. C. B. de Koning, I. R. Green, J. P. Michael, and J. R. Oliveira, *Tetrahedron*, 2001, **57**, 9623.

43. M. P. Winters, M. Stranberg, and H. W. Moore, *J. Org. Chem.*, 1994, **59**, 7572.
44. H. Laatsch, *Liebigs Ann. Chem.*, 1986, 297.
45. D. W. Cameron and H. W.-S. Chan, *J. Chem. Soc.*, 1966, 1825.
46. D. W. Cameron, H. W.-S. Chan, and E. M. Hildyard, *J. Chem. Soc. (C)*, 1966, 1832.
47. L. K. Li, 'The Synthesis of Isochromanes, Isochromenes and Isochromanols', MSc, University of the Witwatersrand, Johannesburg, 2002.
48. E. M. Mmutlane, 'The Synthesis of Aromatic Precursors for Cardinalins and Anthracyclines', PhD, University of the Witwatersrand, Johannesburg, 2004.
49. E. M. Mmutlane, J. P. Michael, I. R. Green, and C. B. de Koning, *Org. Biomol. Chem.*, 2004, **2**, 2461.
50. J. M. Bruce and Y. Roshan-Ali, *J. Chem. Soc., Perkin Trans. 1*, 1981, 2677.
51. W. Baker and O. M. Lothian, *J. Chem. Soc.*, 1939, 274.
52. A. Fürstner, *Angew. Chem. Int. Ed.*, 2000, **39**, 3012.
53. S. T. Nguyen, L. K. Johnson, R. H. Grubbs, and J. W. Ziller, *J. Am. Chem. Soc.*, 1992, **114**, 3974.
54. J. Louie and R. H. Grubbs, *Angew. Chem. Int. Ed.*, 2001, **40**, 247.
55. J. L. Herisson and Y. Chauvin, *Makromol. Chem.*, 1970, **141**, 161.
56. Y. Okimoto, S. Sakaguchi, and Y. Ishii, *J. Am. Chem. Soc.*, 2002, **124**, 1590.
57. W. A. L. van Otterlo, E. L. Ngidi, and C. B. de Koning, *Tetrahedron Lett.*, 2003, **44**, 6483.
58. W. A. L. van Otterlo, R. Pathak, and C. B. de Koning, *Synlett.*, 2003, **12**, 1859.
59. M. Arisawa, Y. Terada, M. Nakagawa, and A. Nishida, *Angew. Chem. Int. Ed.*, 2002, **41**, 4732.
60. S. Krompiec, N. Kuznik, T. Bieg, B. Adamus, J. Majnusz, and M. Grymel, *Polish J. Chem.*, 2000, **74**, 1197.
61. S. Krompiec, M. Pigulla, W. Szczepankiewicz, T. Bieg, N. Kuznik, K. Leszczynska-Sejda, M. Kubicki, and T. Borowiak, *Tetrahedron Lett.*, 2001, **42**, 7095.
62. M. A. Brimble and R. J. R. Elliot, *Tetrahedron*, 2002, **58**, 183.
63. A. K. Mandal, P. K. Jadhav, and H. C. Brown, *J. Org. Chem.*, 1980, **45**, 3543.

64. A. N. C. Lötter, Honours Project, University of the Witwatersrand, Johannesburg, 2003.
65. J. S. Parratt, M. C. Cripps, S. J. Faulconbridge, K. E. Holt, C. L. Rippé, S. P. Savage, and S. J. C. Taylor, *Royal Society of Chemistry Annual reports Book B*, 291.
66. T. H. D. Bugg, 'Introduction to Enzyme and Coenzyme Chemistry', Blackwell Publishing, Oxford, 2004.
67. D. R. Yazbeck, C. A. Martinez, S. Hu, and J. Tao, *Tetrahedron Assymmetry*, 2004, 2757.
68. S. Raza, L. Fransson, and K. Hult, *Protein Science*, 2001, **10**, 329.
69. A. Magnusson, 'Rational redesign of *Candida antarctica* lipase B', PhD, Royal Institute of Technology, Stockholm, 2005 and references therein.
70. M. L. Semmelhack, 'Comprehensive Organometallic Chemistry II', ed. F. G. A. Stone, Pergamon Press, New York, 1995.
71. S. G. Davies, S. J. Cootes, and C. L. Goodfellow, 'Advances in Metal-Organic Chemistry', ed. L. S. Liebeskind, JAI Press, London, 1991.
72. G. Jaouen, S. Top, A. Laconi, D. Couturier, and J. Brocard, *J. Am. Chem. Soc*, 1984, **106**, 2207.
73. C. A. L. Mahaffy and P. Pauson, *Inorg. Synth.*, 1990, **28**, 137.
74. 'Encyclopedia of Chemical Technology', Wiley, New York, 1963.
75. J. Lindley, *Tetrahedron*, 1984, **40**, 1433.
76. J. K. Kochi, 'Organometallic Mechanisms and Catalysis', Academic press, New York, 1978.
77. www.organic-chemistry.org/namereactions/ullmann-reaction.shtm.
78. G. Lindsten, O. Wennerström, and R. Isaksson, *J. Org. Chem.*, 1987, **52**, 547.
79. T. D. Nelson and R. D. Crouch, 'Organic Reactions: Cu, Ni and Pd Mediated Homocoupling Reactions in Biaryl Syntheses: The Ullmann Reaction', ed. L. E. Overman, John Wiley & Sons Inc, New Jersey, 2004.
80. J. F. Bunnett and R. E. Zahler, *Chem. Rev.*, 1951, **49**, 273.
81. G. R. Bacon and H. A. O. Hill, *J. Chem. Soc.*, 1964, 1097.
82. J. Forrest, *J. Chem. Soc.*, 1960, 562.
83. N. Miyaura and A. Suzuki, *Main Group Met. Chem.*, 1987, **10**, 295.
84. J. R. Falck, S. Mohapatra, and S. K. Venkataraman, *Tetrahedron Lett.*, 2002, **43**, 8149.

85. T. R. Kelly and R. L. Xie, *J. Org. Chem.*, 1998, **63**, 8045.
86. J. Finet, A. Y. Fedorov, S. Combes, and G. Boyer, *Curr. Org. Chem.*, 2002, **6**, 597.
87. http://www.organic-chemistry.org/namedreactions/suzuki-coupling.shtm.
88. A. Vilsmeier and A. Haack, *Ber. Dtsch. Chem. Ges.*, 1927, **60B**, 119.
89. A. G. Martinez, R. M. Alvarez, J. O. Barcina, S. d. l. M. Cerero, E. T. Vilar, A.G.Fraile, M. Hanack, and L. R. Subramanian, *J. Chem. Soc. Chem. Commun.*, 1990, 15711572.
90. H. Gross, A. Rieche, and G.Mattey, *Chem. Ber.*, 1963, **96**, 308.
91. O. Garcia, E. Nicolás, and F. Albericio, *Tetrahedron Lett.*, 2003, **44**, 4961.
92. W. S. Johnson and G. H. Daub, 'Organic Reactions: The Stobbe Condensation', ed. R. Adams, John Wiley & Sons Inc, New York, 1951.
93. D. D. Perrin and W. L. F. Armarego, 'Purification of Laboratory chemicals', Pergamon Press, Oxford, 1998.
94. Bruker, in '*SAINT*+Version 6.02 (includes XPREP and SADABS)', Madison, Wisconsin, USA, 1999.
95. Bruker, in 'SHELXTL Version 5.1 (includes XS, XL, XP and XSHELL)', Madison, Wisconsin, USA, 1999.
96. A. L. Spek, *J. Appl. Cryst.*, 2003, **36**, 7.
97. L. M. Harwood, *J. Chem. Soc., Perkin Trans. 1*, 1984, 2577.
98. H. Brunner and R. Störiko, *Eur. J. Inorg. Chem.*, 1998, **6**, 783.
99. E. Hardegger, D. Redlich, and A. Gal, *Helv. Chim. Acta.*, 1945, **28**, 628.
100. R. Taylor, G. G. Smith, and W. H. Wetzel, *J. Am. Chem. Soc.*, 1962, **84**, 4817.
101. K. Hattori, H. Sajiki, and K. Hirota, *Tetrahedron*, 2001, **57**, 4817.
102. J. C. Anderson and D. J. Pearson, *J. Chem. Soc., Perkin Trans. 1*, 1998, 2023.
103. H. G. Kuivila and K. V. Nahabedian, *J. Am. Chem. Soc*, 1960, **83**, 2159.

APPENDIX

A1: Selected ^{1}H and ^{13}C NMR Spectra Related to Part A

A1.1.1 The ^{1}H NMR Spectrum of Compound 107

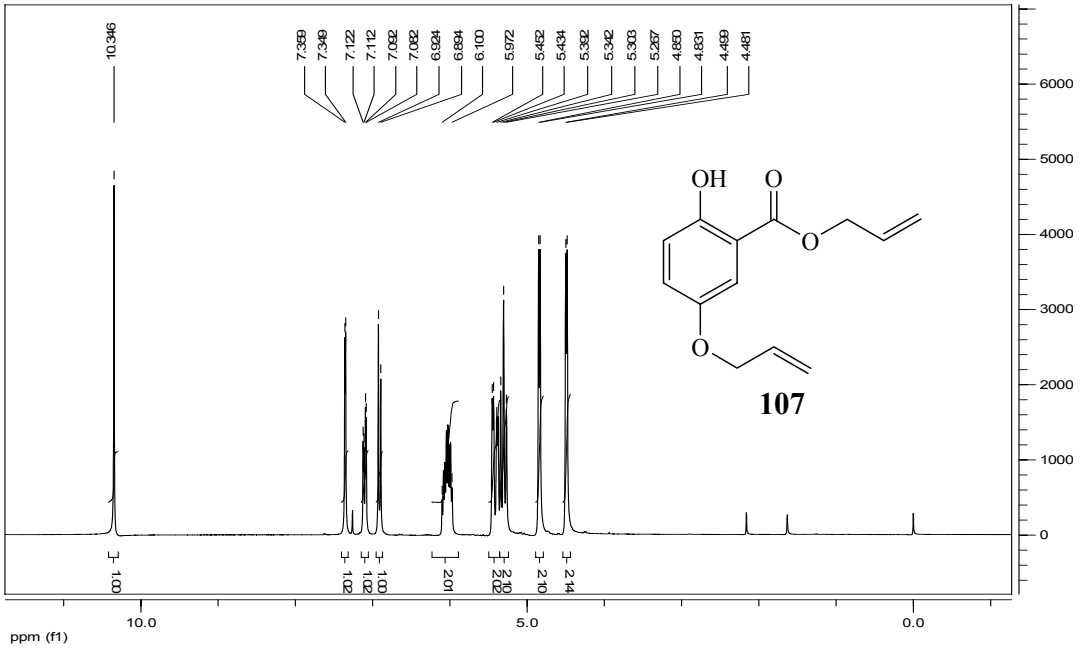

A1.1.2 The ^{13}C NMR Spectrum of Compound 107

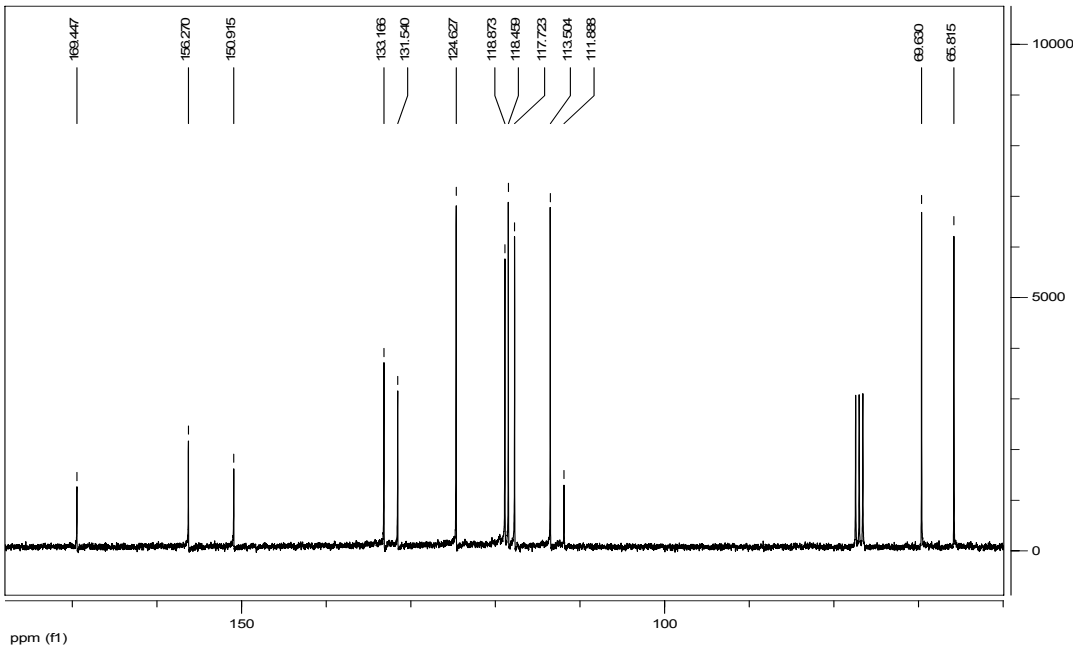

A1.2.1 The ^{1}H NMR Spectrum of Compound 88

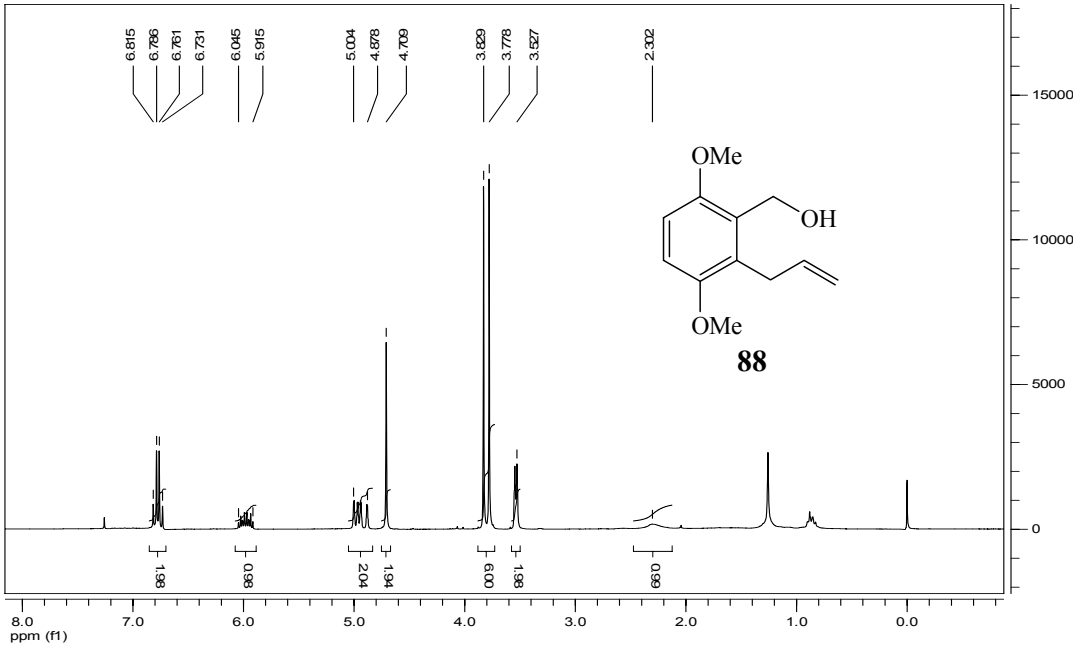

A1.2.2 The ^{13}C NMR Spectrum of Compound 88

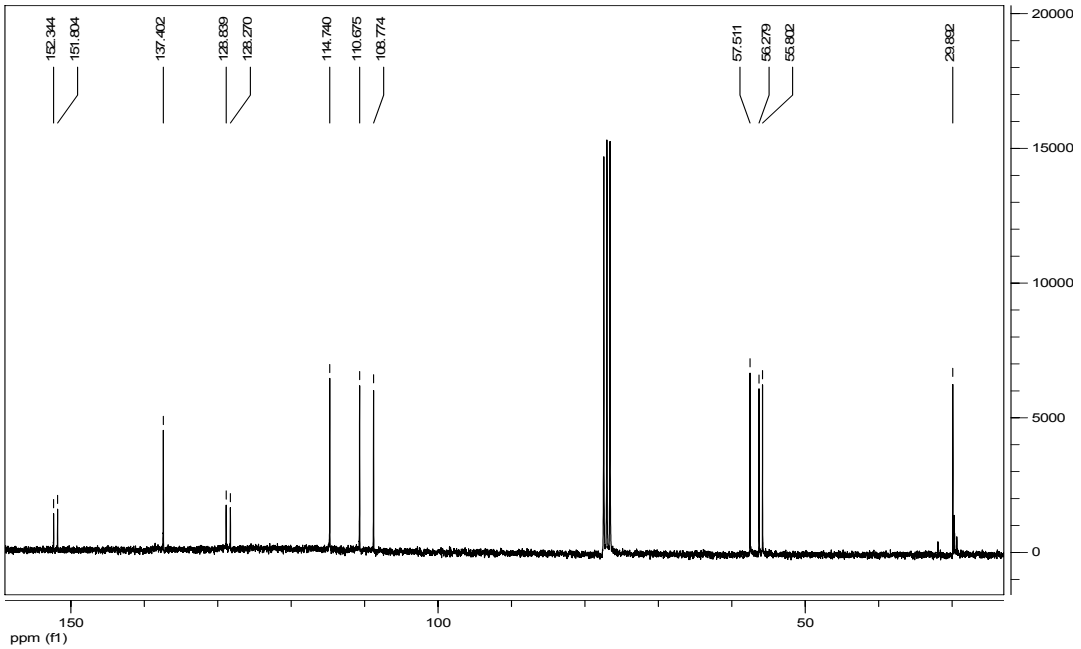

A1.3.1 The ^{1}H NMR Spectrum of Compound 86

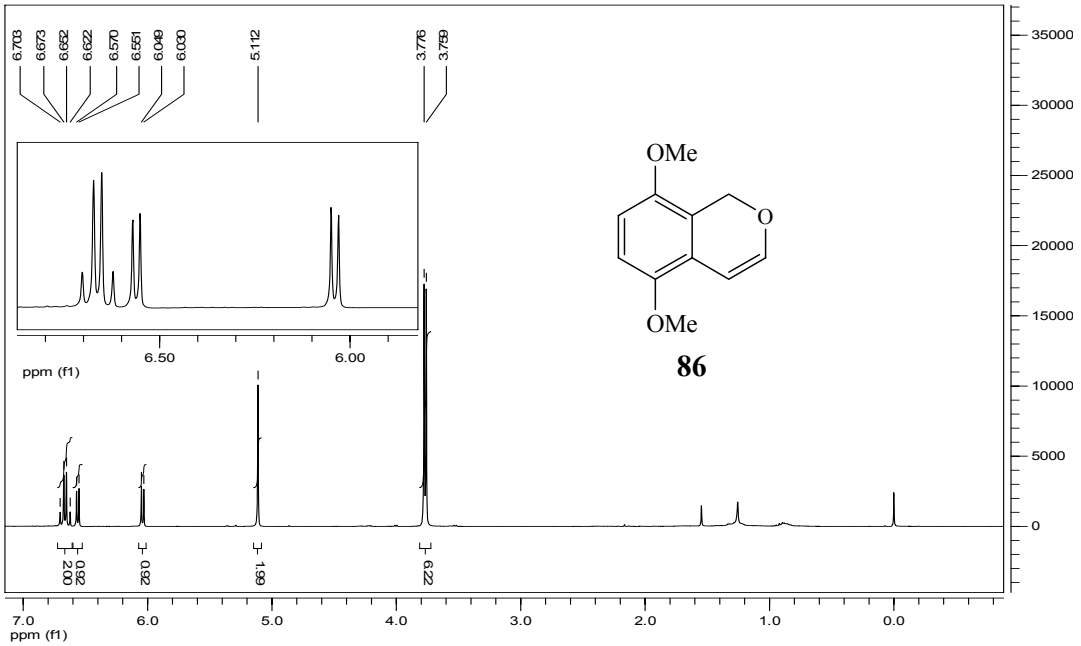

A1.3.2 The ^{13}C NMR Spectrum of Compound 86

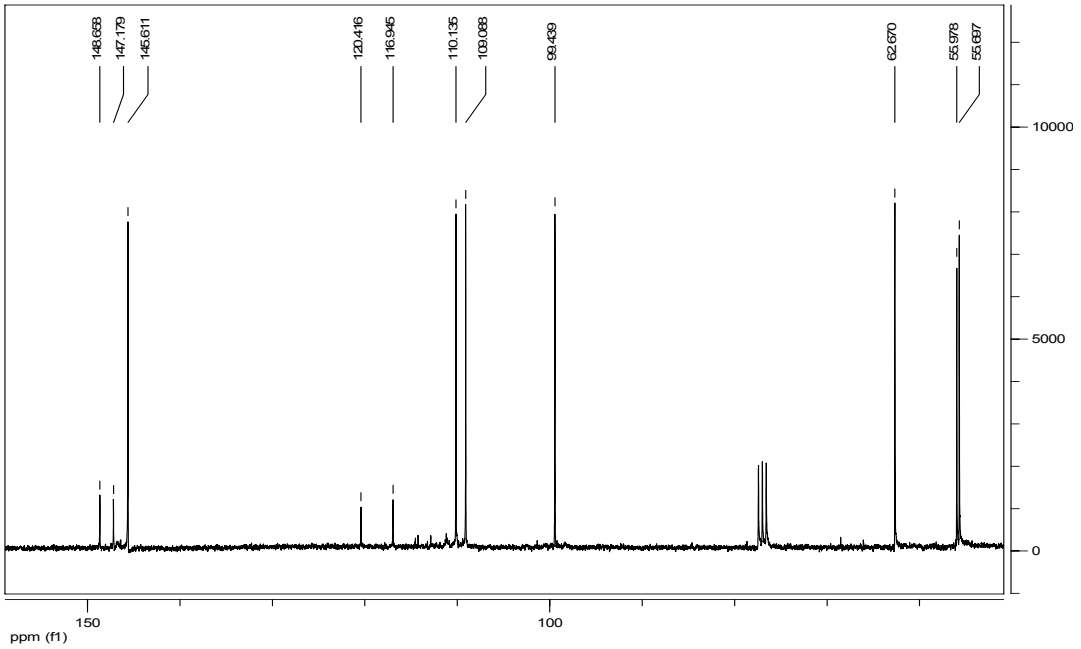

A1.4.1 The ^{1}H NMR Spectrum of Compound 89

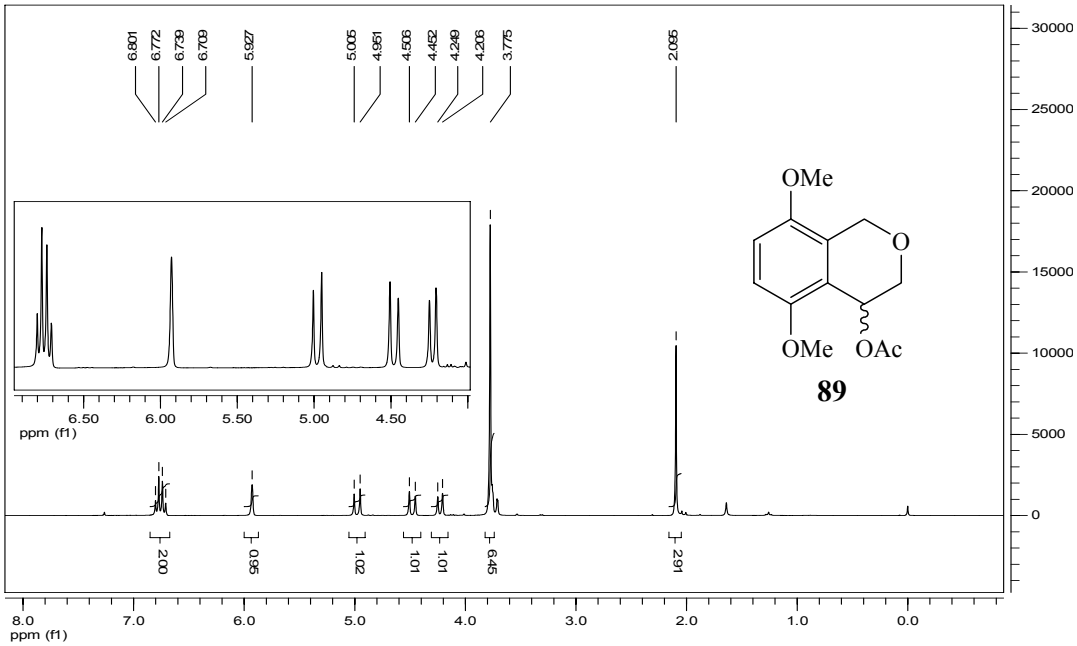

A1.4.2 The ^{13}C NMR Spectrum of Compound 89

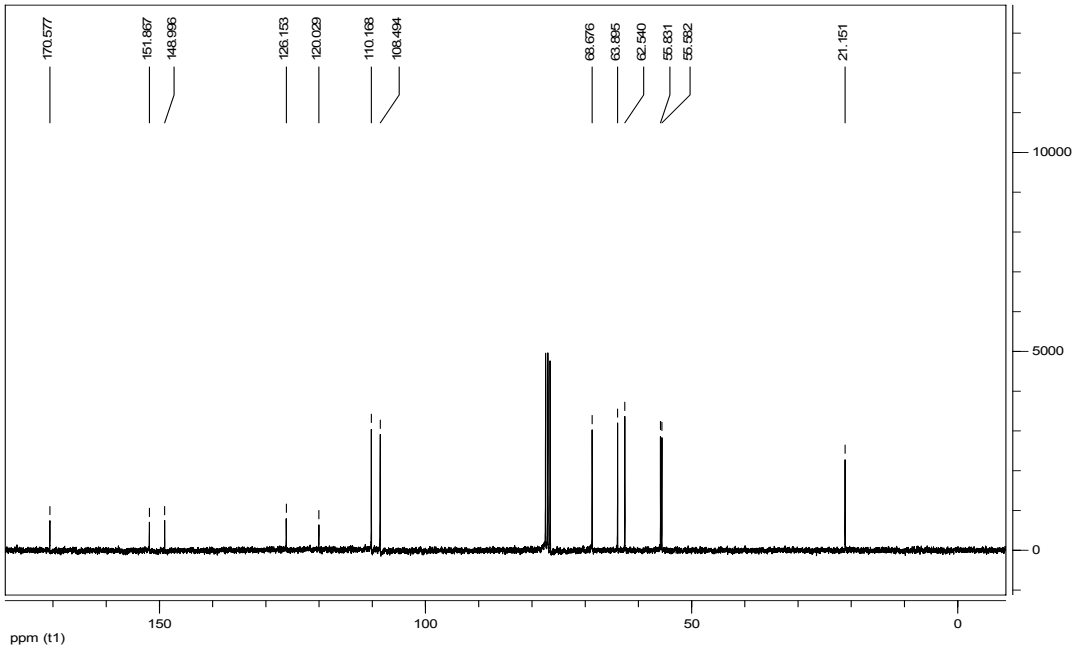

A2: Selected ^{1}H and ^{13}C NMR Spectra Related to Part B

A2.1.1 The ^{1}H NMR Spectrum of Compound 120

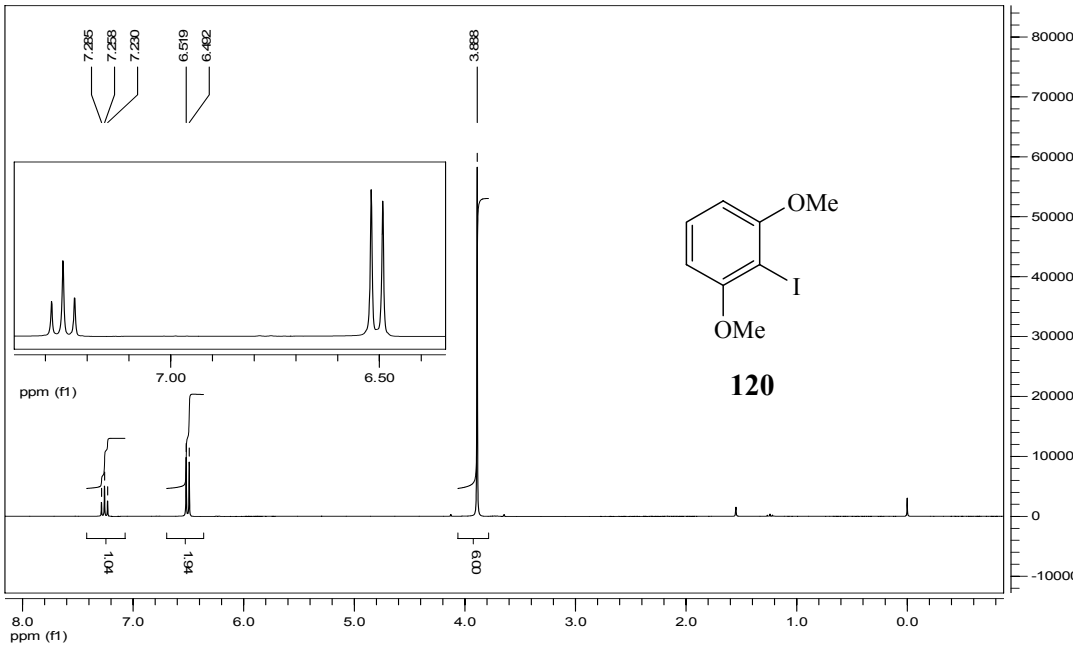

A2.1.2 The ^{13}C NMR Spectrum of Compound 120

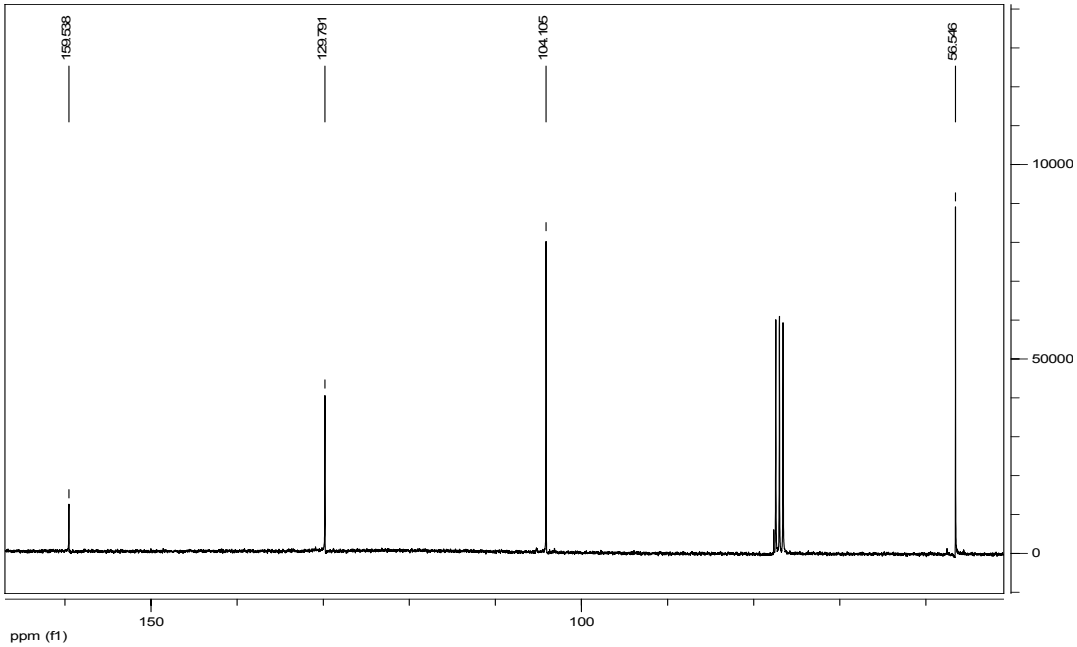

A2.2.1 The ^{1}H NMR Spectrum of Compound 103

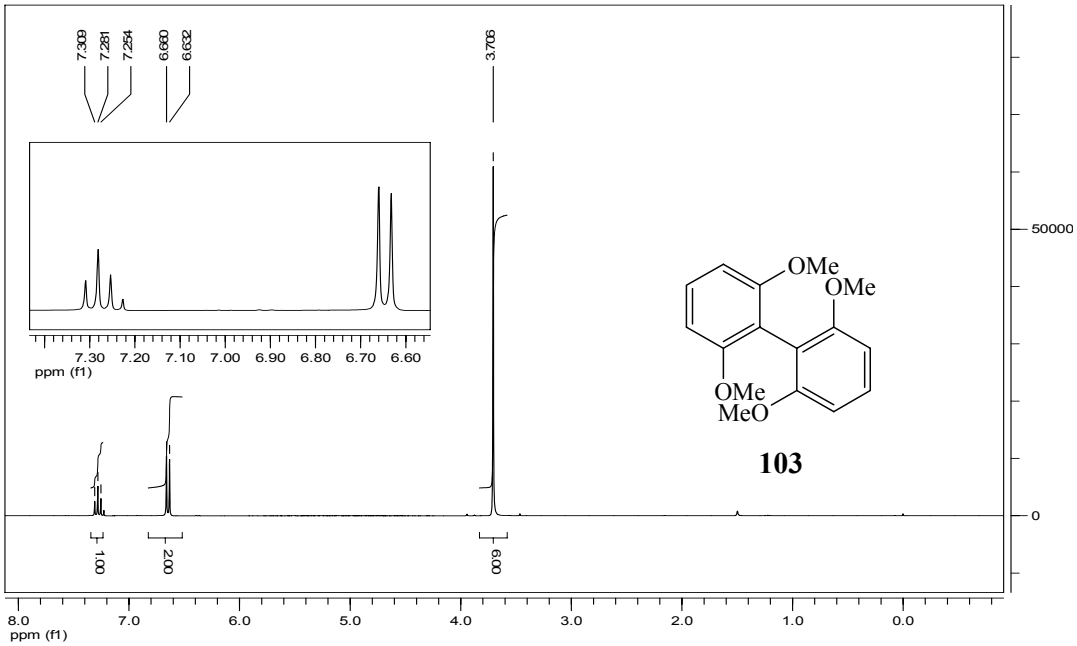

A2.2.2 The ^{13}C NMR Spectrum of Compound 103

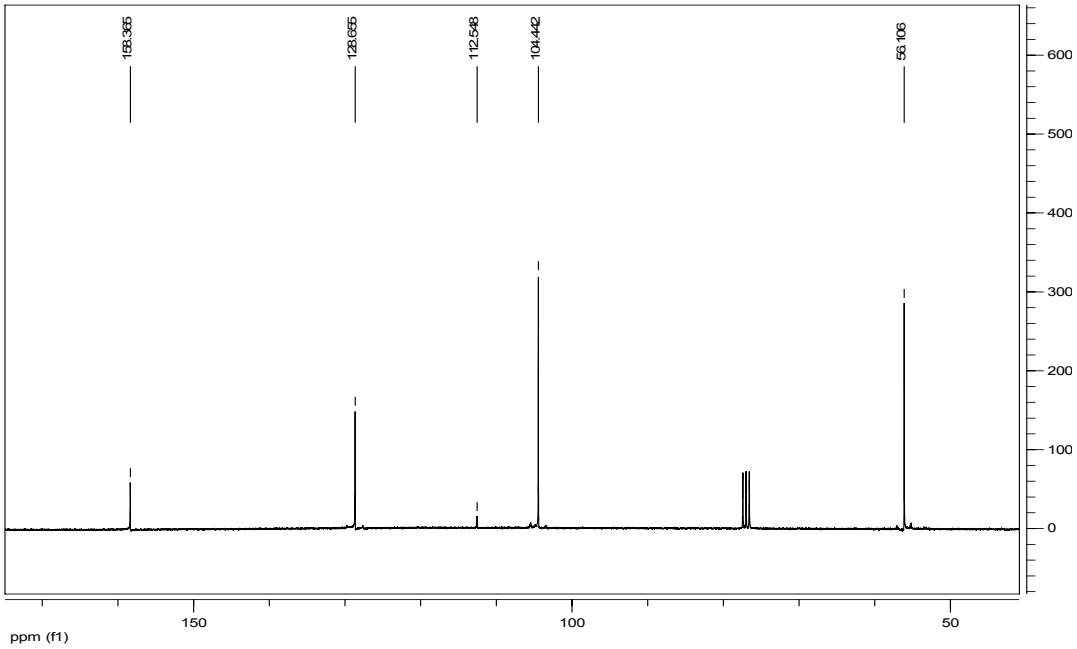

A2.3.1 The ^{1}H NMR Spectrum of Compound 104

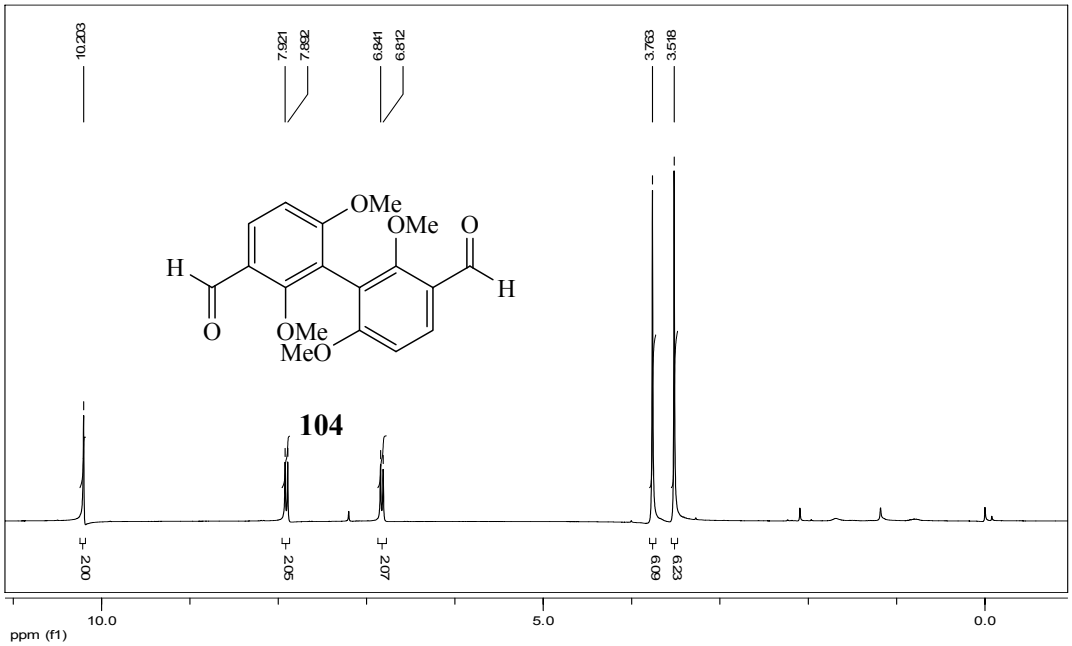

A2.3.2 The ^{13}C NMR Spectrum of Compound 104

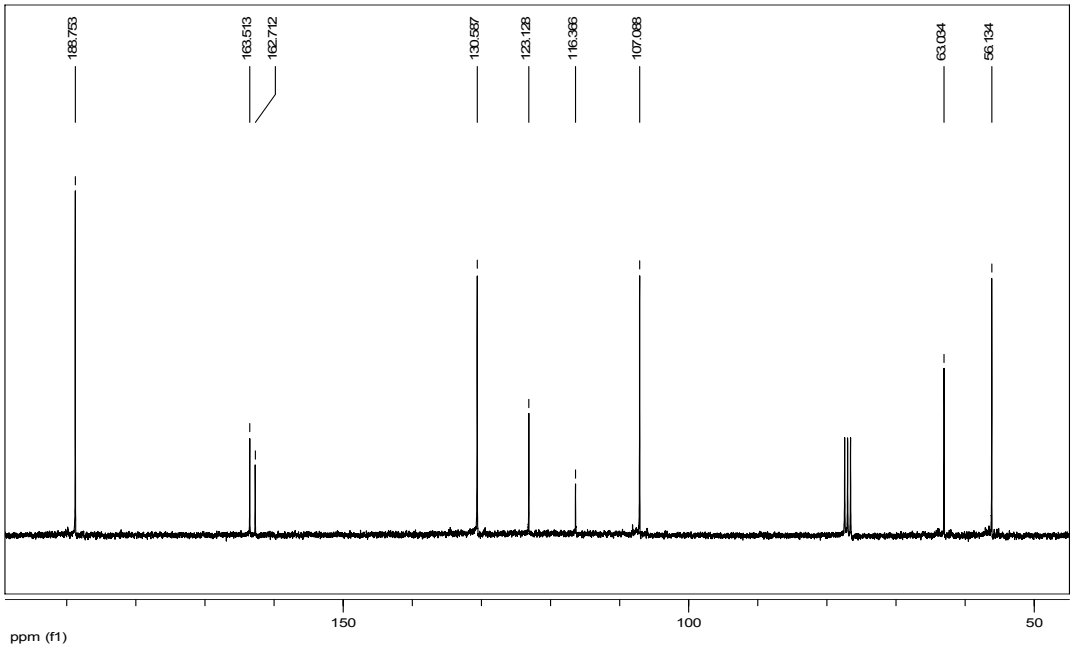

A2.4.1 ^{1}H NMR Spectrum of Compound 105

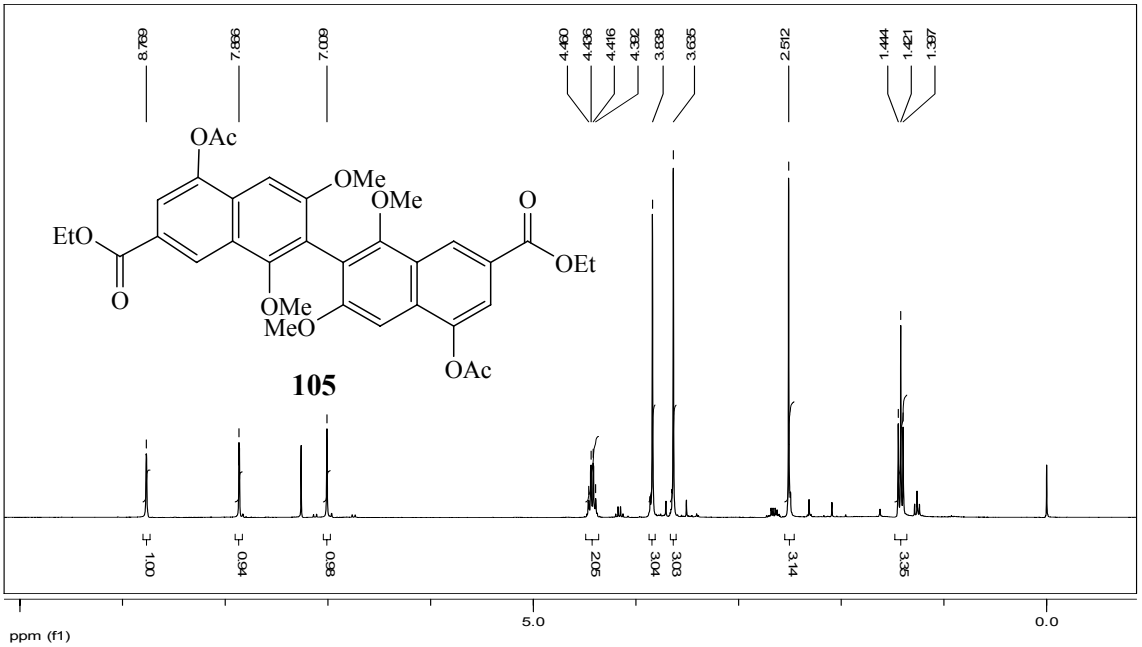

A2.4.2 ^{13}C NMR Spectrum of Compound 105

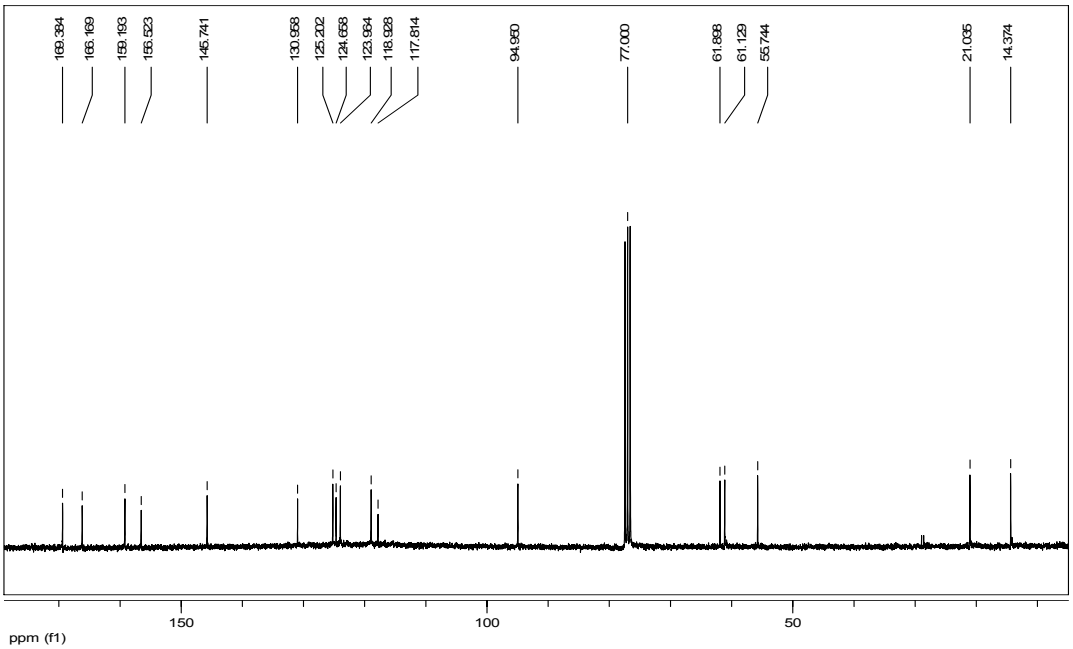

A3: Lipase Screening

A3.1 Commercial Enzymes Utilized

No.	Supplier	Enzyme (and abbreviation used)	Cat. No.
A1	Biochemica	Lipase, immobilised in Sol-Gel-AK from Candida antarctica **(BiLCa)**	62277
A2	Biochemica	Lipase from Mucor javanious **(BLMj)**	62304
A3	Biochemica	Lipase from Rhizopus niveus **(BLRn)**	62310
A4	Biochemica	Lipase from aspergillus **(Bla)**	84205
A5	Biochemica	Lipase from Penicillium roqueforti **(BLPr)**	62308
A6		Control	
B1	Biochemica	Lipase from Candida lipolytica **(BLCl)**	62303
B2	Biochemica	Lipase from Rhizopus arrhizus **(BLRa)**	62305
B3	Biochemica	Lipase from Pseudomonas flourescens **(BLPf)**	62312
B4	Enzymes SA	Lipase PS "Amano" **(ESALPsA)**	LPSAW03506
B5	Enzymes SA	Lipase M "Amano" 10 **(ESALMA10)**	LMW03503
B6		Control	
C1	Enzymes SA	Lipase F-APIS **(ESALFA)**	LFW02523
C2	Amano	Lipase **(AKALAK)**	lot LAKA 0351202
C3	Enzymes SA	Lipase G "Amano" 50 **(ESALGA50)**	LGDW01512
C4	Amano	Lipase AKC-I **(ALAKC-I)**	lot ILAKY0452/02K
C5	Enzymes SA	Lipase AYS "Amano" **(ESALAYSA)**	LAYW045145
C6		Control	
D1	Biochemika	Lipase from Aspergillus niger **(BLAn)**	62301
D2	Biochemika	Lipase from Candida antarctica **(BLCa)**	62299
D3	Biochemika	Lipase from Mucor miehei **(BLMm)**	62298
D4	Altus Biologies	Lipase-CR **(ABLCR)**	lot: ACR-94-001
D5	Biochemika	Lipase from wheatgerm **(BLW)**	62306
D6		Control	

E1	Biochemika	Lipase from Pseudomonas flourescens **(BLPf)**	71548
E2	Amano	Lipase AY "Amano" 30 **(ALAYA30)**	LAYT02510
E3	Biochemika	Lipase from hog pancreas **(BLHP)**	62300
E4	Biocatalysts	Lipase - L056P (P. flourescens) **(BcatLL056P0**	1781981
E5	Biocatalysts	Candida cylindracea-L034 **(BcatLCc)**	1988784
E6		Control	
F1	Biocatalysts	Lipase L115P **(BcatLL115P)**	1768981
F2	Biocatalysts	Lipase **L036P (BcatL036P)**	1493971
F3	Novozymes	Novozym 435 Lipase **(NL435)**	LC2 00015
F4	Biochemika	Lipase from Rhizopus oryzae **(BLRo)**	80612
F5	Novozymes	Lipozyme TL IM **(NLTLIM)**	LA 35000504
F6		Control	
G1	Enzymes SA	Lipolase 100T **(ESAL100T)**	LA 91231/10
G2	Novozymes	Lipozyme RM IM **(NLRMIM)**	LUX 00111
G3	Sigma	Lipase (EC 3.1.1.3) Type II, Crude, from Porcine Pancreas **(SLTIIPP)**	L3126 Lot 70H0688
G4	Novozymes	Novozym 525 **(NL525)**	LCN 01001
G5	Enzymes SA	SP 398 **(ESASP398)**	LAN 00052
G6		Control	
H1	Novozymes	Novozym 388 **(NL388)**	LUN 00020
H2	Biochemika	Esterase from Rhizopus oryzae **(BERo)**	79208
H3	Biochemika	Lipase from Pseudomonas cepacia **(BLPc)**	62309
H4	Biochemika	Esterase from horse liver **(BEHL)**	46069
H5	Biochemika	Esterase immobilized on Eupergit C from Hog liver **(BiEHL)**	46064
H6		Control	

A3.2 Lipase Kits

Columns 1 to 6 in the following tables (**1-5**) contained the alcohol substrate with the acyl donor vinyl acetate and columns 7 to 12 contained the acetate. Both reactions used the tris buffer system and IPA solvent. The positive results for the conversions are highlighted.

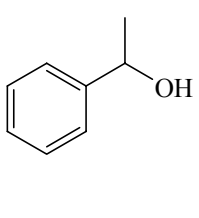

120

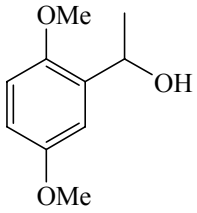

121

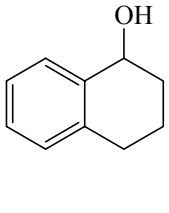

122

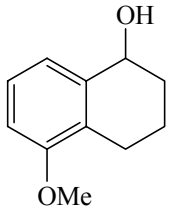

123

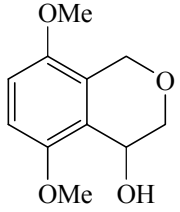

85

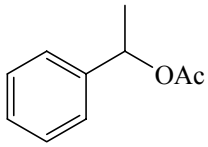

124

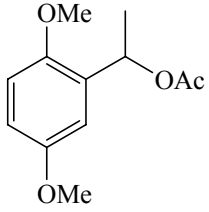

125

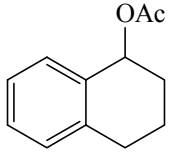

126

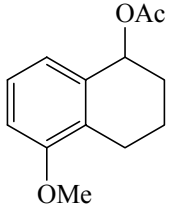

127

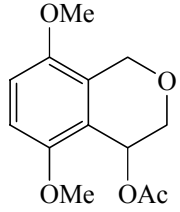

89

Table 1: Compounds 120 and 124

	1	2	3	4	5	6	7	8	9	10	11	12
A	BiL*Ca*	BL*Mj*	BL*Rn*	Bla	BL*Pr*	Control	BiL*Ca*	BL*Mj*	BL*Rn*	Bla	BL*Pr*	Control
B	BL*Cl*	BL*Ra*	BL*Cl*	ESAL*PsA*	ESALMA10	Control	BL*Cl*	BL*Ra*	BL*Cl*	ESAL*PsA*	ESALMA10	Control
C	ESAL*FA*	AL*AK*	ESAL*GA50*	AL*AKC-I*	ESAL*AYSA*	Control	ESAL*FA*	AL*AK*	ESAL*GA50*	AL*AKC-I*	ESAL*AYSA*	Control
D	BL*An*	BL*Ca*	BL*Mm*	ABL*CR*	BL*W*	Control	BL*An*	BL*Ca*	BL*Mm*	ABL*CR*	BL*W*	Control
E	BL*Pf*	AL*AYA30*	BL*HP*	Bcatl*L056P*	BcatL*Cc*	Control	BL*Pf*	AL*AYA30*	BL*HP*	Bcatl*L056P*	BcatL*Cc*	Control
F	Bcatl*L115P*	Bcat*L036P*	NL435	BL*Ro*	NL*TLIM*	Control	Bcatl*L115P*	Bcat*L036P*	NL435	BL*Ro*	NL*TLIM*	Control
G	ESAL*100T*	NL*RMIM*	SL*TIIPP*	NL*525*	ESA*SP398*	Control	ESAL*100T*	NL*RMIM*	SL*TIIPP*	NL*525*	ESA*SP398*	Control
H	NL*388*	BE*Ro*	BL*Pc*	BE*HL*	BiE*HL*	Control	NL*388*	BE*Ro*	BL*Pc*	BE*HL*	BiE*HL*	Control

Table 2: Compounds 121 and 125

	1	2	3	4	5	6	7	8	9	10	11	12
A	BiL*Ca*	BL*Mj*	BL*Rn*	Bla	BL*Pr*	Control	BiL*Ca*	BL*Mj*	BL*Rn*	Bla	BL*Pr*	Control
B	BL*Cl*	BL*Ra*	BL*Cl*	ESAL*PsA*	ESALMA10	Control	BL*Cl*	BL*Ra*	BL*Cl*	ESAL*PsA*	ESALMA10	Control
C	ESAL*FA*	AL*AK*	ESAL*GA50*	AL*AKC-I*	ESAL*AYSA*	Control	ESAL*FA*	AL*AK*	ESAL*GA50*	AL*AKC-I*	ESAL*AYSA*	Control
D	BL*An*	BL*Ca*	BL*Mm*	ABL*CR*	BL*W*	Control	BL*An*	BL*Ca*	BL*Mm*	ABL*CR*	BL*W*	Control
E	BL*Pf*	AL*AYA30*	BL*HP*	Bcatl*L056P*	BcatL*Cc*	Control	BL*Pf*	AL*AYA30*	BL*HP*	Bcatl*L056P*	BcatL*Cc*	Control
F	Bcatl*L115P*	Bcat*L036P*	NL435	BL*Ro*	NL*TLIM*	Control	Bcatl*L115P*	Bcat*L036P*	NL435	BL*Ro*	NL*TLIM*	Control
G	ESAL*100T*	NL*RMIM*	SL*TIIPP*	NL*525*	ESA*SP398*	Control	ESAL*100T*	NL*RMIM*	SL*TIIPP*	NL*525*	ESA*SP398*	Control
H	NL*388*	BE*Ro*	BL*Pc*	BE*HL*	BiE*HL*	Control	NL*388*	BE*Ro*	BL*Pc*	BE*HL*	BiE*HL*	Control

Table 3: Compounds 122 and 126

	1	2	3	4	5	6	7	8	9	10	11	12
A	BiL*Ca*	BL*Mj*	BL*Rn*	Bla	BL*Pr*	Control	BiL*Ca*	BL*Mj*	BL*Rn*	Bla	BL*Pr*	Control
B	BL*Cl*	BL*Ra*	BL*Cl*	ESAL*PsA*	ESALMA10	Control	BL*Cl*	BL*Ra*	BL*Cl*	ESAL*PsA*	ESALMA10	Control
C	ESAL*FA*	AL*AK*	ESAL*GA50*	AL*AKC-I*	ESAL*AYSA*	Control	ESAL*FA*	AL*AK*	ESAL*GA50*	AL*AKC-I*	ESAL*AYSA*	Control
D	BL*An*	BL*Ca*	BL*Mm*	ABL*CR*	BL*W*	Control	BL*An*	BL*Ca*	BL*Mm*	ABL*CR*	BL*W*	Control
E	BL*Pf*	AL*AYA30*	BL*HP*	Bcatl*L056P*	BcatL*Cc*	Control	BL*Pf*	AL*AYA30*	BL*HP*	Bcatl*L056P*	BcatL*Cc*	Control
F	Bcatl*L115P*	Bcat*L036P*	NL435	BL*Ro*	NL*TLIM*	Control	Bcatl*L115P*	Bcat*L036P*	NL435	BL*Ro*	NL*TLIM*	Control
G	ESAL*100T*	NL*RMIM*	SL*TIIPP*	NL*525*	ESA*SP398*	Control	ESAL*100T*	NL*RMIM*	SL*TIIPP*	NL*525*	ESA*SP398*	Control
H	NL*388*	BE*Ro*	BL*Pc*	BE*HL*	BiE*HL*	Control	NL*388*	BE*Ro*	BL*Pc*	BE*HL*	BiE*HL*	Control

Table 4: Compounds 123 and 127

	1	2	3	4	5	6	7	8	9	10	11	12
A	BiL*Ca*	BL*Mj*	BL*Rn*	Bla	BL*Pr*	Control	BiL*Ca*	BL*Mj*	BL*Rn*	Bla	BL*Pr*	Control
B	BL*Cl*	BL*Ra*	BL*Cl*	ESAL*PsA*	ESALMA10	Control	BL*Cl*	BL*Ra*	BL*Cl*	ESAL*PsA*	ESALMA10	Control
C	ESAL*FA*	AL*AK*	ESAL*GA50*	AL*AKC-I*	ESAL*AYSA*	Control	ESAL*FA*	AL*AK*	ESAL*GA50*	AL*AKC-I*	ESAL*AYSA*	Control
D	BL*An*	BL*Ca*	BL*Mm*	ABL*CR*	BL*W*	Control	BL*An*	BL*Ca*	BL*Mm*	ABL*CR*	BL*W*	Control
E	BL*Pf*	AL*AYA30*	BL*HP*	Bcatl*L056P*	BcatL*Cc*	Control	BL*Pf*	AL*AYA30*	BL*HP*	Bcatl*L056P*	BcatL*Cc*	Control
F	Bcatl*L115P*	Bcat*L036P*	NL435	BL*Ro*	NL*TLIM*	Control	Bcatl*L115P*	Bcat*L036P*	NL435	BL*Ro*	NL*TLIM*	Control
G	ESAL*100T*	NL*RMIM*	SL*TIIPP*	NL*525*	ESA*SP398*	Control	ESAL*100T*	NL*RMIM*	SL*TIIPP*	NL*525*	ESA*SP398*	Control
H	NL*388*	BE*Ro*	BL*Pc*	BE*HL*	BiE*HL*	Control	NL*388*	BE*Ro*	BL*Pc*	BE*HL*	BiE*HL*	Control

Table 5: Compounds 85 and 89

	1	2	3	4	5	6	7	8	9	10	11	12
A	BiL*Ca*	BL*Mj*	BL*Rn*	Bla	BL*Pr*	Control	BiL*Ca*	BL*Mj*	BL*Rn*	Bla	BL*Pr*	Control
B	BL*Cl*	BL*Ra*	BL*Cl*	ESAL*PsA*	ESALMA10	Control	BL*Cl*	BL*Ra*	BL*Cl*	ESAL*PsA*	ESALMA10	Control
C	ESAL*FA*	AL*AK*	ESAL*GA50*	AL*AKC-I*	ESAL*AYSA*	Control	ESAL*FA*	AL*AK*	ESAL*GA50*	AL*AKC-I*	ESAL*AYSA*	Control
D	BL*An*	BL*Ca*	BL*Mm*	ABL*CR*	BL*W*	Control	BL*An*	BL*Ca*	BL*Mm*	ABL*CR*	BL*W*	Control
E	BL*Pf*	AL*AYA30*	BL*HP*	Bcatl*L056P*	BcatL*Cc*	Control	BL*Pf*	AL*AYA30*	BL*HP*	Bcatl*L056P*	BcatL*Cc*	Control
F	Bcatl*L115P*	Bcat*L036P*	NL435	BL*Ro*	NL*TLIM*	Control	Bcatl*L115P*	Bcat*L036P*	NL435	BL*Ro*	NL*TLIM*	Control
G	ESAL*100T*	NL*RMIM*	SL*TIIPP*	NL*525*	ESA*SP398*	Control	ESAL*100T*	NL*RMIM*	SL*TIIPP*	NL*525*	ESA*SP398*	Control
H	NL*388*	BE*Ro*	BL*Pc*	BE*HL*	BiE*HL*	Control	NL*388*	BE*Ro*	BL*Pc*	BE*HL*	BiE*HL*	Control

A4: Single Crystal Data and Structure for 2,2',6,6'-Tetramethoxy[1,1′-biphenyl]-3,3′-dicarbaldehyde 104

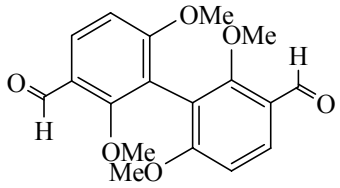

104

Table A4.1. Crystal Data and Structure Refinement for 104

Empirical formula	**C_{18} H_{18} O_6**
Formula weight	330.32
Temperature	173(2) K
Wavelength	0.71073 Å
Crystal system	Monoclinic
Space group	P2(1)/c
Unit cell dimensions	a = 8.0686(13) Å α= 90°.
	b = 15.634(3) Å β= 102.238(8)°.
	c = 13.592(2) Å γ = 90°.
Volume	1675.5(5) $Å^3$
Z	4
Density (calculated)	1.309 Mg/m^3
Absorption coefficient	0.099 mm^{-1}
F(000)	696
Crystal size	0.43 x 0.18 x 0.18 mm^3
Theta range for data collection	2.01 to 27.99°.
Index ranges	-10<=h<=10, -16<=k<=20, -17<=l<=17

Reflections collected	10745
Independent reflections	4048 [R(int) = 0.0588]
Completeness to theta = 27.99°	100.0%
Absorption correction	None
Max. and min. transmission	0.9825 and 0.9588
Refinement method	Full-matrix least-squares on F^2
Data / restraints / parameters	4048 / 0 / 221
Goodness-of-fit on F^2	0.974
Final R indices [I>2sigma(I)]	R1 = 0.0440, wR2 = 0.1133
R indices (all data)	R1 = 0.0795, wR2 = 0.1272
Largest diff. peak and hole	0.211 and -0.224 e.$Å^{-3}$

Table A4.2. Atomic coordinates (x 10^4) and equivalent isotropic displacement parameters ($Å^2$x 10^3) for 104. U(eq) is defined as one third of the trace of the orthogonalized U^{ij} tensor.

	x	y	z	U(eq)
C(1)	1215(2)	2687(1)	4161(1)	29(1)
C(1')	1820(2)	3591(1)	4189(1)	29(1)
C(2)	2355(2)	2010(1)	4352(1)	31(1)
C(2')	2463(2)	3937(1)	3403(1)	31(1)
C(3)	1806(2)	1155(1)	4313(1)	36(1)
C(3')	3107(2)	4777(1)	3458(1)	37(1)
C(4')	3055(2)	5261(1)	4314(2)	45(1)
C(4)	72(2)	1001(1)	4122(1)	40(1)
C(5)	-1103(2)	1652(1)	3947(1)	37(1)
C(5')	2391(2)	4943(1)	5092(1)	43(1)
C(6')	1778(2)	4104(1)	5034(1)	34(1)
C(6)	-532(2)	2496(1)	3937(1)	31(1)

C(7')	952(2)	3363(1)	1856(1)	48(1)
C(7)	4820(2)	2258(1)	5607(1)	54(1)
C(8')	3826(2)	5135(1)	2635(2)	51(1)
C(8)	3030(3)	451(1)	4421(2)	52(1)
C(9')	1200(2)	4161(1)	6702(1)	58(1)
C(9)	-3317(2)	3036(1)	3254(2)	51(1)
O(1)	4069(1)	2186(1)	4551(1)	39(1)
O(1')	2540(1)	3445(1)	2571(1)	39(1)
O(2')	4459(2)	5841(1)	2648(1)	69(1)
O(2)	2645(2)	-305(1)	4383(1)	77(1)
O(3')	1129(1)	3716(1)	5764(1)	44(1)
O(3)	-1574(1)	3183(1)	3710(1)	38(1)

Table A4.3. Bond lengths [Å] for 104.

C(1)-C(2)	1.389(2)
C(1)-C(6)	1.410(2)
C(1)-C(1')	1.492(2)
C(1')-C(2')	1.392(2)
C(1')-C(6')	1.408(2)
C(2)-O(1)	1.3795(18)
C(2)-C(3)	1.406(2)
C(2')-O(1')	1.3804(19)
C(2')-C(3')	1.409(2)
C(3)-C(4)	1.389(2)
C(3)-C(8)	1.465(2)
C(3')-C(4')	1.397(3)
C(3')-C(8')	1.475(3)
C(4')-C(5')	1.374(3)
C(4')-H(4')	0.9500

C(4)-C(5)	1.376(2)
C(4)-H(4)	0.9500
C(5)-C(6)	1.399(2)
C(5)-H(5)	0.9500
C(5')-C(6')	1.399(2)
C(5')-H(5')	0.9500
C(6')-O(3')	1.3595(19)
C(6)-O(3)	1.3588(18)
C(7')-O(1')	1.440(2)
C(7')-H(7'1)	0.9800
C(7')-H(7'2)	0.9800
C(7')-H(7'3)	0.9800
C(7)-O(1)	1.439(2)
C(7)-H(7A)	0.9800
C(7)-H(7B)	0.9800
C(7)-H(7C)	0.9800
C(8')-O(2')	1.215(2)
C(8')-H(8')	0.9500
C(8)-O(2)	1.220(2)
C(8)-H(8)	0.9500
C(9')-O(3')	1.442(2)
C(9')-H(9'1)	0.9800
C(9')-H(9'2)	0.9800
C(9')-H(9'3)	0.9800
C(9)-O(3)	1.4304(19)
C(9)-H(9A)	0.9800
C(9)-H(9B)	0.9800
C(9)-H(9C)	0.9800

Table A4.4. Bond angles [°] for 104

C(2)-C(1)-C(6)	118.10(13)
C(2)-C(1)-C(1')	121.08(13)
C(6)-C(1)-C(1')	120.83(13)
C(2')-C(1')-C(6')	118.81(14)
C(2')-C(1')-C(1)	121.46(13)
C(6')-C(1')-C(1)	119.71(13)
O(1)-C(2)-C(1)	118.77(13)
O(1)-C(2)-C(3)	119.43(13)
C(1)-C(2)-C(3)	121.77(14)
O(1')-C(2')-C(1')	120.07(13)
O(1')-C(2')-C(3')	118.88(14)
C(1')-C(2')-C(3')	121.00(15)
C(4)-C(3)-C(2)	117.92(14)
C(4)-C(3)-C(8)	121.32(15)
C(2)-C(3)-C(8)	120.68(15)
C(4')-C(3')-C(2')	118.24(16)
C(4')-C(3')-C(8')	120.88(16)
C(2')-C(3')-C(8')	120.88(17)
C(5')-C(4')-C(3')	122.09(15)
C(5')-C(4')-H(4')	119.0
C(3')-C(4')-H(4')	119.0
C(5)-C(4)-C(3)	122.26(14)
C(5)-C(4)-H(4)	118.9
C(3)-C(4)-H(4)	118.9
C(4)-C(5)-C(6)	118.90(15)
C(4)-C(5)-H(5)	120.6
C(6)-C(5)-H(5)	120.6
C(4')-C(5')-C(6')	119.07(16)

C(4')-C(5')-H(5')	120.5
C(6')-C(5')-H(5')	120.5
O(3')-C(6')-C(5')	124.31(15)
O(3')-C(6')-C(1')	114.92(13)
C(5')-C(6')-C(1')	120.76(15)
O(3)-C(6)-C(5)	123.99(13)
O(3)-C(6)-C(1)	115.08(12)
C(5)-C(6)-C(1)	120.92(14)
O(1')-C(7')-H(7'1)	109.5
O(1')-C(7')-H(7'2)	109.5
H(7'1)-C(7')-H(7'2)	109.5
O(1')-C(7')-H(7'3)	109.5
H(7'1)-C(7')-H(7'3)	109.5
H(7'2)-C(7')-H(7'3)	109.5
O(1)-C(7)-H(7A)	109.5
O(1)-C(7)-H(7B)	109.5
H(7A)-C(7)-H(7B)	109.5
O(1)-C(7)-H(7C)	109.5
H(7A)-C(7)-H(7C)	109.5
H(7B)-C(7)-H(7C)	109.5
O(2')-C(8')-C(3')	124.4(2)
O(2')-C(8')-H(8')	117.8
C(3')-C(8')-H(8')	117.8
O(2)-C(8)-C(3)	124.27(18)
O(2)-C(8)-H(8)	117.9
C(3)-C(8)-H(8)	117.9
O(3')-C(9')-H(9'1)	109.5
O(3')-C(9')-H(9'2)	109.5
H(9'1)-C(9')-H(9'2)	109.5
O(3')-C(9')-H(9'3)	109.5

H(9'1)-C(9')-H(9'3)	109.5
H(9'2)-C(9')-H(9'3)	109.5
O(3)-C(9)-H(9A)	109.5
O(3)-C(9)-H(9B)	109.5
H(9A)-C(9)-H(9B)	109.5
O(3)-C(9)-H(9C)	109.5
H(9A)-C(9)-H(9C)	109.5
H(9B)-C(9)-H(9C)	109.5
C(2)-O(1)-C(7)	113.87(13)
C(2')-O(1')-C(7')	114.44(12)
C(6')-O(3')-C(9')	118.78(14)
C(6)-O(3)-C(9)	118.36(12)

Symmetry transformations used to generate equivalent atoms:

Table A4.5. Anisotropic displacement parameters ($Å^2$x 10^3)for 104. The anisotropic displacement factor exponent takes the form: $-2\pi^2[h^2a^{*2}U^{11} + ... + 2 h k a^* b^* U^{12}]$

	U^{11}	U^{22}	U^{33}	U^{23}	U^{13}	U^{12}
C(1)	31(1)	30(1)	24(1)	1(1)	3(1)	-3(1)
C(1')	24(1)	27(1)	34(1)	-2(1)	2(1)	0(1)
C(2)	31(1)	33(1)	27(1)	2(1)	2(1)	-2(1)
C(2')	24(1)	29(1)	37(1)	3(1)	3(1)	4(1)
C(3)	44(1)	31(1)	31(1)	4(1)	2(1)	-1(1)
C(3')	25(1)	32(1)	51(1)	9(1)	2(1)	2(1)
C(4')	33(1)	27(1)	68(1)	0(1)	-5(1)	-3(1)
C(4)	49(1)	31(1)	37(1)	2(1)	4(1)	-9(1)
C(5)	35(1)	39(1)	35(1)	-1(1)	3(1)	-10(1)
C(5')	36(1)	36(1)	50(1)	-15(1)	-3(1)	1(1)

C(6')	26(1)	37(1)	36(1)	-3(1)	1(1)	0(1)
C(6)	31(1)	33(1)	27(1)	-1(1)	4(1)	-2(1)
C(7')	53(1)	53(1)	36(1)	-2(1)	6(1)	-3(1)
C(7)	43(1)	59(1)	49(1)	-2(1)	-11(1)	-6(1)
C(8')	34(1)	48(1)	68(1)	26(1)	3(1)	-1(1)
C(8)	54(1)	36(1)	60(1)	6(1)	0(1)	3(1)
C(9')	44(1)	91(2)	38(1)	-22(1)	6(1)	0(1)
C(9)	30(1)	53(1)	63(1)	-7(1)	-3(1)	0(1)
O(1)	31(1)	41(1)	42(1)	4(1)	0(1)	0(1)
O(1')	38(1)	42(1)	37(1)	1(1)	11(1)	5(1)
O(2')	47(1)	56(1)	96(1)	39(1)	0(1)	-11(1)
O(2)	73(1)	33(1)	118(1)	9(1)	2(1)	4(1)
O(3')	46(1)	52(1)	33(1)	-9(1)	10(1)	-4(1)
O(3)	26(1)	37(1)	49(1)	-5(1)	2(1)	-1(1)

Table A4.6. Hydrogen coordinates (x 10^4) and isotropic displacement parameters ($Å^2$x 10^3) for 104.

	x	y	z	U(eq)
H(4')	3492	5827	4361	54
H(4)	-317	427	4113	48
H(5)	-2281	1530	3834	44
H(5')	2350	5289	5661	51
H(7'1)	85	3145	2199	72
H(7'2)	1087	2964	1322	72
H(7'3)	605	3923	1561	72
H(7A)	4312	2742	5893	80
H(7B)	6044	2351	5694	80
H(7C)	4617	1730	5952	80

H(8')	3793	4789	2056	61
H(8)	4199	592	4526	62
H(9'1)	2386	4254	7036	87
H(9'2)	638	3816	7139	87
H(9'3)	622	4713	6569	87
H(9A)	-3393	2631	2696	76
H(9B)	-3853	3577	3000	76
H(9C)	-3900	2797	3756	76

Table A4.7. Torsion angles [°] for 104.

C(2)-C(1)-C(1')-C(2')	76.56(19)
C(6)-C(1)-C(1')-C(2')	-103.17(17)
C(2)-C(1)-C(1')-C(6')	-102.07(17)
C(6)-C(1)-C(1')-C(6')	78.21(19)
C(6)-C(1)-C(2)-O(1)	178.61(13)
C(1')-C(1)-C(2)-O(1)	-1.1(2)
C(6)-C(1)-C(2)-C(3)	0.8(2)
C(1')-C(1)-C(2)-C(3)	-178.94(14)
C(6')-C(1')-C(2')-O(1')	179.13(12)
C(1)-C(1')-C(2')-O(1')	0.5(2)
C(6')-C(1')-C(2')-C(3')	1.8(2)
C(1)-C(1')-C(2')-C(3')	-176.88(13)
O(1)-C(2)-C(3)-C(4)	179.24(14)
C(1)-C(2)-C(3)-C(4)	-3.0(2)
O(1)-C(2)-C(3)-C(8)	-3.7(2)
C(1)-C(2)-C(3)-C(8)	174.05(15)
O(1')-C(2')-C(3')-C(4')	-178.57(13)
C(1')-C(2')-C(3')-C(4')	-1.2(2)

O(1')-C(2')-C(3')-C(8')	1.1(2)
C(1')-C(2')-C(3')-C(8')	178.46(14)
C(2')-C(3')-C(4')-C(5')	-0.4(2)
C(8')-C(3')-C(4')-C(5')	179.99(15)
C(2)-C(3)-C(4)-C(5)	1.8(2)
C(8)-C(3)-C(4)-C(5)	-175.21(16)
C(3)-C(4)-C(5)-C(6)	1.5(2)
C(3')-C(4')-C(5')-C(6')	1.3(3)
C(4')-C(5')-C(6')-O(3')	178.54(14)
C(4')-C(5')-C(6')-C(1')	-0.6(2)
C(2')-C(1')-C(6')-O(3')	179.89(12)
C(1)-C(1')-C(6')-O(3')	-1.4(2)
C(2')-C(1')-C(6')-C(5')	-0.8(2)
C(1)-C(1')-C(6')-C(5')	177.82(14)
C(4)-C(5)-C(6)-O(3)	175.72(14)
C(4)-C(5)-C(6)-C(1)	-3.8(2)
C(2)-C(1)-C(6)-O(3)	-176.91(13)
C(1')-C(1)-C(6)-O(3)	2.8(2)
C(2)-C(1)-C(6)-C(5)	2.6(2)
C(1')-C(1)-C(6)-C(5)	-177.65(14)
C(4')-C(3')-C(8')-O(2')	2.4(3)
C(2')-C(3')-C(8')-O(2')	-177.18(16)
C(4)-C(3)-C(8)-O(2)	-2.2(3)
C(2)-C(3)-C(8)-O(2)	-179.13(19)
C(1)-C(2)-O(1)-C(7)	93.87(17)
C(3)-C(2)-O(1)-C(7)	-88.27(18)
C(1')-C(2')-O(1')-C(7')	79.22(17)
C(3')-C(2')-O(1')-C(7')	-103.36(16)
C(5')-C(6')-O(3')-C(9')	-5.7(2)
C(1')-C(6')-O(3')-C(9')	173.54(14)

C(5)-C(6)-O(3)-C(9)	-13.6(2)
C(1)-C(6)-O(3)-C(9)	165.94(14)
Symmetry transformations used to generate equivalent atoms:	

A4.8 ORTEP Diagrams of 104.